Trabajo de Fin de Grado
Ingeniería Aeroespacial

Analysis and Optimization of Earth Observation Micro-Constellations

Autor: Francisco Pallarés Chamorro

Tutor: Rafael Vázquez Valenzuela

Dpto. Ingeniería Aeroespacial y Mecánica de Fluidos
Escuela Técnica Superior de Ingeniería
Universidad de Sevilla

Sevilla, 2019

Ingeniería Aeroespacial
ESI - Universidad de Sevilla

Trabajo de Fin de Grado
Ingeniería Aeroespacial

Analysis and Optimization of Earth Observation Micro-Constellations

Autor:
Francisco Pallarés Chamorro

Tutor:
Rafael Vázquez Valenzuela
Profesor Titular

Dpto. Ingeniería Aeroespacial y Mecánica de Fluidos
Escuela Técnica Superior de Ingeniería
Universidad de Sevilla

Sevilla, 2019

Trabajo de Fin de Grado: Analysis and Optimization of Earth Observation Micro-Constellations

Autor: Francisco Pallarés Chamorro
Tutor: Rafael Vázquez Valenzuela

El tribunal nombrado para juzgar el trabajo arriba indicado, compuesto por los siguientes profesores:

Presidente:

Vocal/es:

Secretario:

acuerdan otorgarle la calificación de:

El Secretario del Tribunal

Fecha:

Contents

1 Introduction

Remote sensing techniques provide the capacity of collecting information of spots from afar. This tool has an important application on Earth's monitoring from space, a practice which help to gather multiple data from any point on Earth's surface in short periods of time: vegetation biomass, water quality, surface profile, surface temperature, human infrastructures spread... This knowledge is used for a diversity of purposes of human interest, such as military, agricultural, meteorological or ecological ends.

In order to acquire this information by remote sensing practice an entire infrastructure has been set, divided into space and ground segments. The space segment comprises the satellite or satellites, also called *Earth Observation Satellites* (EOS), which are equipped with sensors for the reception of data, usually in the form of electromagnetic signals. These satellites establish transmissions with the ground segment by means of antennas placed in certain spots, in order to sent the information collected. Then the ground segment is responsible for the processing of the data acquired for its use on a particular application.

Earth observation satellites have been used for decades now. Historically, large satellites were required in order to do the observation tasks. These satellites were manually coordinated and their time resolution, linked with the time needed to revisit and acquire data from the exact location [11], was very low. Currently, the miniaturization tendencies have also arrived to the space sector and smaller satellites are now developmed. The emergence of the CubeSats, included in the nanosatellites group, and the growth of the number of their launches make clear the future trend: Earth observation with small and numerous satellites.

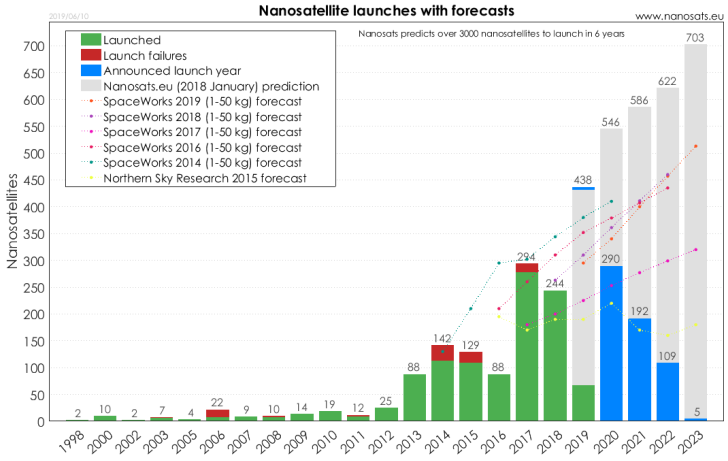

Figure 1.1 Amount and forecast of CubeSats' launches per year.

The increasing amount of EOS will allow a coordinated solution for Earth's surface monitoring with a higher time resolution. However, this concept inevitably requires a more efficient and automatised scheduling of the observations and transmission times for each of the satellites of the constellation involved in the task. In addition, the raise of time resolution together with the specific demands of clients calls for a real-time analysis, in which the computing time for the resolution plays an important roll.

Planet Labs

In the field of Earth remote sensing, the company *Planrt Labs Inc.* stands out for its successful trajectory since its foundation in 2010. The company pursues a daily imaging of the entire Earth to provide a detailed monitoring of changes on its surface. To this end, the company has developed their own satellite model called *Dove*, a Triple-CubeSat equipped with the necessary instrumentation to continuously scan the Earth and send data to the ground stations. The company has been launching their satellites since April 2013 building their *Flock* constellations, groups of satellites on trailing formation along different orbital planes, mostly sun-synchronous ones. With over 200 of their *Doves* in orbit, *Planet Labs Inc.* currently owns the largest satellite fleet.

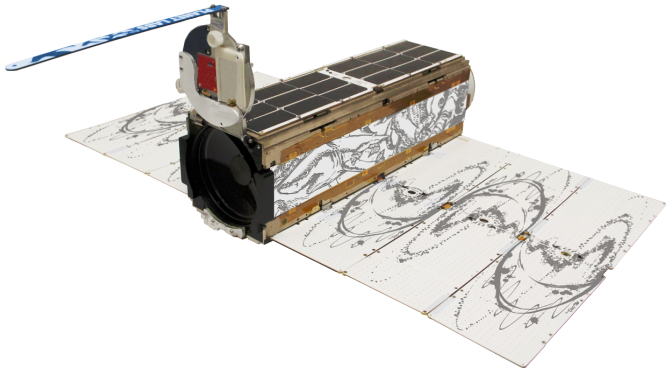

Figure 1.2 *Planet Labs*'s *Dove*.

1.1 Scope of the project

The objective of this project is to provide a an optimised schedule for the observations and transmissions coupled problem using constellations of multiple satellites and diverse spots as ground stations in order to capture a defined region of Earth's surface. Based in other previously done bachelor's thesis ([7] and [6]) and research ([13] and [9]), this project performs a compact analysis of the coupled problem, from the first considerations about the satellite orbits, swaths, ground station and regions of interest, to the final resolution. In order to accomplish this, the mathematical models are developed and explained.

The scheduling policies are governed by a specific guideline, typically in the form of objective which must be minimised, and certain constraints which must be fulfilled. Consequently, the scheduling problem is addressed as a constrained optimisation problem. On a first approach the observations sub-problem is solved by exact algorithms provided by *MATLAB* software and next a heuristic algorithm which provides a solution close to the optimal is developed. Afterwards, the observations and transmissions coupled problem will be solved by an upgraded heuristic algorithm based on the previous one.

The project considers the typical constraints regarding the attitude of satellites, their storage capacity, or the ground stations availability among others. Furthermore, information provided from *Planet Labs Inc.* about their satellites and ground stations is used, in order to carry out as far as possible an accurate analysis.

The use of an heuristic algorithm for the coupled problem in this project is due to the growth in complexity caused by the addition of the constraints regarding the available storage range on each satellite. These constraints complicate a proper modelling of the problem in order to be solved using exact algorithms. The heuristic algorithm used for the observations scheduling sub-problem represents a middle step between the exact resolution of the sub-problem and the heuristic resolution of the complete problem.

Aspects regarding the *Duty-cycle* or energy consumption on the satellites remain outside of the purview of the project. Beyond the scope of this project also are considerations about failed transmissions between satellites and ground stations.

1.2 Structure of the document

A brief description of the structure of this document which reflects the work done on the project is presented below:

- *Chapter 1: Introduction.* On this chapter an explanation of the context in which this project is located is given. The future trends about Earth remote sensing and the importance of efficiently solving the scheduling problem is introduced. The chapter also establishes the considerations under the scope of the project.
- *Chapter 2: Preliminary considerations.* The chapter contains a description of the entities and phenomena taking part on the Earth observation activities. For each of them, some modelling is carried out in order to introduce the mathematical resolution of the problem.
- *Chapter 3: Computational geometry modelling.* Here in this chapter, the mathematical entities needed to uniquely identify the scheduling problem are defined from the basis set on the *Preliminary considerations.*
- *Chapter 4: Problem optimization.* This chapter describes mathematically the optimisation problem, defined by its objective function and the constraints which must be fulfilled. A relaxation of the observations and transmissions problem where only observations are considered is firstly stated. Then, the complete problem is addressed.
- *Chapter 5: Results.* This chapter is exclusively dedicated to the exhibition of the results obtained for both relaxed and complete problems and an their analysis.
- *Chapter 6: Conclusions and future work.* On the final chapter, an overall analysis of the project is done and possible future consideration are mentioned in order to improve the study are suggested.

It is also important to inform about the specifications of the device in which the algorithms are executed in order to contextualise the computational demands of the methods used.

- Processor: *Intel®Core™* i7-8750H CPU @ 2.20 GHz x64 (6 cores)
- RAM: 16.0 GB
- Software: *MATLAB* 9.5 (*R2018b*)

2 Preliminary considerations

2.1 Set up

In order to provide a proper spatial description of the situation, the definition of the used reference frames is given below. The reference frames necessary to locate and orient both Earth's surface and a satellite is a first step for the mathematical description of the problem.

2.1.1 Geocentric equatorial frame

The geocentric equatorial frame ($_\oplus$) is defined by the direction of the Vernal equinox (γ-point) which corresponds to the $X_\oplus$-axis direction. The $Z_\oplus$-axis points towards the celestial north pole so that the equator lies on the $XY_\oplus$-plane (Inertial Earth-centred frame). The orbit propagator uses this frame to describe the situation of the satellite at every instant of time.

Together with the modulus of the position vector ($R_{sat} = |\vec{R}_{sat}\rfloor_\oplus|$), invariant under frame rotation, it is usual to use two angles to describe the situation of a certain point on this frame:

- **Right Ascension (α)**: Angle between $X_\oplus$-axis and the plane containing the satellite and normal to the equatorial $XY_\oplus$-plane.
- **Declination (δ)**: Angle between the position vector $\vec{R}_{sat}$ ($\vec{r}$ in Fig. 2.1) and the equatorial $XY_\oplus$-plane.

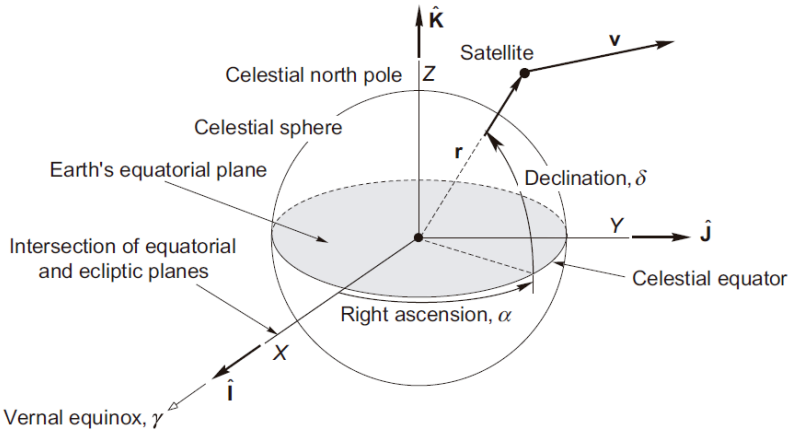

Figure 2.1 Geocentric reference frame [1].

Hence, the position vector can be described as:

$$\vec{R}_{sat}\rfloor_\oplus = R_{sat}\begin{pmatrix}\cos(\alpha)\cos(\delta)\\ \sin(\alpha)\cos(\delta)\\ \sin(\delta)\end{pmatrix} \tag{2.1}$$

2.1.2 Perifocal frame

The perifocal reference frame ($_{pf}$), is used for the description of an orbit. The frame is centred on the celestial body governing the orbital motion, meanwhile, the X_{pf}-axis points the position of the periapsis of the orbit,

$$\vec{i}_{pf} \parallel \vec{e}, \tag{2.2}$$

the Z_{pf}-axis is along the angular momentum direction,

$$\vec{k}_{pf} \parallel \vec{h}, \tag{2.3}$$

and the Y_{pf}-axis is defined to complete the coordinate system,

$$\vec{j}_{pf} \parallel \vec{h} \times \vec{e}, \tag{2.4}$$

The rotation between the perifocal and geocentric equatorial frame is governed by three orbital angles which locate the orbital plane, XY_{pf}-plane, in the geocentric coordinate system. First, the ascending and descending nodes are defined as the points where the orbiting body cross the equatorial plane northwards and southwards respectively. This two points define the node line direction, N. The angles can be defined thanks to the definition of this vector,

- **Right Ascension of the Ascending Node (Ω)**: Angle between $X_{\oplus}$-axis and the line of nodes direction, N-axis.
- **Inclination (i)**: Angle between the $Z_{\oplus}$-axis and the direction of the angular momentum $\vec{h}$.
- **Argument of Perigee (ω)**: Angle between the ascending node direction, N-axis, and the direction of the perigee of the orbit, $\vec{e}$.

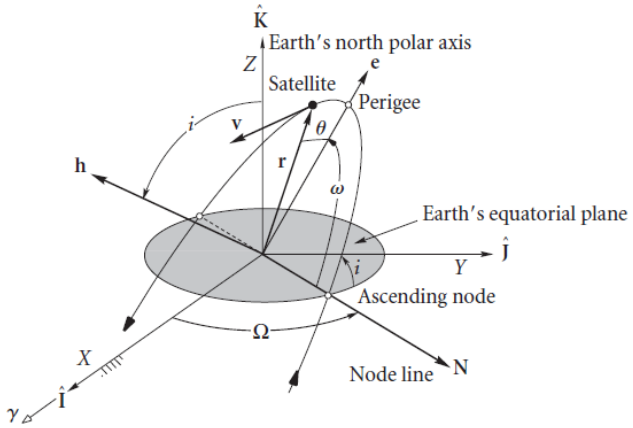

Figure 2.2 Perifocal and geocentric equatorial frames [1].

Thanks to this description, the rotation between frames can be described decomposing it into three different rotation along the $Z_{\oplus}$-axis, N-axis and Z_{pf}-axis.

$$T_\Omega = \begin{pmatrix} \cos(\Omega) & \sin(\Omega) & 0 \\ -\sin(\Omega) & \cos(\Omega) & 0 \\ 0 & 0 & 1 \end{pmatrix}, \tag{2.5}$$

$$T_i = \begin{pmatrix} 1 & 0 & 0 \\ 0 & \cos(i) & \sin(i) \\ 0 & -\sin(i) & \cos(i) \end{pmatrix}, \tag{2.6}$$

$$T_\omega = \begin{pmatrix} \cos(\omega) & \sin(\omega) & 0 \\ -\sin(\omega) & \cos(\omega) & 0 \\ 0 & 0 & 1 \end{pmatrix}. \tag{2.7}$$

Therefore, the rotation matrix from perifocal to geocentric equatorial frame is defined as follows,

$$T_{pf}\rfloor_\oplus = \left(T_\oplus\rfloor_{pf}\right)' = (T_\omega T_i T_\Omega)' = T_\Omega' T_i' T_\omega', \tag{2.8}$$

$$T_{pf}\rfloor_\oplus = \begin{pmatrix} \cos(\Omega)\cos(\omega) - \sin(\Omega)\cos(i)\sin(\omega) & -\cos(\Omega)\sin(\omega) - \sin(\Omega)\cos(i)\cos(\omega) & \sin(\Omega)\sin(i) \\ \sin(\Omega)\cos(\omega) + \cos(\Omega)\cos(i)\sin(\omega) & -\sin(\Omega)\sin(\omega) + \cos(\Omega)\cos(i)\cos(\omega) & -\cos(\Omega)\sin(i) \\ \sin(i)\sin(\omega) & \sin(i)\cos(\omega) & \cos(i) \end{pmatrix} \tag{2.9}$$

2.1.3 Geographic equatorial frame

The geographic equatorial frame ($_{gph}$), as the geocentric equatorial frame, also place the XY_{gph}-plane containing the equator; however, its X_{gph}-axis is defined by the intersection between the equator and the Greenwich meridian, rotating with the planet (Non-inertial Earth-centred frame).

As in the geocentric frame, once the modulus of the position vector ($R_{sat} = |\vec{R}_{sat}\rfloor_{gph}|$) is known, two angles may be defined for a description of any position on this frame:

- **Longitude (λ)**: Angle between X_{gph}-axis (Greenwich meridian) and the plane containing the satellite normal plane to XY_{gph}-plane which defines Local meridian (Λ in Fig. 2.3).
- **Latitude (ϕ)**: Angle between the position vector $\vec{r}_\oplus$ and the equatorial XY_{gph}-plane.

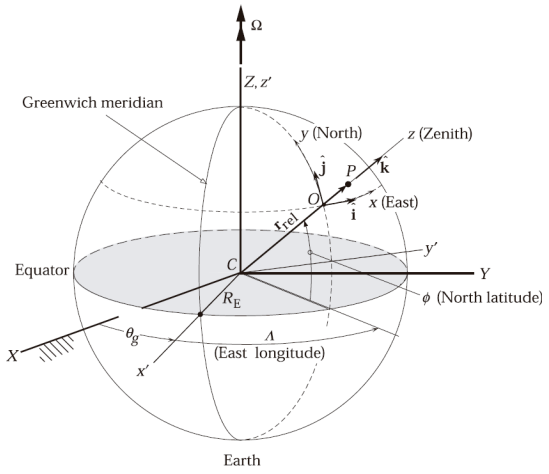

Figure 2.3 Geographic reference frame [1].

$$\vec{R}_{sat}\rfloor_{gph} = R_{sat} \begin{pmatrix} \cos(\lambda)\cos(\phi) \\ \sin(\lambda)\cos(\phi) \\ \sin(\phi) \end{pmatrix} \tag{2.10}$$

The relationship between this frame and the geocentric equatorial frame is given from the Greenwich mean sidereal time at the instant of time (GMST), which states the angle between the Vernal equinox ($X_{\oplus}$-axis) and the Greenwich meridian (X_{gph}-axis).

$$\theta_g = GMST \cdot 15 \frac{^o}{hr} \tag{2.11}$$

$$\cos(\theta_g) = \vec{i}_{\oplus} \cdot \vec{i}_{gph} \tag{2.12}$$

Hence, taking into account the right ascension (α) and declination (δ) angles definition on the Geocentric frame, the transformation between the frames is immediate:

$$\lambda = \alpha + \theta_g \tag{2.13}$$

$$\phi = \delta \tag{2.14}$$

This is the key frame for the representation and computation of geographical zones and allows to relate the model of visibility used with the topography on Earth's surface. It is also appropriate to indicate that for this project, a simplification of ideal spheric Earth has been used.

2.1.4 Vehicle Velocity, Local Horizontal frame

In order to analyse the attitude of the satellite a local reference frame is used. On the Vehicle Velocity, Local Horizontal frame ($_{VVLH}$), Z_{VVLH}-axis is along the negative position vector (nadir):

$$\vec{k}_{VVLH} \parallel -\vec{R}_{sat} \tag{2.15}$$

while Y_{VVLH}-axis is defined along the negative orbit normal:

$$\vec{j}_{VVLH} \parallel -\vec{R}_{sat} \times \vec{V}_{sat} \tag{2.16}$$

Hence, the X_{VVLH}-axis is towards velocity, but not necessary parallel to it.

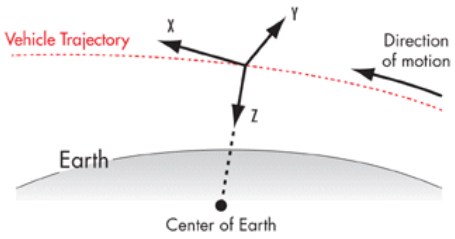

Figure 2.4 VVLH reference frame.

The rotation from VVLH frame to Geographical frame can be described by means of the following equivalences:

$$\vec{i}_{VVLH}\rfloor_{gph} = \vec{j}_{VVLH}\rfloor_{gph} \times \vec{k}_{VVLH}\rfloor_{gph} \tag{2.17}$$

$$\vec{j}_{VVLH}\rfloor_{gph} = -\frac{\vec{R}_{sat}\rfloor_{gph} \times \vec{V}_{sat}\rfloor_{gph}}{|\vec{R}_{sat}\rfloor_{gph} \times \vec{V}_{sat}\rfloor_{gph}|} \tag{2.18}$$

$$\vec{k}_{VVLH}\rfloor_{gph} = -\frac{\vec{R}_{sat}}{|\vec{R}_{sat}|}, \tag{2.19}$$

therefore, the rotation matrix between the two frames is:

$$T_{VVLH\rfloor gph} = \left(\vec{i}_{VVLH\rfloor gph} \;\middle|\; \vec{j}_{VVLH\rfloor gph} \;\middle|\; \vec{k}_{VVLH\rfloor gph} \right) \tag{2.20}$$

It is important to note that VVLH frame is a local frame while the Geographic frame is an Earth-centred; thus, not only a rotation, but also a translation defined by the vector $\vec{R}_{earth}$, which represents Earth's center position from the satellite, is needed for changing between these two frames.

$$\vec{R}_{earth\rfloor VVLH} = R_{sat} \begin{pmatrix} 0 \\ 0 \\ 1 \end{pmatrix} \tag{2.21}$$

2.1.5 Spacecraft frame

The spacecraft reference frame ($_{sc}$) is bounded to the satellite and rotates with it. At an initial instant before the manoeuvring, when the sensor(Z_{sc}-axis) points towards the nadir, the Spacecraft frame matches the VVLH frame. The manoeuvre achieves the desired aim direction by rotations along the X_{sc}, Y_{sc} and Z_{sc}-axes, directing Z_{sc}-axes towards the objective:

$$\vec{k}_{sc} \quad = \quad \vec{u}_{aim} \tag{2.22}$$

Once the definitions between these two last frame is made , it is important to identify the attitude angles of a satellite.

- **Roll angle (ω)**: Angle defined along the positive X_{sc}-axis direction.
- **Pitch angle (φ)**: Angle defined along the positive Y_{sc}-axis direction.
- **Yaw angle (χ)**: Angle defined along the positive Z_{sc}-axis direction.

In order to aim at a certain objective on Earth's surface, only two manoeuvres along their axes are needed. In our case, first rolling (ω) followed by pitching (φ) manoeuvres have been chosen. These rotations can be described by their rotation matrices:

$$T_{roll} \quad = \quad \begin{pmatrix} 1 & 0 & 0 \\ 0 & \cos(\omega) & \sin(\omega) \\ 0 & -\sin(\omega) & \cos(\omega) \end{pmatrix}, \tag{2.23}$$

$$T_{pitch} \quad = \quad \begin{pmatrix} \cos(\varphi) & 0 & -\sin(\varphi) \\ 0 & 1 & 0 \\ \sin(\varphi) & 0 & \cos(\varphi) \end{pmatrix}. \tag{2.24}$$

Therefore, the matrix of aiming, which corresponds to the rotation matrix from VVLH frame to Spacecraft frame, is:

$$T_{aim} = T_{pitch} T_{roll} = \begin{pmatrix} \cos(\varphi) & \sin(\omega)\sin(\varphi) & -\cos(\omega)\sin(\varphi) \\ 0 & \cos(\omega) & \sin(\omega) \\ sin(\varphi) & -\sin(\omega)\cos(\varphi) & \cos(\omega)\cos(\varphi) \end{pmatrix}. \tag{2.25}$$

The rotation matrix from the Spacecraft frame to the VVLH frame, as well as the expression of the Z_{sc}-axis in the VVLH frame are as follows:

$$T_{sc}\rfloor_{VVLH} = T'_{aim} = \begin{pmatrix} \cos(\varphi) & 0 & \sin(\varphi) \\ \sin(\omega)\sin(\varphi) & \cos(\omega) & -\sin(\omega)\cos(\varphi) \\ -\cos(\omega)\sin(\varphi) & \sin(\omega) & \cos(\omega)\cos(\varphi) \end{pmatrix}, \tag{2.26}$$

$$\vec{k}_{sc}\rfloor_{VVLH} = \vec{u}_{aim}\rfloor_{VVLH} = \begin{pmatrix} \sin(\varphi) \\ -\sin(\omega)\cos(\varphi) \\ \cos(\omega)\cos(\varphi) \end{pmatrix} \tag{2.27}$$

2.1.6 Normalised frame

The normalised frame ($_{norm}$) represents a Non-inertial Earth-centred frame and is used for the computation of the limits of the visibility swath or visible region. It is defined by the position of the satellite ($\vec{R}_{sat}$), which belongs to X_{norm}-axis; and the aim direction, contained in the XZ_{norm}-plane and pointing to the positive values of the Z_{norm}-axis. For the computation mentioned, the radius of Earth ($R_{\oplus}$) is used to nondimensionalise the distances; therefore, the points obtained from the algorithm are multiplied by this magnitude to get the real position on this frame.

The Normalised frame is described by means of its relation with the local frames, VVLH frame and the Spacecraft frame, as follows:

$$\vec{i}_{norm} \parallel -\vec{k}_{VVLH}, \tag{2.28}$$

$$\vec{j}_{norm} \parallel \vec{i}_{norm} \times \vec{u}_{aim}, \tag{2.29}$$

$$\vec{k}_{norm} \parallel \vec{i}_{norm} \times \vec{j}_{norm}. \tag{2.30}$$

It is important to define the off-nadir angle (Γ) which measures the angle between the aim direction and the nadir, strongly related with the quality of the images taken by the satellite. For larger angles of aim the satellite capture Earth's surface farther from the normal, worsening the quality of the taken image.

$$\cos(\Gamma) = \vec{u}_{aim} \cdot \left(-\vec{i}_{norm}\right) = \vec{u}_{aim} \cdot \vec{k}_{VVLH} = \cos(\omega)\cos(\varphi). \tag{2.31}$$

The rotation from Normalised frame to VVLH frame can be expressed by means of the previous equivalences:

$$\vec{i}_{norm}\rfloor_{VVLH} = \begin{pmatrix} 0 \\ 0 \\ -1 \end{pmatrix}, \tag{2.32}$$

$$\vec{j}_{norm}\rfloor_{VVLH} = -\frac{\vec{i}_{norm}\rfloor_{VVLH} \times \vec{u}_{aim}\rfloor_{VVLH}}{|\vec{i}_{norm}\rfloor_{VVLH} \times \vec{u}_{aim}\rfloor_{VVLH}|} \tag{2.33}$$

$$\vec{k}_{norm}\rfloor_{VVLH} = \vec{i}_{norm}\rfloor_{VVLH} \times \vec{j}_{norm}\rfloor_{VVLH}. \tag{2.34}$$

therefore, the rotation matrix is:

$$T_{norm}\rfloor_{VVLH} = \left(\vec{i}_{norm}\rfloor_{VVLH} \;\middle|\; \vec{j}_{norm}\rfloor_{VVLH} \;\middle|\; \vec{k}_{norm}\rfloor_{VVLH} \right) \tag{2.35}$$

As in the transformation between VVLH and Geographic frames, the Normalised frame is Earth-centred and a translation given by the vector $\vec{R}_{sat}$ is needed for the change of frame.

$$\vec{R}_{sat}\rfloor_{norm} = R_{sat} \begin{pmatrix} 1 \\ 0 \\ 0 \end{pmatrix} \tag{2.36}$$

2.2 Orbital Mechanics

On Earth observation missions, the satellite's position determination along time is an essential task. Once the attitude and specifications of the sensor are fixed, the relative position between this one and Earth's surface defines which area is within its visibility limits. For this reason an accurate position determination is required in this project.

With this in mind, an introduction to orbital mechanics is presented in this section, in order to determine the orbits and positions of the satellites considered, taking also into account the most representative perturbation involved in the problem.

2.2.1 Two-body problem

The position of the satellites on this problem is ruled by Newton's laws of motion, by which is stated the relation between the forces and the accelerations governing the movement of any body. In particular, Newton's second law establishes the relation between the acceleration of a body, $\vec{a}_i$, described on an inertial frame, and the sum of the forces, $\vec{F}_{ij}$, acting on it by introducing the gravitational mass of this body, m_i,

$$\sum_{\forall j} \vec{F}_{ij} = m_i \vec{a}_i.$$

By the integrations of the body's acceleration, its velocity and position are determined along time. Hence, the motion of the satellite is uniquely defined by their masses and the forces acting on them once an initial state has been set.

Newton's gravitational law

The gravitational force is the main factor governing the orbital motion of bodies. This force, F, describes the attraction between two particles with masses, m_1 and m_2, as proportional to each of their masses and inversely proportional to the square of the distance, r, between them,

$$F = G\frac{m_1 m_2}{r^2}$$

where G is established as the gravitational constant,

$$G = 6.6742 \times 10^{-11} \frac{m^3}{Kg\,s^2}$$

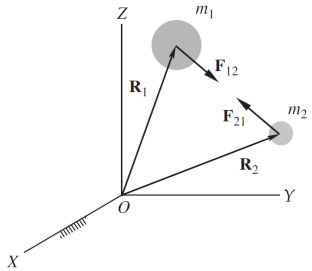

Figure 2.5 Gravitational forces [1].

Therefore, including the vectorial analysis of the attraction between the two point of masses described by their positions, $\vec{R}_1$ and $\vec{R}_2$, the force, $\vec{F}_{12}$ acting on 1 due to 2 attraction,

$$\vec{F}_{12} = G\frac{m_1 m_2}{|\,\vec{R}_2 - \vec{R}_1\,|^3}\left(\vec{R}_2 - \vec{R}_1\right),$$

or defining the relative distance, $r = |\,\vec{R}_2 - \vec{R}_1\,|$, and the versor pointing 2 from 1, $\vec{u}_{12} = \frac{\vec{R}_2 - \vec{R}_1}{|\vec{R}_2 - \vec{R}_1|}$,

$$\vec{F}_{12} = G\frac{m_1 m_2}{r^2}\vec{u}_{12}.$$

The force acting in the other body is defined by Newton's third law,

$$\vec{F}_{21} = -\vec{F}_{12}.$$

Equations of motion

Given an inertial reference frame, and the position vectors of both point of masses relative to this frame, $\vec{R}_1$ and $\vec{R}_2$, the motion of each one is defined by Newton's second law,

$$m_1\ddot{\vec{R}}_1 = G\frac{m_1 m_2}{r^2}\vec{u}_{12}, \tag{2.37}$$

$$m_2\ddot{\vec{R}}_2 = -G\frac{m_1 m_2}{r^2}\vec{u}_{12}. \tag{2.38}$$

The potential energy, V, of the gravitational force, $\vec{F}$, between these two masses is established by,

$$V = -\frac{Gm_1 m_2}{r}, \tag{2.39}$$

from which the gravitational force can be derived thanks to its conservative character,

$$\vec{F} = -\nabla V. \tag{2.40}$$

It is important to describe thoroughly the relative motion of one point, *2*, around the other, *1*, due to the non-inertial character of this approximation. Consequently, the relative acceleration,

$$\ddot{\vec{r}} = \ddot{\vec{R}}_2 - \ddot{\vec{R}}_1, \tag{2.41}$$

$$\ddot{\vec{r}} = -\frac{G(m_1+m_2)}{r^2}\vec{u}_r, \tag{2.42}$$

and defining the gravitational parameter, μ,

$$\mu = G(m_1+m_2), \tag{2.43}$$

the equation of relative motion can be rewritten as,

$$\ddot{\vec{r}} = -\frac{\mu}{r^3}\vec{r}. \tag{2.44}$$

The Eq. (2.44) consists on a non-linear second-order differential equation which governs the motion of the point of mass *2*, relative to *1*. The double integration of this equation together with its six constraints of integration, such as initial relative velocity and position, lead to the description of the relative position as function of time.

This equations describe the ideal situation with two point masses, while the bodies involved in this project are the satellites and the planet Earth. However, by considering the Earth as a perfect sphere, its gravitational field created outside its interior region is identical to the created one by a point mass in the center of this sphere with the Earth's mass, $M_\oplus$. In addition, due to the difference of masses, $M_\oplus \gg m_{sat}$, and sizes, the satellite can be as well considered as a point mass and the previous description for the relative motion can be used to describe the position in space between these two entities. The gravitational parameter, once again due to the difference between masses, is practically function of the greater mass only, and it is defined for the planet Earth,

$$\mu \approx GM_\oplus = 3.986004 \times 10^5 \frac{Km^3}{s^2}.$$

Position in the orbit

Once the differential equation which describes the relative motion of the satellite around the Earth is established, by introducing the angular momentum of the orbit, h, which is a constant, together with other

necessary of parameters, the relative position of the orbiting body can be defined directly on its orbital plane,

$$r = \frac{h^2}{\mu}\frac{1}{1+e\cos\theta}. \tag{2.45}$$

This one represent a parametric equation of a conic curve, where e is the eccentricity of the orbit, related to the type of conic curve, and θ is the true anomaly, the angle between the position vector of the orbiting body and the position vector of the periapsis point, i.e. the point of minimum distance between the satellite and the central body.

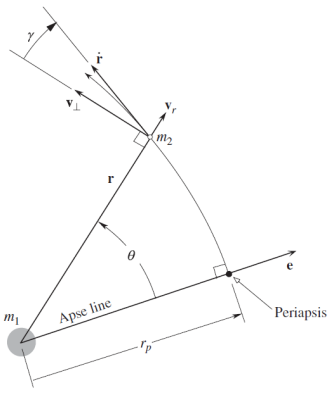

Figure 2.6 Orbital plane description [1].

The artificial satellites orbits around Earth are elliptical, hence the eccentricity,

$$e < 1,$$

and in particular, with regard to Earth observation satellites, their orbits are practically circular,

$$e \simeq 0.$$

This description defines the position of the orbiting body in the perifocal reference frame ($_{pf}$). From the coordinates on this frame, the position in the geocentric equatorial ($_{\oplus}$) frame can be established by a rotation transformation (Subsec. 2.1.2).

Position as function of time

In order to describe the variation of the position in time two additional angles are established:

- **Eccentric anomaly:**

  The definition of the eccentric anomaly, E, is shown in Fig. 2.7 using the auxiliary circle which cirumscribes the ellipse.

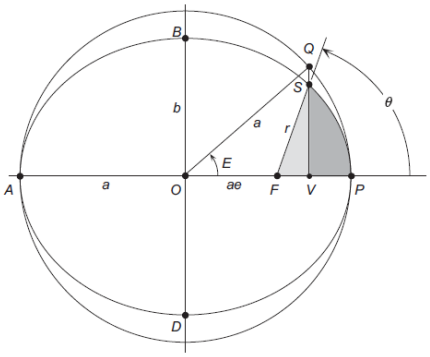

Figure 2.7 Eccentric anomaly definition [1].

The eccentric anomaly, E, is related to the true anomaly, θ, through the next equation:

$$\tan\frac{\theta}{2} = \sqrt{\frac{1+e}{1-e}}\tan\frac{E}{2}. \tag{2.46}$$

- **Mean anomaly:**

  In this case, the mean anomaly, M, is the angle between the vector of a fictitious body moving around the ellipse at a constant angular speed, $n = \sqrt{\frac{\mu}{a^3}}$, and the periapsis vector. This angular speed defines an orbital period, T, equal to the one involving the real object.

$$M = nt = \frac{2\pi}{T}t. \tag{2.47}$$

  The mean anomaly, M, is also described by the eccentric anomaly by the relation,

$$M = E - e\sin E, \tag{2.48}$$

  also known as the *Kepler's equation*.

Therefore, the true anomaly, θ, of the object and the elapsed time, t, are related using the previous expressions.

2.2.2 Orbit perturbations

The previous model for the determination of the position of an orbiting object lies in the assumption of a situation where the gravitational field created by a perfect homogeneous sphere of matter is the only agent with which the body interacts. However, in the real situation other factors participate in satellite's motion, perturbing the ideal one. This factors, also called perturbations, need to be analysed in order to get a precise position of the orbiting bodies.

A model used in order to address the problem of perturbation might be rewriting Eq. (2.44) adding a term, $\vec{p}$, representing the acceleration due to the perturbations,

$$\ddot{\vec{r}} = -\frac{\mu}{r^3}\vec{r} + \vec{p}. \tag{2.49}$$

The effects of some of the perturbation which affect a generic satellite orbiting Earth at a height of 1000 *km* can be estimated by stating the orders of magnitude of the perturbing acceleration:

$$a_0 = \frac{\mu}{r^2}$$

- Earth's oblateness: $p \sim 10^{-2}a_0$
- Lunar gravity: $p \sim 10^{-7}a_0$
- Solar gravity: $p \sim 10^{-7}a_0$
- Solar radiation pressure: $p \sim 10^{-9}a_0$
- Atmospheric drag: $p \sim 10^{-10}a_0$

In case of the atmospheric drag, its perturbation becomes rapidly negligible with altitudes. Nevertheless, for altitudes of the Earth observation satellites orbits, its presence manifests and it should be considered.

The other predominant perturbation considered in this analysis is the effect of the gravitational field created by a non-spherical Earth. Due to the heterogeneity of Earth, its gravitational field does not perfectly matches the one created by a perfect homogeneous sphere and an analysis of its potential should be carried out.

The effects of the perturbations mentioned are divided into three groups:

- **Secular effects:** represent linear variations in the orbital elements.
- **Long-period effects:** represent periodic variations in the orbital elements whose periods is greater than the orbital one.
- **Short-peeriod effects:** represent periodic variations in the orbital elements whose periods is less than the orbital one.

Atmospheric Drag

The atmospheric drag is caused by the interaction between the spacecraft and the particles of the atmosphere. The dependence of atmospheric air's density on the altitude has been an important matter of study for the aerospace sector, and as a result several models has been developed, most of them by interpolating values of density of the air at certain altitudes. In Fig. 2.8 is presented the *US Standard Atmosphere 1976*.

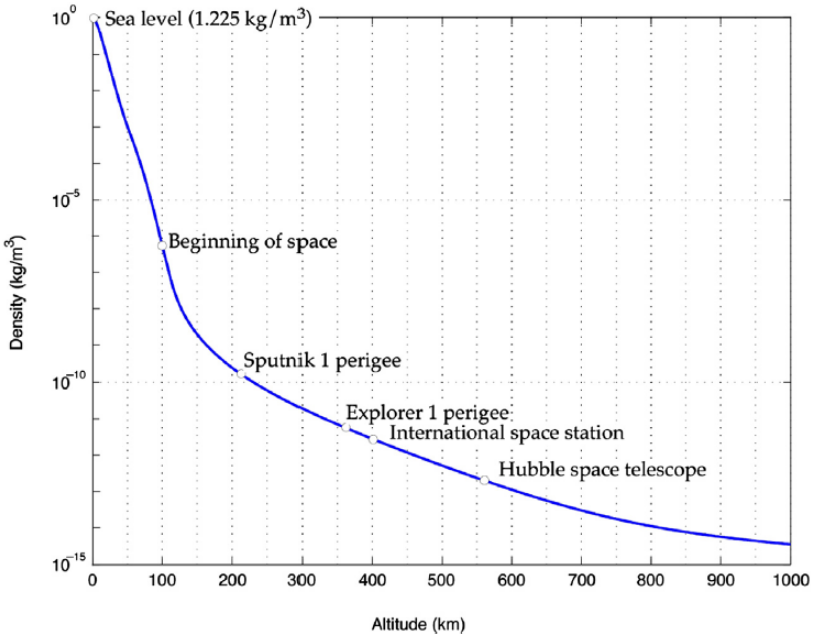

Figure 2.8 *US Standard Atmosphere 1976* [1].

As shown, the density at the altitudes where orbiting bodies exist is low, but their effects still can be noticed eventally deorbiting the satellites.

The drag is modelled as a force which oppose to the relative velocity of an object moving on a fluid, in this case the atmosphere, therefore the relative velocity between the satellite and an atmosphere which rotates with Earth must be established,

$$\vec{v}_{rel} = \vec{v} - \vec{v}_{atm} = \vec{v} - \vec{\Omega}_e \times \vec{r},$$

with $\vec{\Omega}_e$ the angular velocity vector of Earth,

$$\vec{\Omega}_e \rfloor_{\oplus} = \begin{pmatrix} 0 \\ 0 \\ 7.2921159 \times 10^{-5} \end{pmatrix} \frac{rad}{s}.$$

Then the drag can be expressed as the vector,

$$\vec{D} = -D\vec{u}_{rel},$$

defining the versor, $\vec{u}_{rel}$, with the direction of the relative velocity, $\vec{v}_{rel}$,

$$\begin{aligned} v_{rel} &= |\,\vec{v}_{rel}\,| \\ \vec{u}_{rel} &= \frac{\vec{v}_{rel}}{v_{rel}}. \end{aligned}$$

The magnitude of the drag, D, can be estimated thanks to the drag coefficient of the body, C_D, the density at the altitude of the orbit, ρ and the frontal area of the body A,

$$D = \frac{1}{2}\rho v_{rel}^2 C_D A,$$

from which the perturbing acceleration can be completely defined,

$$\vec{p} = -\frac{1}{2}\rho v_{rel}\left(\frac{C_D A}{m}\right)\vec{v}_{rel}.$$

Usually, the model uses the ballistic coefficient, B, in stead of the drag coefficient,

$$B = \frac{C_D A}{m},$$

or the analogous BSTAR coefficient, B^*, which employs a reference value of the air density, ρ_0,

$$B^* = \frac{\rho_0 B}{2} = \frac{\rho_0 C_D A}{2m}.$$

Gravitational perturbations

The gravitational potential per unit of mass given a perfect and homogeneous sphere is given by Eq. (2.39),

$$V = -\frac{\mu}{r},$$

and the acceleration is given by its gradient,

$$\vec{a} = -\nabla V = -\mu\frac{\vec{r}}{r^3}.$$

Nevertheless, the Earth's form is not a perfect sphere, but more similar to an oblate spheroid. This fact has consequences on the gravitational field which is generated. In order to model the gravitational perturbation, a term representing the perturbation of the gravitational potential, $\Phi(r,\phi)$, is used,

$$V = -\frac{\mu}{r} + \Phi(r,\phi).$$

This term only considers the zonal harmonics, this is the differences between a perfect sphere and Earth along the latitudes; for this reason it is called the rotationally symmetric perturbation, and it is only function of the distance, r, and the latitude, ϕ.

The rotationally symmetric perturbation potential can be expressed as infinite series:

$$\Phi(r,\phi) = \frac{\mu}{r}\sum_{k=2}^{\infty} J_k\left(\frac{R}{r}\right)^k P_k(\cos\phi)$$

where J_k are the zonal harmonics, R is the equatorial radius and P_k are the *Legrende polynomials*. Some of the first zonal harmonics are,

$$\begin{aligned} J_2 &= 0.00108263 \\ J_3 &= -2.33936\times10^{-3}\,J_2 \\ J_4 &= -1.49601\times10^{-3}\,J_2 \\ &\ldots \end{aligned}$$

while the *Legrende polynomials* can be obtained from Rodrigues' formula,

$$P_k(x) = \frac{1}{2^k k!}\frac{d}{dx^k}\left(x^2-1\right)^k$$

Finally, the acceleration due to gravitational perturbations can be derived from the gradient of the rotationally symmetrical perturbation potential,

$$\vec{p} = -\nabla\Phi$$

Sun-synchronous orbits:

An important secular effect of the gravitational perturbations strongly related with Earth observation satellites is the nodal regression, whereby the right ascension of the ascending node of the orbit, Ω, varies along time due to the effect of the first zonal harmonic, J_2. This variation can be expressed as,

$$\dot{\Omega} = -\frac{3}{2}\frac{nJ_2R^2}{a^2\left(1-e^2\right)^2}\cos i$$

where a is the semimajor axis of the elliptical orbit, and n represents the mean motion of the orbit,

$$\begin{aligned} a &= \frac{h^2}{\mu}\frac{1}{1-e^2}, \\ n &= \sqrt{\frac{\mu}{a^3}}. \end{aligned}$$

For a given combination of semimajor axis, a, and eccentricity, e, the inclination of the orbit, i, fixes the variation of the right ascension, $\dot{\Omega}$. This fact can be used to achieve a desired rate of change. In case of Earth observation, the variation matches the variation of the sun position during the Earth translation movement, hence the illumination of the spot captured by the sensor at a given latitude remains approximately equal during the year.

For the considered LEO satellites on this project:

$$\begin{aligned} n &\simeq 15.26\,\frac{rev}{day}, \\ a &\simeq 6866\,km, \\ e &\simeq 0, \\ i &\simeq 97.4^{\,o}, \end{aligned}$$

establishing a value for the nodal regression of $\dot{\Omega} \sim 0.99\,\frac{^o}{day}$, which matches the sun position variation around the geocentric frame of reference.

2.2.3 Orbit propagation

At this point, the necessary definitions for the determination of the position of the satellites at every instant of time have been set out. However, regarding orbital perturbations, in stead of numerically integrate the equation of motion (2.49), it is usually preferred to describe the orbital elements at a given instant of time, and analyse their evolution by using a propagation.

Here is explained the procedure to establish an initial state of the satellite and propagate it along time.

Two Line Element set

The state of a satellite at a certain instant of time, or *epoch*, is described in its *Two Line Element* (TLE) set. This data format gather the orbital elements of the object into two lines of 69 characters which are used for the propagation (osculating parameters).

Card #	Satellite Number	Class	International Designator			Yr	Epoch Day of Year (plus fraction)	Mean motion derivative (rev/day /2)	Mean motion second derivative (rev/day2 /6)	Bstar (/ER)	Eph	Elem num	Chk Sum
			Year	Lch#	Piece			S	S.	S. S E			
1	16609	U	86017A			93	352.53502934	.00000789	00000-0	10529-3	0	342	
			Inclination (deg)			Right Ascension of the Node (deg)		Eccentricity	Arg of Perigee (deg)	Mean Anomaly (deg)	Mean Motion (rev/day)		Epoch Rev	Chk
2	16609		51.6190			13.3340		.0005770	102.5680	257.5950	15.591140		70447	869

Figure 2.9 *Two Line Element* set format [12].

Simplified General Perturbations 4 propagator

The data provided by the TLE set is used for the propagation of the satellite state. Then, the propagator uses a certain model to perform such propagation. The most common models for propagation are the *Simplified perturbations models*, a set of mathematical models aimed at the propagation of near or far Earth-orbiting objects.

For the analysis carried out in this project, the mathematical model used is the *Simplified General Perturbations 4* model or *SGP4* [3]. This model was designed for near orbiting objects with an orbital period of less than 225 minutes, providing an error of ± 0.5 *km* at epoch which can grow up to 3 *km* per day.

This algorithm follows a procedure in order to get the velocity and position at each instant [6]:

1. Orbital elements acquisition from the TLE set.
2. Secular effects due to atmospheric drag and gravitational perturbations addition.
3. Long-period effects due to the gravitational perturbation addition.
4. Kepler's equation resolution.
5. Short-period effects due to the gravitational perturbation addition.
6. Position and velocity computation from the calculated orbital elements.

2.3 Objective Regions

The scheduling problem requires finding out an optimal (simple, affordable, ...) schedule for the observations of a previously defined set of objective regions on Earth's surface. These regions may have all kinds of morphologies and locations around the globe which have to be established for the algorithm. Therefore, the geometry of the objective regions is described by the points defining its frontier.

In this project, the objective regions are directly identified as the political territories of certain chosen countries, considering all their non connected regions. Specifically, the regions of Spain and Italy territories will be used. However, the territory which is the subject of observation can be simply defined by any polygon over Earth's surface by just specifying its vertices.

Region processing algorithm

The considered geometry of the political zones is imported from a file containing the coordinates of the border points. A *polyshape* object is built thanks to these points and then its non-connected regions are detected and separated in different elements of a *polyshape* array.

In order to handle with these objective regions in the subsequent algorithm, a modification process of the *polyshape* is carried out:

1. The regions whose area is less than a tolerance, $tolA$, are neglected and subtracted from the set of objective regions.
2. For each objective region, a reduction of its number of border points is made in order to simplify the future algorithms. To do so, a shrink factor, $Shrink \in [0,1]$, is considered as the parameter which govern the reduction of the points.

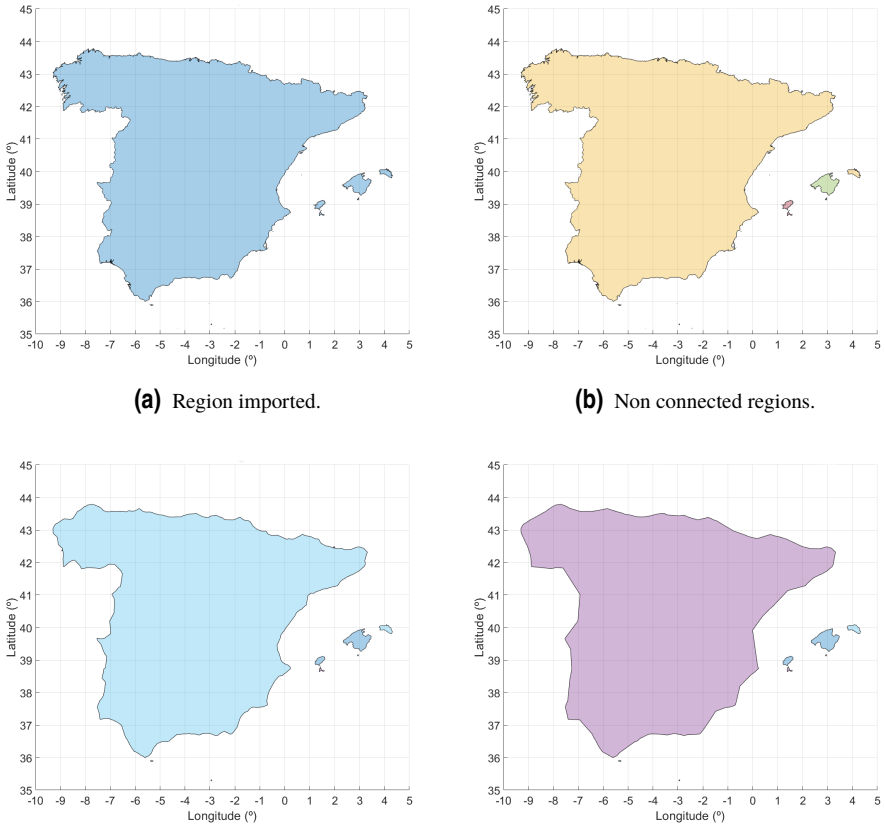

(a) Region imported.

(b) Non connected regions.

(c) Simplified regions (Shrink = 0.4).

(d) Simplified regions (Shrink = 0.1).

Figure 2.10 Region of interest modification.

In some cases where there are regions close to each other, an independent simplification produces overlapped regions. In order to solve this issue an inclusion routine has been added to the algorithm:

1. The regions are ordered from bigger to smaller area.
2. The independent simplification of a region is carried out.
3. If the result overlaps with the previous simplified regions, a group simplification is done with all the affected regions.
4. The next unsimplified region is considered.

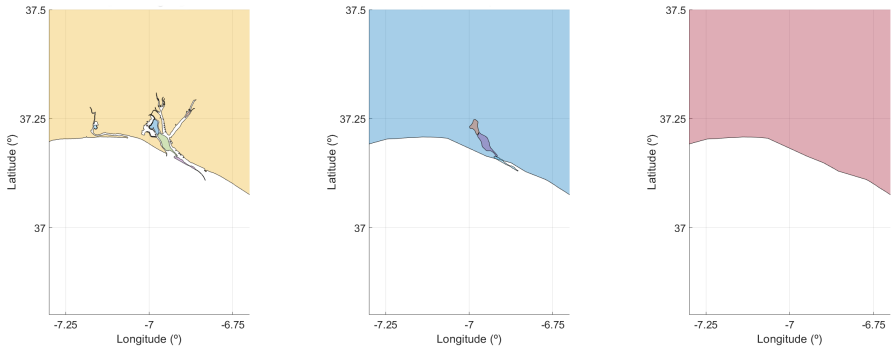

(a) Unsimplified neighbouring regions.

(b) Independently simplified regions.

(c) Inclusive simplification.

Figure 2.11 Region overlapping solution.

2.4 Satellites

Earth observation satellites (EOS) are the responsible for the remote sensing of Earth and there is an entire variety of these satellites depending on their sizes, orbits or gathering information techniques. Some meteorological satellites take advantage of the geostationary orbit (GEO) strengths, but most of the observation satellites are placed in low Earth orbits (LEO) in order to improve their captures quality among other benefits.

The LEO are located at a height of around 750 *Km* above the surface, which defines its orbital period of approximately 100 *min*. Consequently, each revolution to the orbit they make takes an Earth's rotation of about 25^o, shifting west-wards the satellite's ground-track the same amount as it passes through the equator.

In addition the orbits of the observation satellites with optical sensors receiving the Sun's light reflection from the surfaces are typically sun-synchronous (Subsec. 2.2.2), which allows to cover almost all the latitudes thanks of their inclination ($i \approx 97^o$). Furthermore, the images taken from different locations on different dates have the same light incidence over the Earth's surface, improving the results when comparing them.

The satellites are equipped with the necessary instrumentation in order not only to acquire, storage and transmit the data (sensors, memory, antennas...), but also to be capable of performing other functions, such as energy control or navigation. With regard to this project, the navigation and attitude instrumentation has special importance since it controls the aiming direction of the satellite choosing which surface region is observed. To do so, diverse attitude sensors (gyroscopes, MRU, ...) and actuators (RCS, Momentum wheels) are onboard depending on the size of the satellite.

Each slew manoeuvre takes some time to fully accomplish it which mainly depends on the capability of the instrumentation. This slew time can be estimated by establishing the maximum rotation speeds of the spacecraft on their attitude axis, and assuming all rotations are made simultaneously:

$$t_\omega = \Omega_\omega \Delta\omega, \tag{2.50}$$
$$t_\varphi = \Omega_\varphi \Delta\varphi, \tag{2.51}$$
$$t_\chi = \Omega_\chi \Delta\chi, \tag{2.52}$$
$$t^{slew} = \max\{t_\omega, t_\varphi, t_\chi\}; \tag{2.53}$$

denoting Ω_x the x-rotation velocities and the Δx the absolute change on the x-angle of attitude.

Planet Labs

In this project, the satellites of *Planet Labs* company are used to solve the problem. The number of their satellites with which the analysis will be developed is reduced for reasons of computing capabilities. In particular the constellations of the 12 *Flock 2P* satellites over the same orbital plane will be considered as well as the constellation of satellites *Flock 3P*, formed by 88 of them. Both constellations lie on the approximately same sun-synchronous orbital plane.

Table 2.1 *Planet Labs*' *Flock 2P* and *3P* constellations .

$$Date of Epoch \quad : \quad 22/08/2019 \quad 14:00:00.001$$

FLOCK 2P			***FLOCK 3P***		
i	=	$97.365 \pm 0.004\,^o$	i	=	$97.402 \pm 0.004\,^o$
Ω	=	$298.723 \pm 0.435\,^o$	Ω	=	$301.238 \pm 0.466\,^o$
e	=	0.001120 ± 0.000054	e	=	0.000622 ± 0.000087
ω	=	$149.15 \pm 5.23\,^o$	ω	=	$286.2 \pm 23.3\,^o$
n	=	$15.261 \pm 0.006\,\frac{rev}{day}$	n	=	$15.264 \pm 0.010\,\frac{rev}{day}$

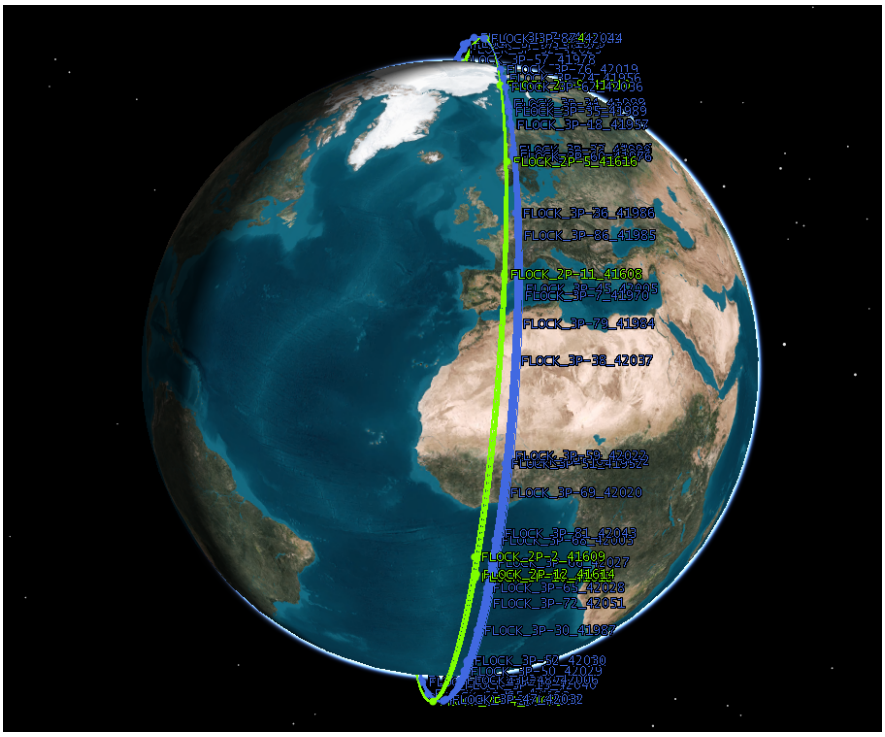

Figure 2.12 *Flock 2P* and *Flock 3P* constellations.

The observations of these satellites often require good visibility which may not be achieved due to meteorological conditions. This inclusion of meteorological considerations remains out of the scope of this project as mentioned in Subsec. 1.1. Nevertheless, the implemented procedure of satellite scheduling can distinguish the observations produced at day or night time in order to give the option to discard the unwanted ones. This is important for EOS equipped with optical sensors, due to the dependence of these sensors on the amount of reflected light from Earth's surface.

2.5 Ground stations

On a space mission a ground segment is needed to collect the data gathered by the spacecraft as well as to guide their operations. Ground stations have a crucial role on ground functions since represent the link between the spacecraft and the ground segment itself. The ground stations consist in terrestrial radio stations designed to establish telecommunications links with space probes and satellites, or even to receive radio waves form astronomical radio sources. In case of LEO Earth observation satellites, the ones this project concerns about, the transmission of data is possible by using radio waves typically from the super high frequency (SHF) bands (3.0 - 30.0 GHz).

The location of the ground stations are important factors which influence the performance of transmission schedules. They are strongly related to the satellite's orbit from which the transmission is sent. As an example, for geostationary satellites, the ground stations communicating with the them need to be located on the face of Earth visible from the the satellite involved, to ensure permanent communication with it.

Another important aspect to take into account about operating a ground station is the fact that they need some time to configure the transmission. This means, after a communication occurs, the ground station cannot immediately receive the next transmission from a satellite without a reset time. This reset time, t_{reset} , must be consider in the transmission scheduling problem.

Planet Labs

The company *Planet Labs Inc.* has built its own ground station infrastructures and rented some others, including 22 active dishes allocated in 8 spots spread around the globe. The company works in the X-band ($\sim$ 8.2 GHz) high speed downlink (HSD) radio to collect the data from their satellites [2].

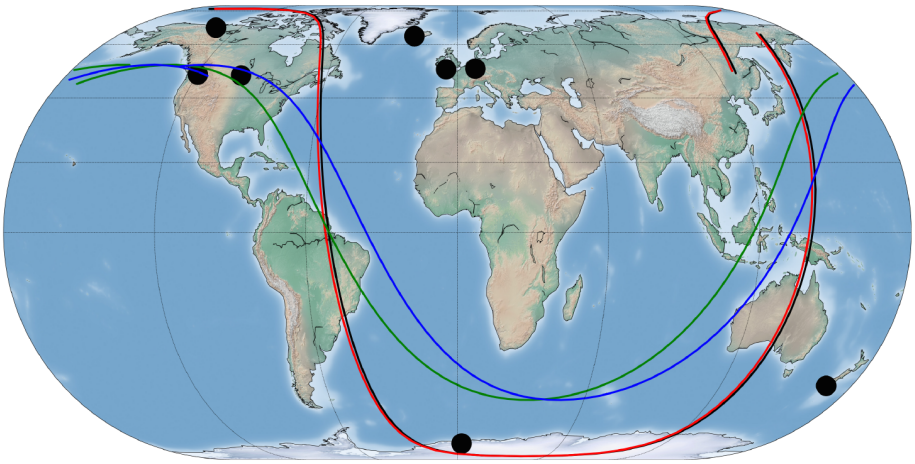

Figure 2.13 *PlanetLabs* ground stations spots and ground tracks of representative *Doves* satellites [2].

As it can be seen, the majority of the ground stations sites are located at extreme latitudes. This can be explained by the fact that almost all satellites *Planet Labs* orbits are close to polar, which makes the satellites fly over the poles on every orbit revolution. Consequently, a polar ground station allows a greater number of visibility windows than at other latitudes.

In this project some of the locations represented in Fig. 2.13 are selected as ground stations sites where transmission are received. Their geographical coordinates has been estimated and are shown bellow:

Table 2.2 *Planet Labs* ground stations (2017) .

no.	λ	ϕ
1	-130^{o}	65^{o}
2	-120^{o}	47^{o}
3	-100^{o}	47^{o}
4	-20^{o}	65^{o}
5	-5^{o}	50^{o}
6	0^{o}	-85^{o}
7	10^{o}	50^{o}
8	170^{o}	45^{o}

2.6 Observations

The Earth's observation satellites are equipped with different instrumentation in order to acquire information. Depending on the objective of these satellites, the sensor used will consist in particular systems dedicated to access to the needed information over Earth's surface. This sensor can be classified following different criteria, but the prevalent analysis concerns the source of the information acquired [8]:

- The **passive sensors** receive the information generated thanks to an external agent, the Sun for instance, which illuminates the objective. This group includes different radiometers and spectrometers which generally operate in the visible, infrared, thermal infrared and microwave bands of the electromagnetic spectrum.
- The **active sensors** use its own energy source to generate the information they receive by typically emitting radiation which illuminates the target and receiving back its reflection. In most of these sensors the radiation employed corresponds to the microwave band of the electromagnetic spectrum

Planet Labs

With regard to *Planet Labs*' satellites, the instrumentation used include a telescope and a frame CCD camera equipped with Bayer-mask filter which receive the sun's photons reflected on the Earth's surface

[10]. Therefore, these sensors belong to the passive remote sensing technique, working with the visible electromagnetic radiation of the spectrum.

The observation satellites receive the radiation from an Earth's field of view (FOV) guided by the aiming direction in which they are pointing depending on their attitude. The attitude angles (ω, φ, χ) might be adjusted to achieve certain spots over the surface. The observation region captured by the sensor shifts while the satellite follows its orbit, gathering data from a swath over the surface.

Due to the importance of the observation swath's geometry needed to carry out the project, a whole model with the objective of obtaining the lateral limits of this swath is presented below. This model defines the mentioned limits depending on the satellite's orbit, attitude and sensor's parameters, which are defined from *Planet Labs* existing satellites.

2.6.1 Swaths

The description of the visible region and swath will be pursued using the three-dimensional space and linear algebra, initially characterised using a normalised frame ($_{norm}$) and then rotating and translating in order to change between different frames of reference (Sec. 2.1). In order to achieve that, a mathematical description of the entities participating in the situation is made, followed by the computation of the limits themselves, and concluding by changing their characterisation to the proper frame of reference.

Entities

- **Earth:** Earth is modelled as a sphere centred on the origin whose radius is unity in terms of dimensionless distance.

$$\underline{P}_{sph} : \begin{cases} r = 1 \\ -\pi \leq \varphi < \pi \\ 0 \leq \rho < \pi \end{cases} \tag{2.54}$$

- **Satellite:** The satellite is located on the X-axis, at a certain nondimensional distance A from the origin ($A = R_{sat}/R_{earth}$).

$$\underline{P}_{sat} = \begin{pmatrix} A \\ 0 \\ 0 \end{pmatrix} \tag{2.55}$$

- **Aim Line:** The line which joins the satellite and the objective on Earth's surface is defined as the Aim Line and described by the point P_{sat} and a unit vector, $\vec{u}_{aim}$, which varies its direction depending on the off-nadir angle, Γ.

$$\vec{r}_{sat} = \underline{P}_{sat} + \lambda \vec{u}_{aim} \, ; \tag{2.56}$$

$$\vec{u}_{aim} = \begin{pmatrix} -\cos(\Gamma) \\ 0 \\ \sin(\Gamma) \end{pmatrix} . \tag{2.57}$$

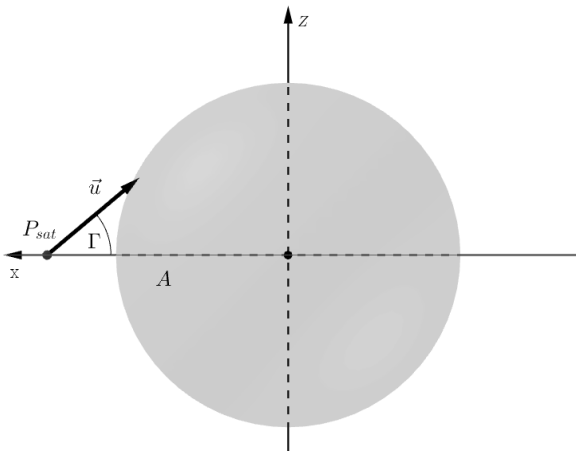

Figure 2.14 Simplified geometrical situation.

- **Cone of vision:** The vision of the satellite's sensor will be modelled as the points from the space inside a cone. This cone will be defined by its vertex, P_{sat}, its axis vector, $\vec{u}_{aim}$, and its aperture angle, FOV (Field of vision). In order to define in a better way the surface points of this cone, an auxiliary vector perpendicular to the axis, $\vec{w}$, will be used. The sum of these two vectors is equal to a third vector, $\vec{v} = \vec{u}_{aim} + \vec{w}$, which defines the generatrix lines of the cone's surface through it vertex, P_{sat}.

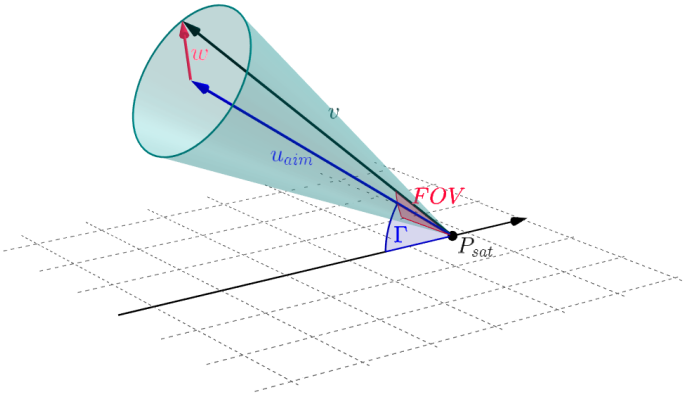

Figure 2.15 Cone of Vision.

The vector $\vec{w}$ depends on the parameter θ, defined as the angle between the vector and the plane $y = 0$. For each value of θ the points define a surface line of the cone which contains the vertex.

$$\vec{r}_{cone}(\theta) = \underline{P}_{sat} + \sigma[\vec{u}_{aim} + \vec{w}(\theta)]\,. \tag{2.58}$$

Hence, the vector is defined as follows,

$$\vec{u}_{aim} \cdot \vec{w} = 0\,, \tag{2.59}$$

$$|\vec{w}| = |\vec{u}_{aim}| \tan\left(\frac{FOV}{2}\right), \tag{2.60}$$

$$\vec{w} \cdot \vec{j} = |\vec{w}| \sin(\theta)\,. \tag{2.61}$$

Defining $\vec{u}_{aim}$ as a versor (unity vector),

$$|\vec{u}_{aim}| = 1\,,$$

therefore,

$$|\vec{w}| = \tan\left(\frac{FOV}{2}\right), \tag{2.62}$$

$$\vec{w} \cdot \vec{j} = \tan\left(\frac{FOV}{2}\right) \sin(\theta)\,; \tag{2.63}$$

finally, taking into account Eq. (2.57)

$$\vec{w} = \begin{pmatrix} -\tan\left(\frac{FOV}{2}\right) \sin(\Gamma)\cos(\theta) \\ \tan\left(\frac{FOV}{2}\right) \sin(\theta) \\ -\tan\left(\frac{FOV}{2}\right) \cos(\Gamma)\cos(\theta) \end{pmatrix}. \tag{2.64}$$

- **Scan sector:** In case the observation region is shifted creating a swath, the vision entity which describes the gathered area is simplified from the cone of vision to a scan sector. This sector sweeps the surface under the satellite while is moving acquiring the desired information. The scan sector is defined by

its vertex or center, which corresponds to the satellite's position (P_{sat}); its angle, equal to the angle of vision of the sensor (FOV); and the plane in which it lies, containing the aim line. The orientation of this plane will be set relying on the definition of vector $\vec{w}$ (2.64), which is established as perpendicular to the satellite's ground track at every time step. Once, known the velocity of the satellite on the simplified situation frame ($P_{sat} \in X$), it is useful to determine the versor which defines the trajectory parallel to Earth's surface, to wit, the satellite's ground track.

$$\vec{N} = \vec{V}_{sat} - \left(\vec{V}_{sat} \cdot \vec{i}\right)\vec{i}, \tag{2.65}$$

$$\vec{n} = \frac{\vec{N}}{|\vec{N}|}; \tag{2.66}$$

therefore, the expression for vector $\vec{n}$ is:

$$\vec{n} = \begin{pmatrix} 0 \\ n_y \\ n_z \end{pmatrix}; \tag{2.67}$$

The computation of the edges of the sector can be deduced from the algorithm of computation of the generatrix lines of the cone of vision (Eq. (2.58) to (2.64)). Nevertheless, as mentioned before, the vector $\vec{w}$ satisfies the equation:

$$\vec{w} \cdot \vec{n} = 0\,. \tag{2.68}$$

Taking into account the expression of $\vec{w}$ described on Eq. (2.64), the values of θ for the sector edges fulfill:

$$\tan(\theta) = \frac{n_z}{n_y}\cos(\Gamma); \tag{2.69}$$

which give a pair of values for θ:

$$\theta_1 = \arctan\left(\frac{n_z}{n_y}\cos(\Gamma)\right), \tag{2.70}$$

$$\theta_2 = \arctan\left(\frac{n_z}{n_y}\cos(\Gamma)\right) + 180^o\,. \tag{2.71}$$

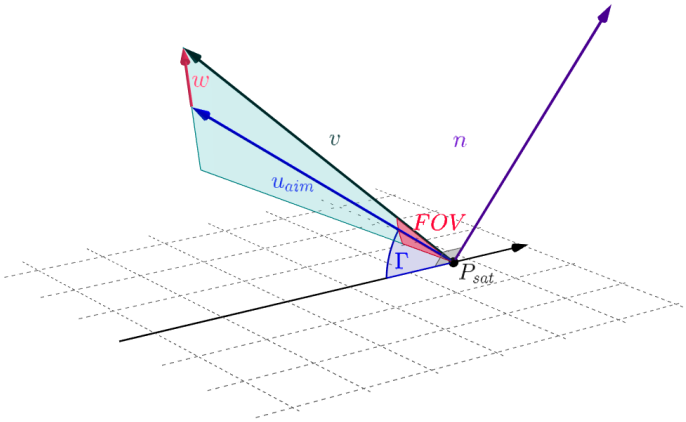

Figure 2.16 Scan Sector.

Instantaneous visible region

For the first situation, in which a single shot of Earth's surface is taken on a certain moment from the satellite's position, the computation of every point of intersection between the cone of vision, which models the visible space region for the satellite's sensor, and the sphere is needed to define the visible surface region at this instant. This intersection between the cone and the sphere is computed for each line as follows:

For a given $\overline{\theta}$,

$$\underline{P}^{\star} = \underline{P}_{sat} + \sigma^{\star}[\vec{u}_{aim} + \vec{w}(\overline{\theta})], \tag{2.72}$$

$$\sigma^{\star} : |\overline{OP}^{\star}| = 1. \tag{2.73}$$

Covering all the values for $\overline{\theta}$, $0 < \theta < 2\pi$, all the intersection points are calculated.

In case the cone intersects the sphere only partially, the rest of the points needed to close the visibility region are computed considering tangent lines to the sphere through the point $\underline{P}_{sat}$. The points selected are the points of tangency between these lines and the sphere which are inside the cone of vision, and represent the limit of visibility not because of the sensor's aperture (FOV), but due to Earth's curvature.

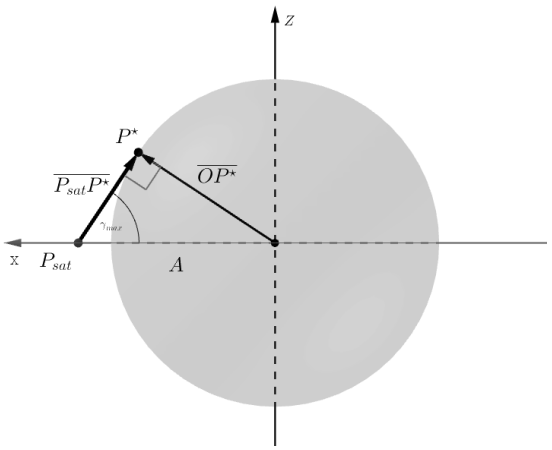

Figure 2.17 Limit of possible visibility.

These points fulfill the equations deducted from the tangency condition:

$$\overline{OP^{\star}} \perp \overline{P_{sat}P^{\star}}, \tag{2.74}$$

$$|\overline{OP}^{\star}| = 1, \tag{2.75}$$

which implies,

$$x^{\star} = \frac{1}{A}, \tag{2.76}$$

$$y^{\star 2} + z^{\star 2} = 1 - \frac{1}{A^2}. \tag{2.77}$$

In order to visualise the results, three examples are shown (Fig. 2.18a, and 2.18b). First two of them have the same position of the satellite ($A = 1.3$) and aperture ($FOV = 10^{o}$), however in the second (Fig. 2.18b) a bigger off-nadir angle ($\Gamma = 45.3^{o}$) is considered, obtaining a much more elongated shape of the visible region. On the third example (Fig. 2.18c), a greater off-nadir angle ($\Gamma = 50^{o}$) produces a partial intersection and the limits for the visible region are computed as discussed before.

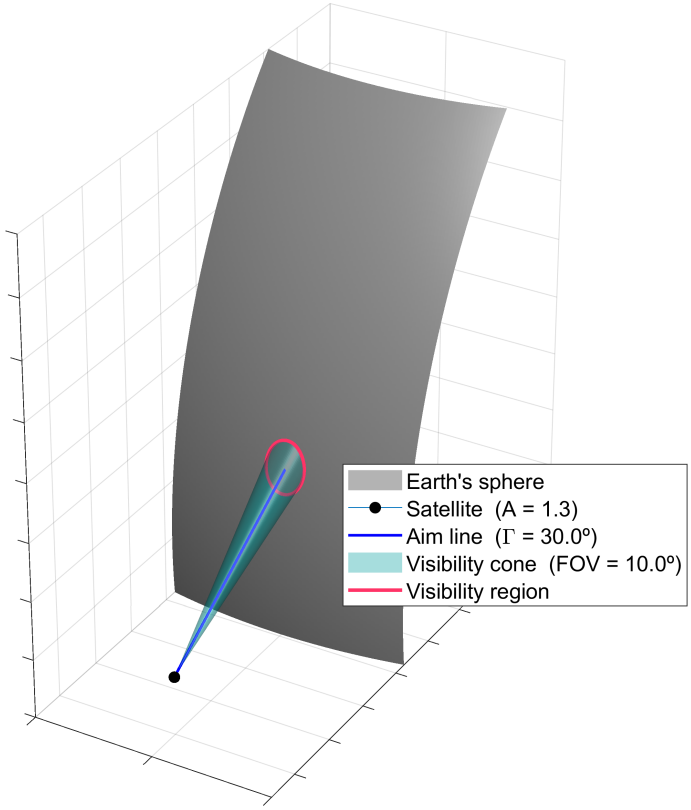

(a) Intersection Cone-Sphere, Example 1 .

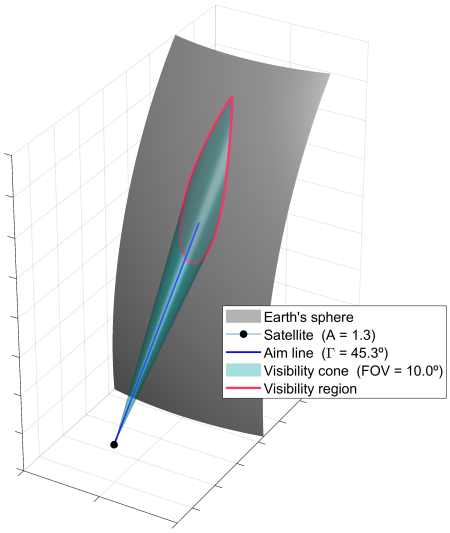

(b) Intersection Cone-Sphere, Example 2 .

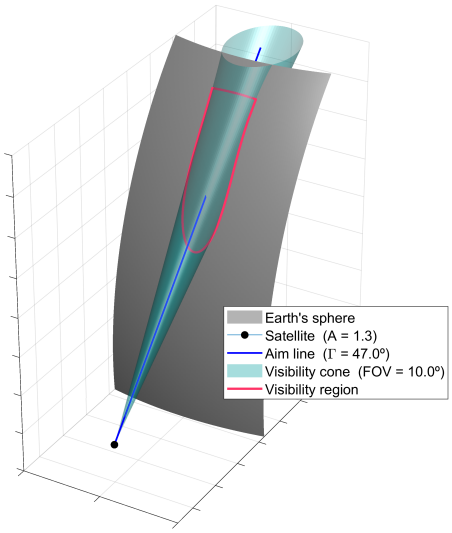

(c) Intersection Cone-Sphere, Example 3 .

Figure 2.18 Visibility regions.

Shifted visible region

In case the satellite carries out a "scanning" of Earth's surface while moving, the resolution is similar to the one already explained. However, instead of modelling the vision of the satellite as the region inside a cone of visibility, it is defined as the surface scanned by a sector whose vertex corresponds to the position of the satellite. The intersection between the edges of the scan sector and Earth's surface at each time step produces both limits of the swath of visibility while the satellite moves.

The rest of the algorithm used to compute the intersection points between these two lines and the sphere is identical to the one used previously to compute the intersection of the cone (Eq. (2.72) to (2.77)), with

the exception that now the angle θ only takes values of θ_1 and θ_2, generating the pair of points pursued $P_1^\star = P^\star(\theta_1)$ and $P_2^\star = P^\star(\theta_2)$.

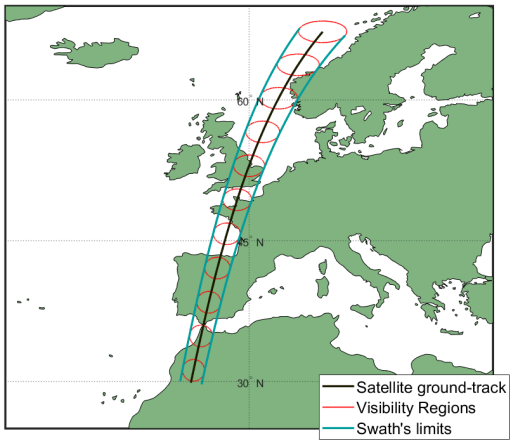

$FOV = 30^o, \Gamma = 0^o$

Figure 2.19 Visibility swath and regions .

As shown on Fig. 2.19, it can be deduced that the limits of the visibility swath are tangent on every point of a certain region of visibility produced by the visibility cone model. Nevertheless, due to the complexity of tangency computation on every single visibility region, a simpler model has been chosen and the definition used for the scan sector, although providing good results for combinations of small sensor aperture (FOV) and aiming angle (Γ), does not fulfill the tangency condition between regions and swath under certain extreme conditions.

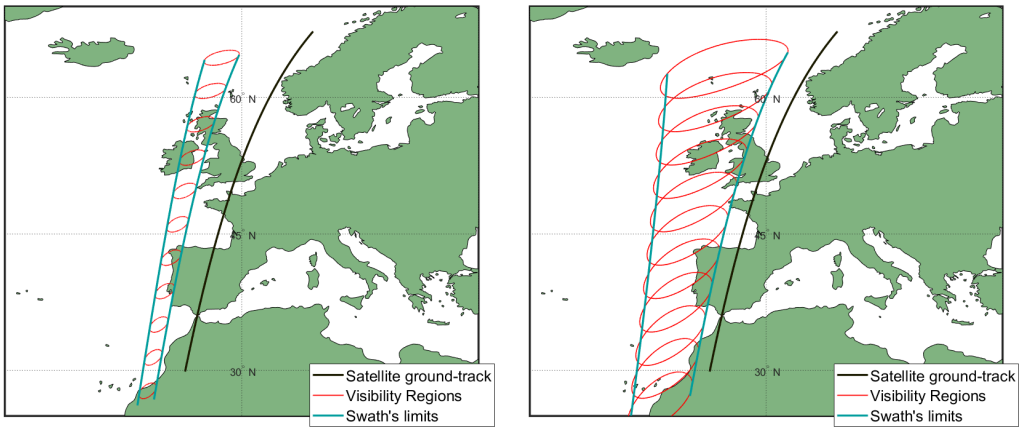

(a) $FOV = 10^o, \Gamma = 50^o$. **(b)** $FOV = 30^o, \Gamma = 50^o$.

Figure 2.20 Swath's limits tangency error.

It is important to mention that this algorithm is not prepared to compute the swath on situations where the cone of visibility intersects only partially Earth's sphere. These situations often involve large aperture angles of the sensor and/or angles of aim not small enough to generate a proper surface image, hence they are not the scope of this project.

Geographical frame description

Once the visibility limits are described in the normalised frame ($_{norm}$), the coordinates of their points are changed to the geographical frame ($_{gph}$) in order to locate the visibility regions with respect to other geographical data present on Earth's surface.

These changes of reference frames are guided by algebraic transformation which apply the translation vectors and rotation matrices already described on this document (Sec. 2.1).

Some results obtained for different latitudes are shown below. The orbital parameters for the EOS Satellite no.1 from the *Planet Labs*' constellation *Flock 2P* have been used,

$$\begin{aligned} Date of Epoch &: 22/08/2019 \quad 14:00:00.001 \\ B^{\star} &= 0.22087 \times 10^{-3} R_{\oplus}^{-1} \\ i &= 97.3677^{o} \\ \Omega &= 299.1570^{o} \\ e &= 0.0010827 \\ \omega &= 152.8799^{o} \\ M &= 308.5990^{o} \\ n &= 15.26243907 \, \frac{rev}{day} \end{aligned}$$

as well as a hypothetical value for the aperture of the sensor $FOV = 10^{o}$. In stead of a defined objective to observe on Earth's surface, different fixed values for roll and pitch angles have been used. All simulations correspond to time windows defined by their Universal Time on 24 August, 2019.

- **Western Europe 10:30:00 - 10:40:00**

  To begin with, the results for the mentioned observation satellite as it flies over western Europe are presented. As can be seen, at medium latitudes not so far from the equator, the swath's limits are practically parallel to the satellite's ground-track, whereas approaching the pole they start to be distorted.

Figure 2.21 Nadir aiming observation.

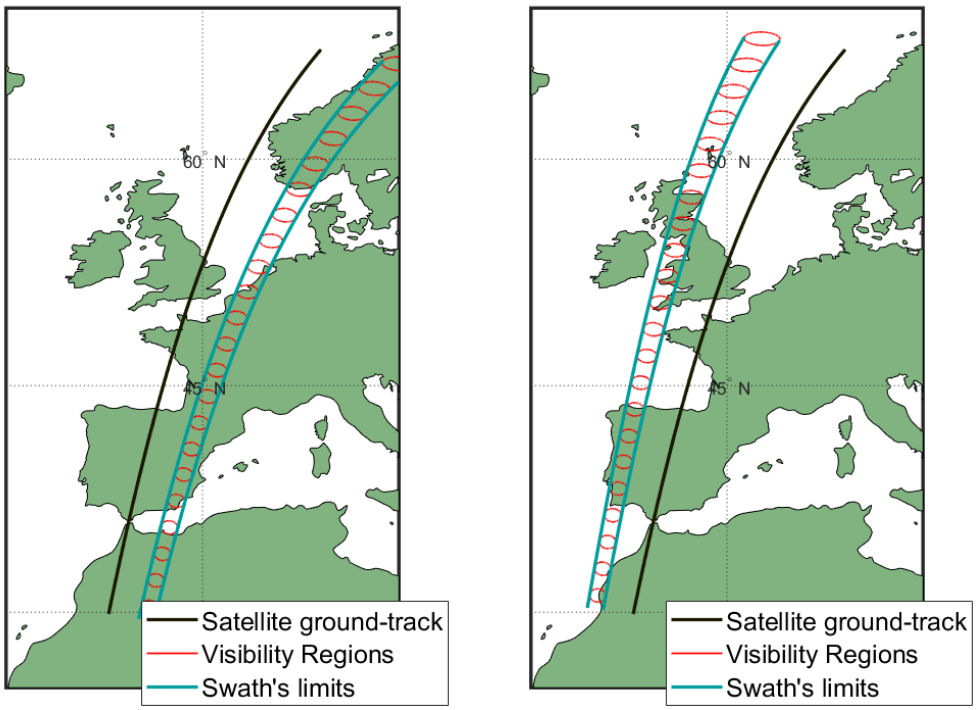

(a) $\omega = 30^o, \varphi = 0^o$. **(b)** $\omega = -30^o, \varphi = 0^o$.

Figure 2.22 Rolling observation.

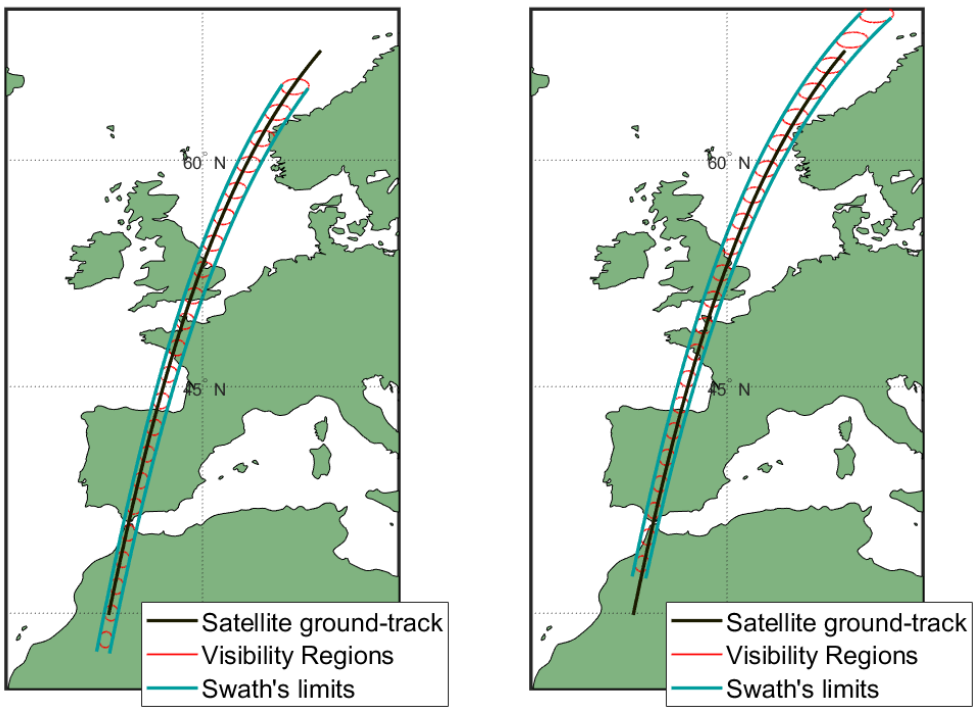

(a) $\omega = 0^o, \varphi = 30^o$. **(b)** $\omega = 0^o, \varphi = -30^o$.

Figure 2.23 Pitching observations.

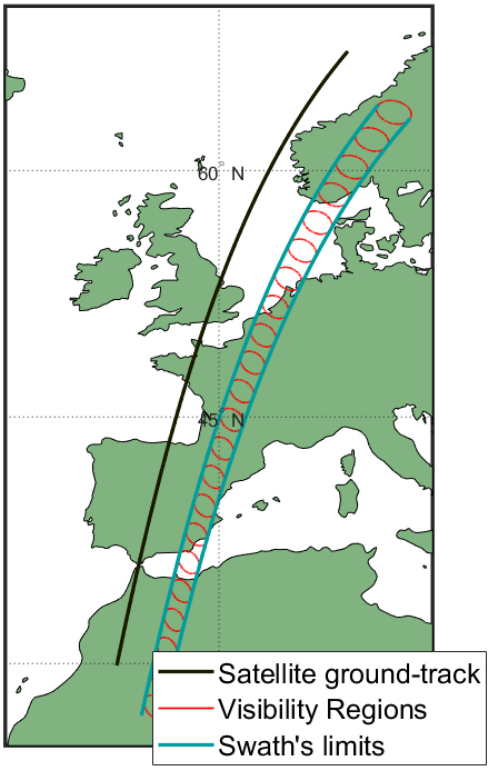

(a) $\omega = 30^o, \varphi = 30^o$.

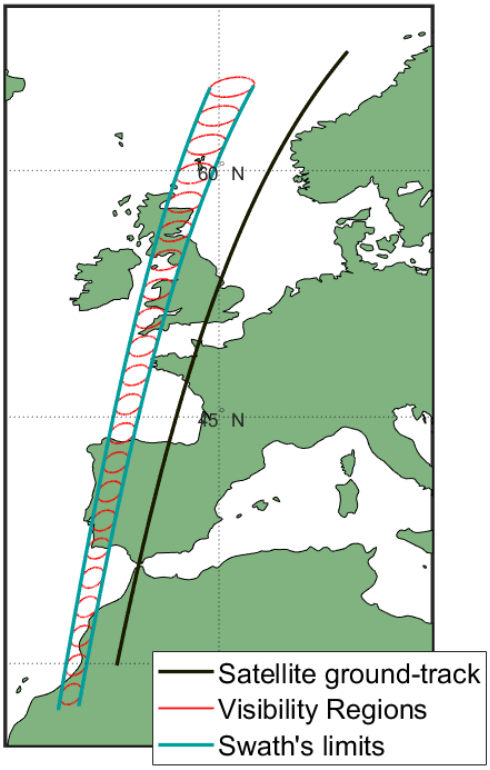

(b) $\omega = -30^o, \varphi = 30^o$.

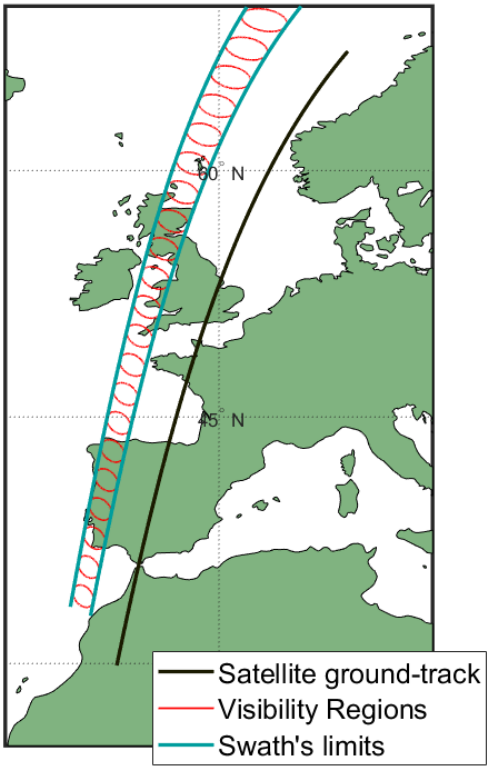

(c) $\omega = -30^o, \varphi = -30^o$.

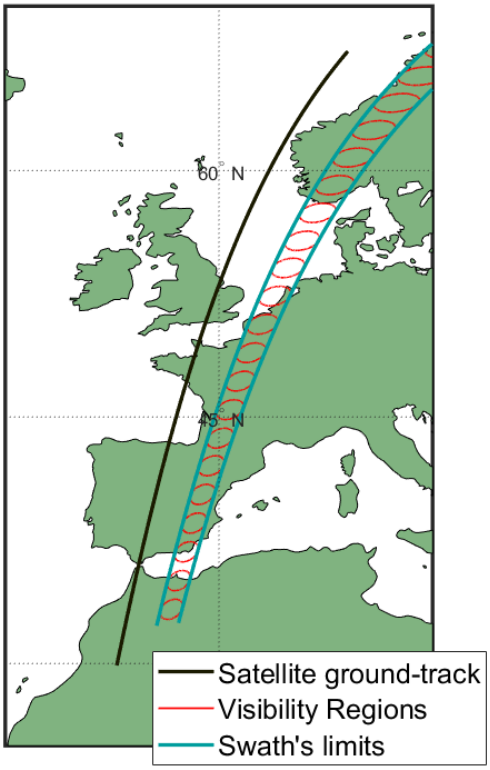

(d) $\omega = 30^o, \varphi = -30^o$.

Figure 2.24 Rolling and pitching observations.

- **North Pole 11:55:00 - 12:05:00**

  In order to study the behaviour of the algorithm around the poles, this extreme situation has been simulated.

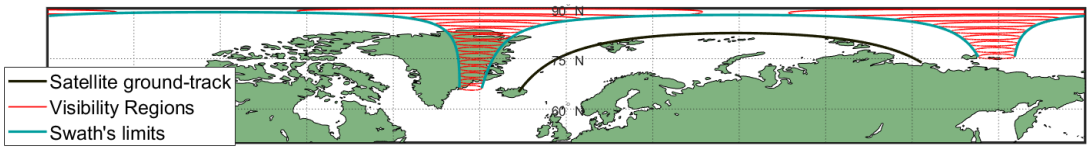

$\omega = -55^o, \varphi = 0^o$

Figure 2.25 Pole coverage.

As it is shown, the procedure taken to define the limits of the visible regions and swath has the capability to properly perform around the singularity of the poles

- **South Pole 11:05:00 - 11:10:00**

  An additional exposition of observation results is done for extreme latitudes, in this case, over the south pole by analysing different satellite rolling attitudes.

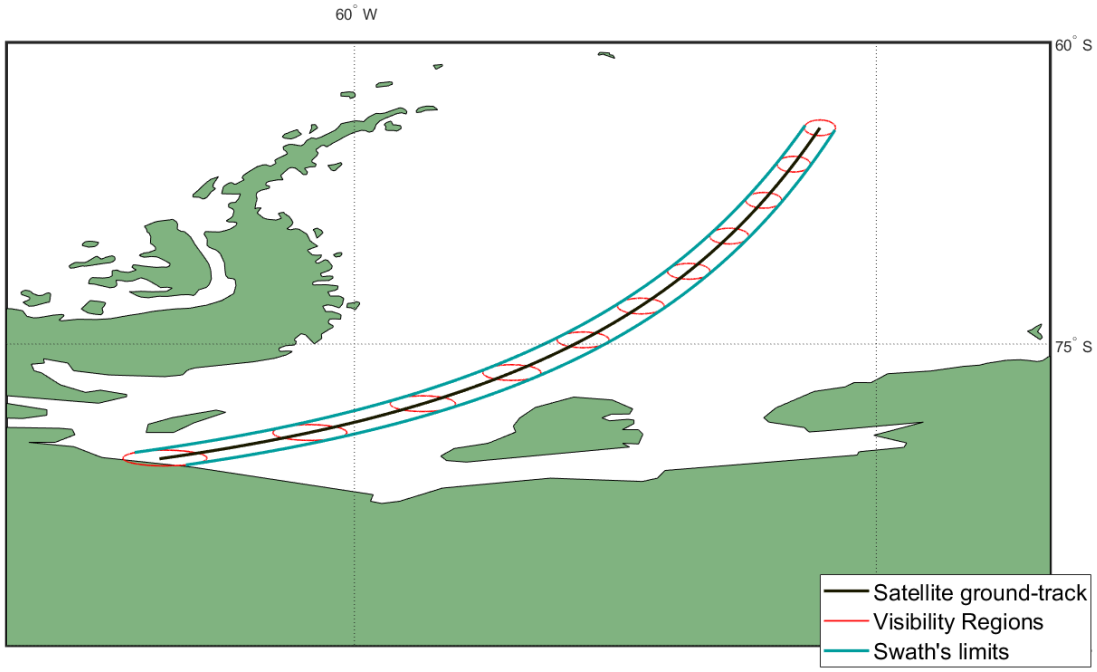

(a) $\omega = 0^o, \varphi = 0^o$.

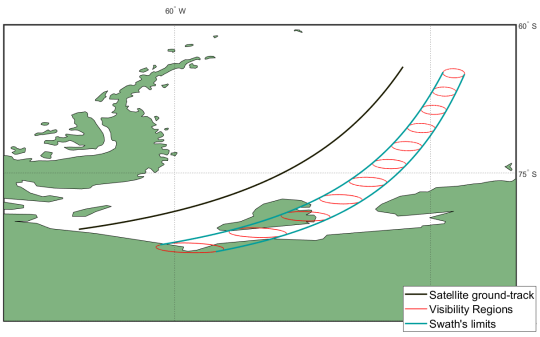

(b) $\omega = 30^o, \varphi = 0^o$.

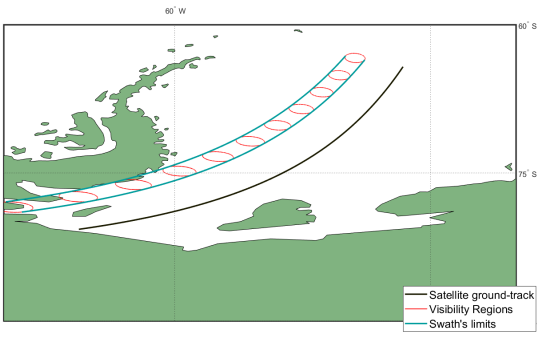

(c) $\omega = -30^o, \varphi = 0^o$.

Figure 2.26 South pole observations.

2.6.2 Modes

Concerning the attitude configuration for the analysis of the scheduling project under the scope of this project, once the observation window of an objective region from a satellite begins the attitude is fixed until it finishes the capture. After the observation concludes, the satellite is allowed to accomplish a slew manoeuvre in order to change its attitude.

Nevertheless, while the available attitudes configuration are not continuous, in order to address the problem by computational methods a discretisation is needed. Consequently, each attitude configuration involving specific values for roll, ω, and pitch, φ, angles is identified as a mode of observation of the satellite; while a finite number of modes are established to create the observation swaths of every satellite.

As a consequence of considering different modes of observation for the same satellite, the algorithm should consider the presence of observations which are nor compatible between each other. The aspect of incompatibility between windows will be discussed in following sections.

2.7 Satellite-Antenna transmissions

While there still is free space, the acquired observation by the satellites are stored in their RAM. These memories have a maximum storage capacity, which implies that the data must be transmitted to the ground stations, not only for making it accessible, but also for allowing the satellite to continue with its observations. Therefore, the transmissions consist on radio communication between a satellite and a ground station, both provided with the necessary instrumentation, such as the antennas. To establish the communications certain conditions must be fulfilled, mostly related with the visibility conditions. As the satellite orbits, a transmission with certain ground station is available while it flies over a zone where there is good visibility between both agents, i.e. when the satellite is within the ground station's line of sight. The requirement compliance might be affected not only by the relative position between the ground station, the satellite and the surface of Earth, but also due to other factors such as meteorological phenomena.

Elevation for transmission

Although the meteorological phenomena remains out of the scope of this project, the atmospheric interference is taken into account. Therefore, a transmission will be available granted that the elevation, γ, of the satellite from the ground station location exceeds a minimum value, so that the microwaves travel along a shorter path inside the atmosphere.

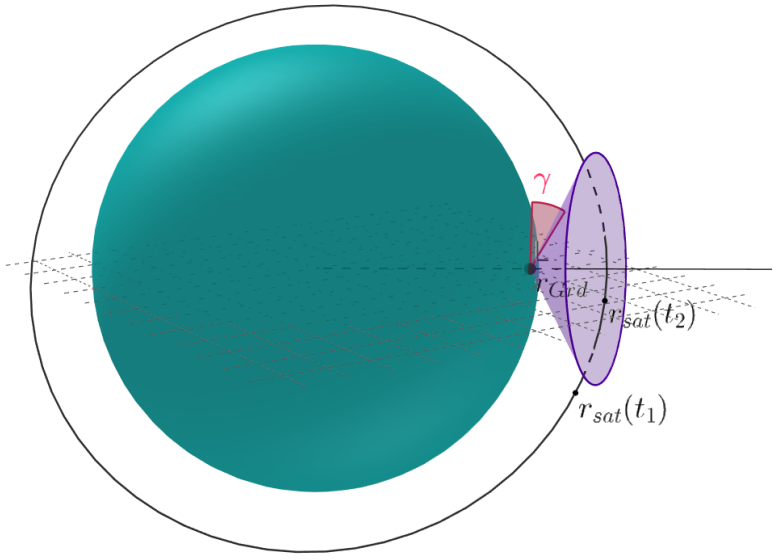

Figure 2.27 Minimum elevation for transmission.

The minimum elevation constraint generates a cone which defines the points at which the transmission is possible. Hence, for an arbitrary scenario of ground station location and orbiting satellite (Fig. 2.27), at the t_1 instant the transmission is not available, while at t_2 it is.

Antenna Pointing

As a consequence of the antennas gain, in both satellite and ground station, they must be directed towards each other for a proper communication. In the model adopted for this analysis, the operation to keep the alignment between the two entities is assumed. The antenna at the ground station will be directed towards the satellite, while the satellite will change its attitude to point the ground station with its antenna, whose directivity matches the sensor aiming direction.

Notwithstanding the assumption of alignment preservation, the attitude of the satellite at the starting and finishing instant of the transmission must be consider. The attitude of the satellite at these instants is fixed in order to proceed with the transmission and slew operations may be involved in order to change a pre-existing attitude. This slew manoeuvres require a slew time which might not be small enough to establish the compatibility of the transmission with the previous satellite's operation.

Transmission speed

An important parameter in the telecommunications between satellite and ground station is the downlink or transmission speed. *Planet Labs Inc.* uses its X-band high speed downlink (HSD) which allows transmission which reach speeds of 220 Mbps using 16APSK modulation [2].

However, for the purpose of this project, the transmission speed is characterised by directly comparing it to the observation speed. The transmission-observation speed ratio, δ^{trs}, is defined as ratio between the time spent collecting data while an observation occurs and the time needed to transmit the same amount of data.

$$\delta^{trs} = \frac{DR_{trs}}{DR_{obs}}; \tag{2.78}$$

defining DR_{trs} and DR_{obs} as the transmission data-rate and the observation analogous data-rate respectively.

3 Computational geometry modelling

On this chapter the previous instances needed as inputs for the resolution of the observation-transmission scheduling problem will be described. In order to get this instances, a mathematical model for each element participating in the situation will be carried out.

3.1 Geometry

The geometrical shapes involved have been modelled with the *Computational Geometry Toolbox* from *MATLAB*, more precisely thanks to the *Elementary Polygons* functions [4]. This tool allows to define polygons in terms of their ordered two-components vertices as *polyshape* objects.

As an example for the boundary vertices defined in cartesian coordinates:

$$A = (0,0)$$
$$B = (1,0)$$
$$C = (1,1)$$
$$D = (0,1)$$

the tool is able to build the *polyshape*:

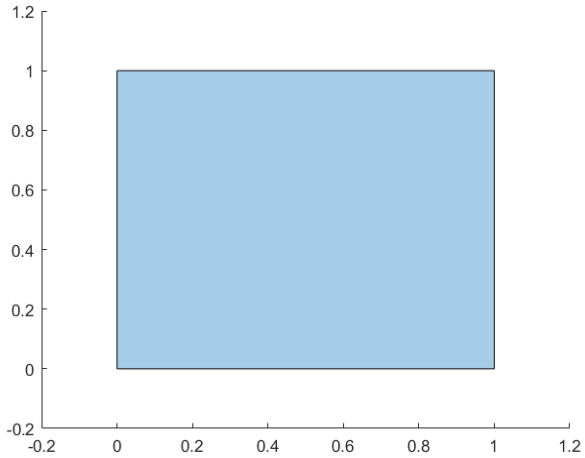

Figure 3.1 Example 1 of *polyshape* object.

The mechanism for building the *polyshape* uses the established boundaries, each of one defined by the two-coordinates points and separated by *NaN* components. In addition, the algorithm is able to detect the

number of holes and non-connected regions for a defined *polyshape*. Hence, as an example, we can add the next boundaries to the previous example:

$$E = (0.2,0.2) \qquad I = (1.2,0.8)$$
$$F = (0.6,0.2) \qquad J = (1.4,0.8)$$
$$G = (0.6,0.6) \qquad K = (1.4,1)$$
$$H = (0.2,0.6) \qquad L = (1.2,1)$$

So the new *polyshape* has two disconnected regions and a hole:

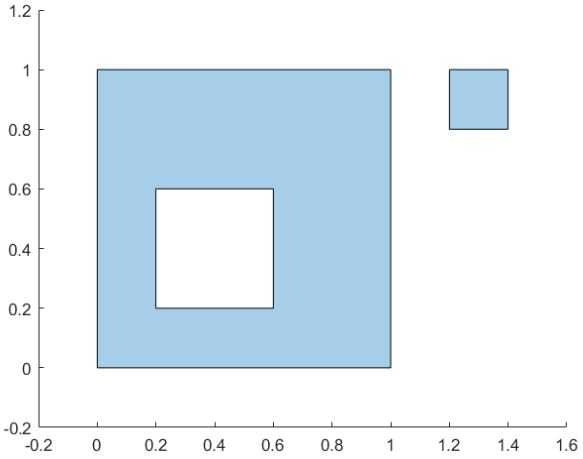

Figure 3.2 Example 2 of *polyshape* object.

The *Computational Geometry Toolbox* is a powerful tool which offers different features for the *polyshape* objects. Some of them are used in this project to compute needed data for the resolution and are briefly described below.

Modification

- **Hole removal:** Given a *polyshape* object, the toolbox allows to generate he same *polyshape* without holes.

- **Boundary outlier removal:** Given a *polyshape* object and a certain tolerance tol, the toolbox allows to generate he same *polyshape* removing the outliers whose ratio $\frac{a}{b}$ is bigger than the tolerance tol, as it is shown:

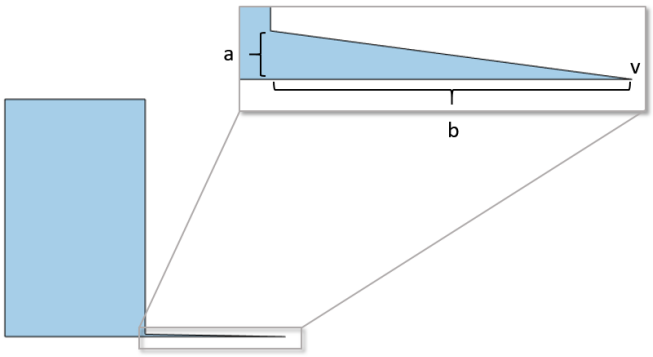

Figure 3.3 *Polyshape* with outlier.

Query and visualize

- **Overlapping detection:** Given two or more *polyshape* objects it can be determined if these overlap or not among each other.
- **Regions division:** Given a single *polyshape* object, it can be divided into different *polyshapes* saved in a *polyshape* array with same number of elements as number of disconnected regions the single *polyshape* has.

Geometric quantities

- **Area determination:** It computes the area enclosed by the *polyshape*.

Boolean operations

In the case of the boolean operations, the next situation of two polyshapes will be taken into account for the examples:

- **Intersection:** Given two or more *polyshapes*, the intersection between all of them can be computed.
- **Subtraction:** Given two *polyshapes*, the subtraction of one from the other can be computed.
- **Union:** Given two or more *polyshapes*, the union of all of them can be carried out.

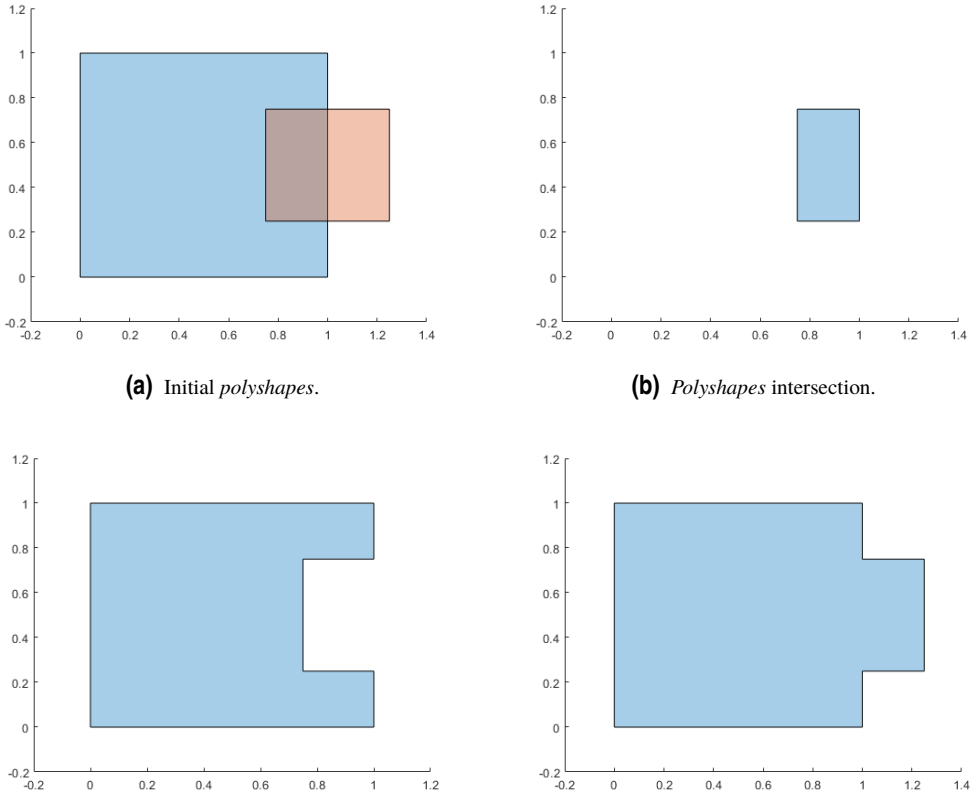

(a) Initial *polyshapes*.

(b) *Polyshapes* intersection.

(c) *Polyshapes* subtraction.

(d) *Polyshapes* union.

Figure 3.4 Boolean operations.

3.2 Observation windows

Swath *polyshapes*

After defining the swath's limits for each considered satellite (Subsec. 2.6.1) the swath *polyshapes* is build by properly rearranging the computed points. The large swath obtained is split into other swaths whose longitudes are contained into the common longitudes interval $[-180^{o},180^{o}]$.

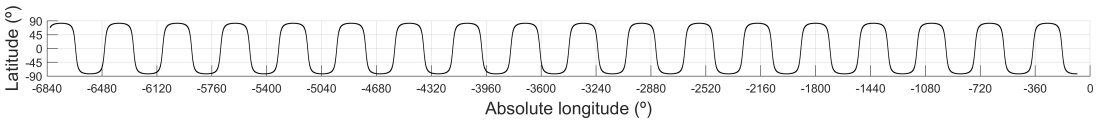

(a) Continuous swath.

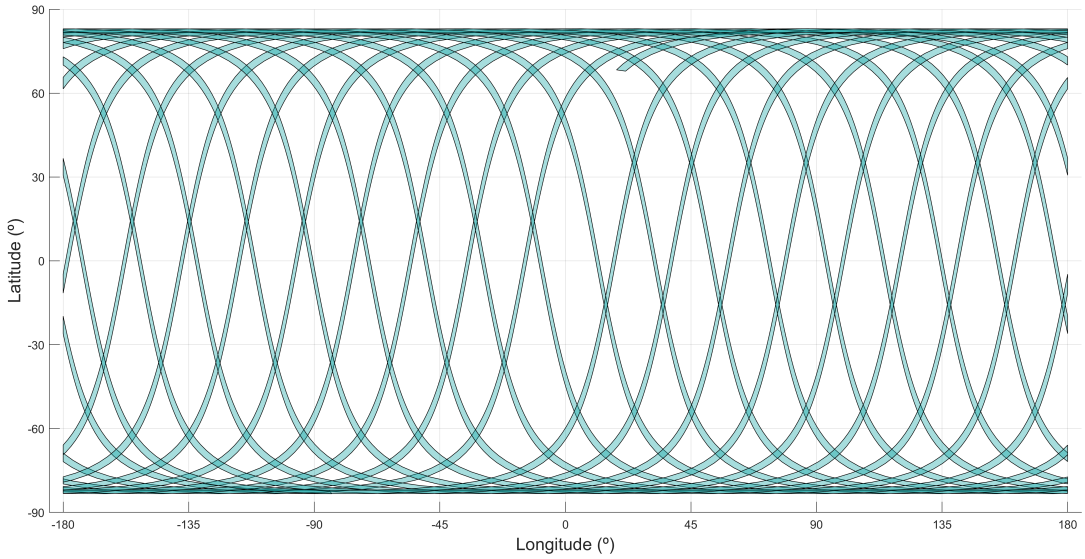

(b) Split swath.

Figure 3.5 Swath *polyshapes* for a certain satellite.

Observation edges

The observation windows are defined as portions of swaths whose start and end are defined in order to cover a specific objective region. Consequently, apart from the relation with the satellite, its attitude and the number of revolutions from epoch; each observation window is related to two specific times of start and end delimiting its edges. In order to define both edges, for each combination of swath and objective region an algorithm is used to get the start and finish times and limits:

1. The intersection points between the swath and the objective region also belonging to the last of the mentioned regions are identified. In case there is no intersection there is not available observation window of the objective region using the considered swath.

2. The elements of the swath's limit points vector are run on a ordered loop depending on the limit which we are defining:

   - **Start limit:** the points are considered in time-increasing order.
   - **Finish limit:** opposite to the starting point, the points are considered in time-decreasing order.

   The distances between the considered swath's limit point and each intersection points identified in **1.** are computed and stored.

3. Once one of the distances computed increases with respect to the previous stored value, the start/finish limit of the observation window has been crossed. Therefore, the swath's limit point considered before the minimum distance point defines the start/finish limit for the observation window and the correspondent time is stored as the start/finish time, t^s/t^f, for the observation window.

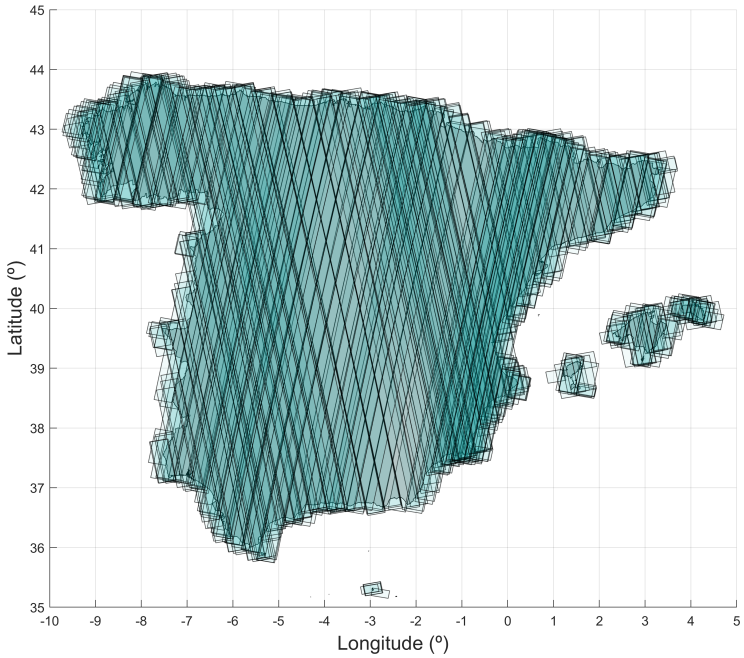

Figure 3.6 Observation windows for Iberian and Balearic Spanish regions, created by *Flock 3P* constellation.

Observations post-processing

As additional information about the observation windows, a characterisation of each one is made by classifying them in two groups depending on the direction with which they occur:

- **Northward observation**: the latitude at the finish of the observation window is greater than the latitude at its start.
$$\phi^f - \phi^s > 0$$

- **Southward observation**: the latitude at the finish of the observation window is less than the latitude at its start.
$$\phi^f - \phi^s < 0$$

This classification helps to identify which observations occurs while day or night times. Since the orbits considered are sun-synchronous, the satellites will keep ascending or descending when flying over the same sun-exposed face of Earth.

It is important to mention that the algorithm which computes the observation windows divides the discontinuous observation windows caused by the geometry of the objective region into different independent observation windows which are continuous, that is to say, observation window *polyshapes* formed by only one region.

Furthermore, once the computation of each observation has been carried out, as a cause of distinguishing between objective regions even though they may be located close to each other, observation windows related to the same satellite whose start and finish are not enough separated in time (or even overlap) might be present. This would lead to the waste of one of them in case the other is acquired due to the incompatibility between them. In favour of addressing this issue, an algorithm (algo. 1) has been developed with which this

observation windows are merged into just one.

$OW^{new} \leftarrow \emptyset$;
$OW' \leftarrow OW^{old}$;
while $OW' \neq \emptyset$ **do**
  $j' \leftarrow j \in OW'$;
  $OW'' \leftarrow OW' - j'$;
  $OW^{new} \leftarrow OW^{new} \cup j'$;
  while $OW'' \neq \emptyset$ **do**
    $j'' \leftarrow j \in OW''$;
    $t_{tot} \leftarrow \max\{t^f_{j'}, t^f_{j''}\} - \min\{t^s_{j'}, t^s_{j''}\}$;
    $t_{use} \leftarrow (t^f_{j'} - t^s_{j'}) + (t^f_{j''} - t^s_{j''})$;
    if $t_{tot} - t_{use} \geq t_{min}$ **then**
      $OW'' \leftarrow OW'' - j''$;
    else
      $j^\star \leftarrow j' \cup j''$;
      $t^s_{j^\star} \leftarrow \min\{t^s_{j'}, t^s_{j''}\}$;
      $t^f_{j^\star} \leftarrow \max\{t^s_{j'}, t^s_{j''}\}$;
      $OW'' \leftarrow \emptyset$;
      $OW^{new} \leftarrow OW^{new} - j'$;
      $OW^{new} \leftarrow OW^{new} \cup j^\star$;
    end
  end
  $OW' \leftarrow OW' - j'$
end

Algorithm 1: Observation windows joining algorithm

3.3 Transmission windows

As the observation windows, the transmission ones are as well defined by their start an finish points, governed by the only considered restriction of satellite minimum elevation (Sec. 2.7). In order to identify each one of the edges and define the satellite's attitude for each window, the next procedure has been followed:

1. For each satellite, its positions during time are analysed and checked whether the elevation relative to the any of ground stations fulfills the restriction established or not.
2. Once the transmission availability with each ground station is characterised for every point of the satellite's orbit, the first and last points where the transmission is available for each interval are established as the window's start and finish points.
3. For the start and finish instants of each window the relative positions of the ground station and satellite are used to calculate its pointing attitudes.
4. Each transmission window is described by the satellite and ground station involved and the start and finish times, t^s and t^f, while the start and finish attitudes will be employed to determine the slew times to accomplish the transmission.

Idle time

The transmission window is defined in terms of transmission availability regarding the relative positions between receiver and transmitter. Nonetheless, as a result of the transmission data-rate and the data hypothetically stored in the satellite's memory, all data might be transmitted before the transmission window closes. In this case, the time between the end of the data transmission, $\bar{t}$, and the finish of transmission window, t^f, is defined as the idle time of the transmission, t^{idle}.

$$t^{idle} = t^f - \bar{t}; \quad t^s \leq \bar{t} \leq t^f.$$

During this intervals of time, the transmissions are still available but no needed. In order to implement the *foresee-download* policy in the scheduling algorithm [14], the idle periods of time must be take into account to state which transmission windows are not completely exploited.

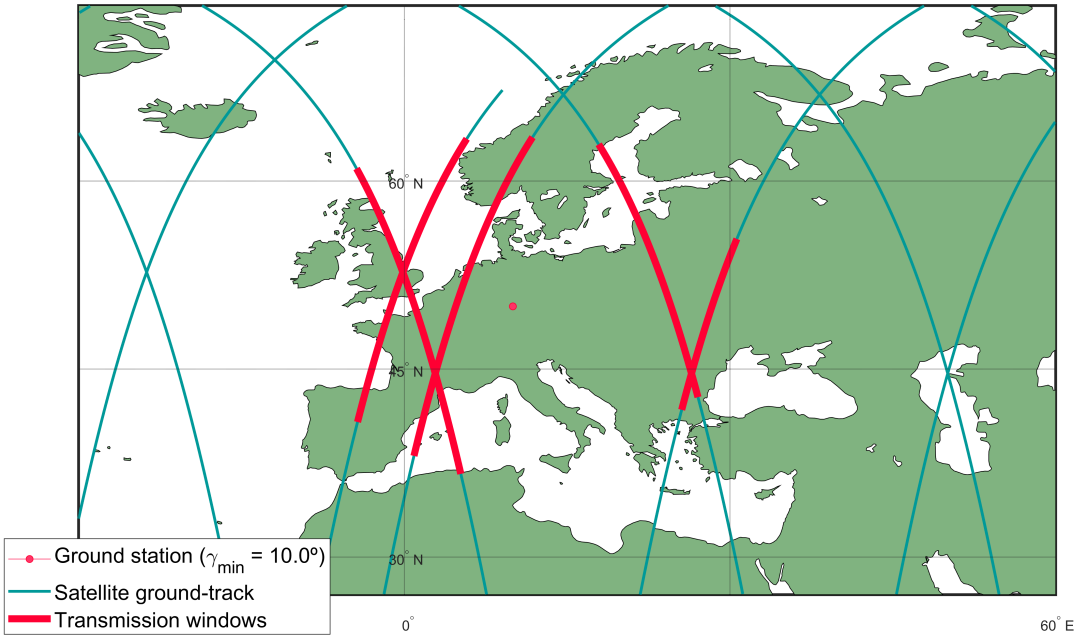

Figure 3.7 Transmission windows between a satellite and a ground station given the minimum elevation, γ_{min}.

3.4 Windows incompatibility

The established windows, observation or transmission ones, are defined for any available occasion between satellites and observation regions or ground stations. Nevertheless, not every combination of selected windows for the scheduling solution is feasible. As an example a satellite cannot acquire two different observations happening simultaneously. The incompatibility of the windows is strongly related with the time management on every source, ground station or satellite. Not only one observation or transmission operation is allowed at each instant, but also the auxiliary operations must be considered, such as the satellite slew operations or the ground stations resetting. Hence the incompatibility must be identified for every combination of windows.

Observations incompatibility

For two observations, $\{1,2\}$, performed by the same satellite a time is required for the slew operation, $t_{1,2}^{slew}$ (2.53). Therefore the compatibility of both observation windows is defined by the following inequation:

$$\max\{t_1^f, t_2^f\} - \min\{t_1^s, t_2^s\} \geq (t_1^f - t_1^s) + (t_2^f - t_2^s) + t_{1,2}^{slew}. \tag{3.1}$$

Transmission incompatibility

In case of two transmissions, $\{1,2\}$, received by the same ground station, the resetting time of the ground station must be obeyed (Sec. 2.5), t_{reset}. The compatibility condition between both transmission windows is established as:

$$\max\{t_1^f, t_2^f\} - \min\{t_1^s, t_2^s\} \geq (t_1^f - t_1^s) + (t_2^f - t_2^s) + t_{reset}. \tag{3.2}$$

Mixed incompatibility

Not only the slew operations are needed in order to accomplish two different observations with different attitudes; when a transmission is started or finished the attitude of the satellite is such that its antenna points the ground station involved. Hence a slew manoeuvre will be carried out between observations and transmission windows. Three situations may be presented:

- **Observation before transmission** ($t^f_{obs} \leq t^s_{trs}$): In this case the attitudes considered for the slew operation are the attitude for the observation, $\{1\}$, and the attitude at the transmission start, $\{2^s\}$. The compatibility restriction is described as follows:

$$\max\{t^f_1, t^f_2\} - \min\{t^s_1, t^s_2\} \geq (t^f_1 - t^s_1) + (t^f_2 - t^s_2) + t^{slew}_{1,2^s}. \tag{3.3}$$

- **Transmission before observation** ($t^f_{trs} \leq t^s_{obs}$): For this situation the attitudes considered to establish the slew operation are the attitude at the transmission finish, $\{1^f\}$, and the attitude for the observation, $\{2\}$. The compatibility restriction is described as follows:

$$\max\{t^f_1, t^f_2\} - \min\{t^s_1, t^s_2\} \geq (t^f_1 - t^s_1) + (t^f_2 - t^s_2) + t^{slew}_{1^f,2}. \tag{3.4}$$

- **Simultaneous observation and transmission**: Under this situation the windows are inherently incompatible. The simultaneity of both windows is described by the expression

$$\max\{t^f_1, t^f_2\} - \min\{t^s_1, t^s_2\} \leq (t^f_1 - t^s_1) + (t^f_2 - t^s_2) \tag{3.5}$$

3.5 Subregions

Considering one observation window related to an objective region (Fig. 3.8), this is divided into sub-parts which can be classified into two groups:

- **Covered zones**: The zones born from the intersection between the objective region and the observation are covered by the observation itself.
- **Uncovered zones**: The zones defined by the subtraction of the observation from the objective region are not covered by the considered observation.

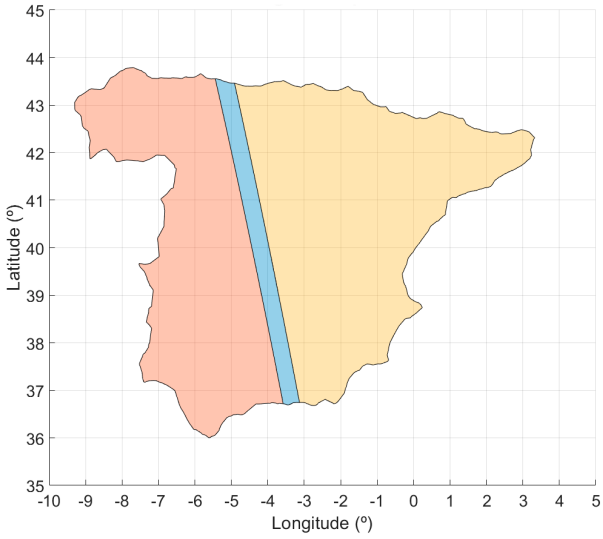

Figure 3.8 Objective region divided by observation .

Based on the previous idea, examining the interactions between all the objective regions and the entire number of observation windows generated, the objective region is divided into a series of distinct zones. This regions will be named subregions (*SR*), and each one of them will be covered by certain satellites with certain modes after certain number of orbit revolutions. The objective of the optimization algorithm is to determine which subregion is covered by which observation window in order to fulfill some specific constraints and optimize a certain feature of this coverage.

Subregions algorithm

In order to define the geometry of the subregion a recursive algorithm has been used in which, starting from the original objective region, one at a time, every observation window is considered, and the new subregions generated are included to the previous subregion set.

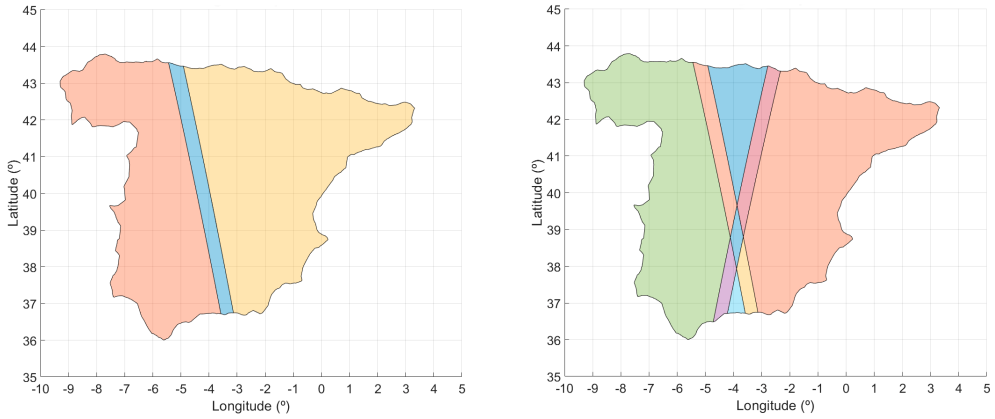

(a) First considered observation window.

(b) Second considered observation window.

Figure 3.9 Subregions computation algorithm.

As seen in Fig. 3.9, the algorithm takes the existing subregions set at the previous step and define the new one by carrying out boolean operations between the new observation window and the subregions. This algorithm is better explained in algo. 2. Meanwhile the algorithm build the new subregions, these ones are characterized with information about the objective region to which they belong as well as the satellites an attitudes used for covering them. In addition the coverage matrix, Q_{ij}, defined later in this document, containing information about the coverage relation between subregions and observation windows is set up.

$SR^{new} \leftarrow \emptyset$;
while $SR^{old} \neq \emptyset$ **do**
  $i^\star \leftarrow i \in SR^{old}$;
  $Q_{ij}^{new} \leftarrow Q_{ij}^{old} \quad \forall i \neq i^\star, j$;
  $Inters \leftarrow i^\star \cap j^\star$;
  while $Inters \neq \emptyset$ **do**
    $i' \leftarrow i \in Inters$;
    $SR^{new} \leftarrow SR^{new} \cup i'$;
    $Q_{i'j}^{new} \leftarrow Q_{i^\star j}^{old} \quad \forall j$;
    $Q_{i'j^\star}^{new} \leftarrow 1$;
    $Inters \leftarrow Inters - i'$;
  end
  $Subtr \leftarrow i^\star - j^\star$;
  while $Subtr \neq \emptyset$ **do**
    $i' \leftarrow i \in Subtr$;
    $SR^{new} \leftarrow SR^{new} \cup i'$;
    $Q_{i'j}^{new} \leftarrow Q_{i^\star j}^{old} \quad \forall j$;
    $Q_{i'j^\star}^{new} \leftarrow 0$;
    $Subtr \leftarrow Subtr - i'$;
  end
end

Algorithm 2: Subregion set, SR, and coverage matrix, Q, update given a new considered observation window, $j^\star$.

Since the boolean operation must be executed between the new observation window and the whole number of pre-existing subregions, the complexity of this algorithm increases exponentially with the number of

observation windows already considered. This might raise the computation time for large objective regions in which a great number of observation windows are involved.

With the objective of avoiding this problem, a *divide-compute-assemble* process is implemented for each objective region:

1. Maximum values for latitude height, $\Delta\phi_{max}$, and longitude width, $\Delta\lambda_{max}$, are set depending on the orientation of the observation windows. The objective region is checked to fit into the geographical rectangle established by these values and, in case not, it is divided into parts which fulfill the maximum width and height guidelines.
2. The algorithm described (Fig. 2) is executed for each one of the parts in which the objective region has been divided.

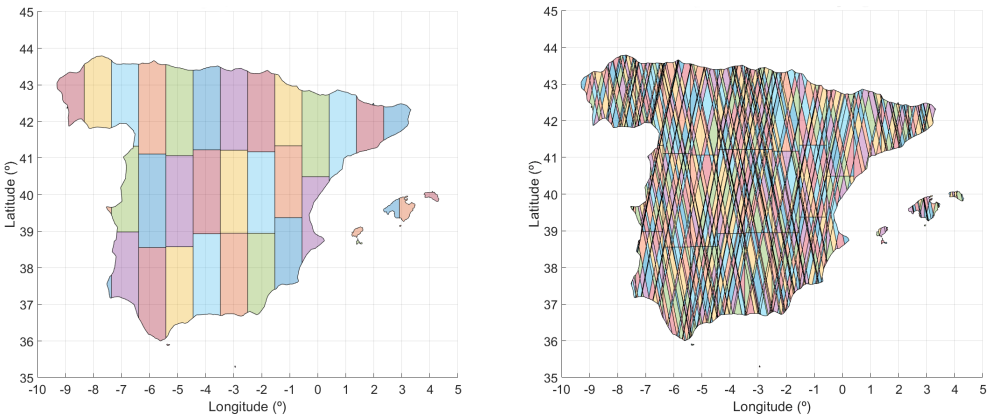

(a) Division of the regions into smaller auxiliary ones. **(b)** Subregion computation for each auxiliary region.

Figure 3.10 Subregions computation process.

3. Once the subregions are defined for each part, an assemblage of the parts occurs. The contiguous subregions of different parts are merged into one subregion by the union boolean operation.

This process is repeated for every objective region participating in the problem. In Fig. 3.11 a final result of the algorithm is presented for the Iberian Spanish territory and Balearic Islands

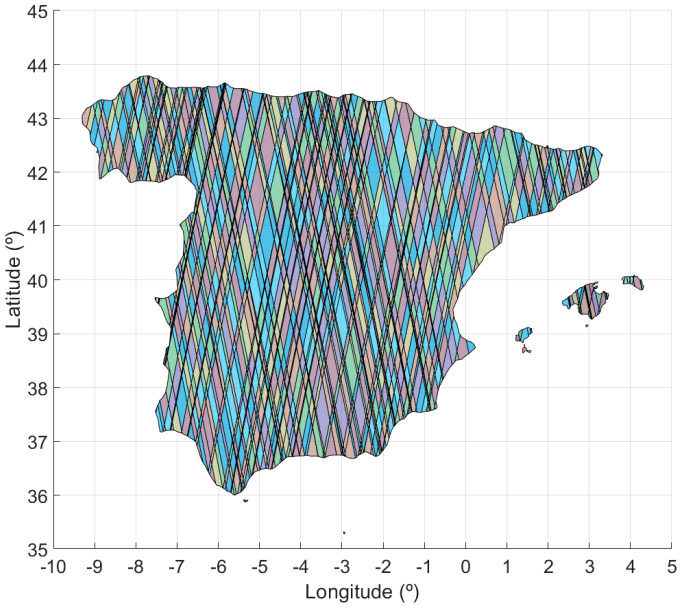

Figure 3.11 Subregions for certain objective regions and satellites.

4 Problem optimization

A final mathematical description about the model used to address the observations and transmissions scheduling problem as well as the algorithms and tools used to solve it are presented in this chapter.

4.1 Mathematical description

For the resolution of the problem is convenient to thoroughly describe it before. The scheduling problem, as an optimization problem, is governed by a number of constraints which must be obeyed and an objective to optimize. The constraints define the set of feasible solution: schedules which fulfill a series of previously stated requirements, while the objective determines the best schedule (or schedules) from the feasible solution set. For the observation and transmission scheduling problem constraints might take into account limitations such as the available energy of the satellites to perform slew and observation operations, whereas the objective might consist in minimizing the transmission of data or the total cost of the operations.

In order to address the problem with the optimization algorithms, a mathematical model of these constraints and objective must be done. Once the parameters and variables are precisely described, the mathematical form of the problem goal consist on a objective function of the variables governed by the parameters which has to be maximized; and the constraints are expressed as equalities or inequalities related to the variables and governed by the parameters as well.

In particular, the observation and transmission scheduling problem is typically modelled in terms of integer variables, more specifically, most of them binary data, indicating dual information about the entities (covered or not, scheduled or not, compatible or not...).

A description of this model used for the particular problem of observation-transmission problem under the scope of the project is made as follows:

4.1.1 Mathematical entities

Time interval

The scheduling problem is considered to be solved during a time interval characterized by initial and final instants, $t \in [t_1, t_{end}]$. The magnitude of the time span, $t_{span} = t_{end} - t_1$, characterises the scale of the scheduling problem, allowing a greater number of objective regions observed but less rescheduling responsiveness for longer time spans and vice versa.

A discretisation of the continuous time interval is made to address the problem. The time step, t_{step}, establishes the distance between the discrete time instants and, as a consequence, the number of subintervals between each discrete instants given a time span,

$$N_{subi} = \left\lceil \frac{t_{span}}{t_{step}} \right\rceil,$$

as well as the number of time instant when the state is defined,

$$N = N_{subi} + 1,$$

and therefore the discrete instants,

$$t_1 \leq t_\tau \leq t_{end} : \tau = 1, 2, \dots, N.$$

Hence, an integer time parameter, τ, is defined for the complete time characterisation of the problem:

$$\tau = \left\lceil \frac{t_\tau - t_1}{t_{step}} + 1 \right\rceil : \tau \in \mathbb{Z}, 0 \leq \tau \leq N. \tag{4.1}$$

Objective regions set

The union of the R disconnected regions, r, whose observation is required establishes the objective regions set, $ObjReg$:

$$\bigcup_{\forall r} r = ObjReg.$$

Ground stations set

The union of the G ground stations, g, considered for the data transmission forms the ground stations set, $GrdSt$:

$$\bigcup_{\forall g} g = GrdSt.$$

Observation satellites set

The union of the S satellites, s, participating in the capture and transmission of data defines the observation satellites set, $ObsSat$:

$$\bigcup_{\forall s} s = ObsSat.$$

Modes set

The M fixed modes, m, used by the satellite to capture Earth's surface form the modes set, $Modes$:

$$\bigcup_{\forall m} m = Modes.$$

Observation configurations set

Based on the previous definitions, each combination of satellite, s, and mode of observation, m, generates an specific observation configuration, k. The K observation configurations, k, generate the Observation configurations set, $ObsConf$:

$$\bigcup_{\forall k} k = ObsConf.$$

Hence, a direct relation between the observation configurations and the observation satellites and modes of observation is established:

$$k \Leftrightarrow s, m.$$

Observation windows set

The observation windows set, OW, is composed by the J observation windows, j, produced thanks to the combinations of the previous parameters:

$$\bigcup_{\forall j} j = OW.$$

A given observation window is determined by the e-th observation chance of the r objective region by the k observation configuration, involving the satellite $s = s(k)$ and observation mode $m = m(k)$. Given the previous entities the start, τ^s_{rke}, and finish, τ^f_{rke}, times are extracted for each observation window j. Therefore:

$$j = \{[\tau^s_{rke}, \tau^f_{rke}] : r \in ObjReg, k \in ObsConf, e \in \mathbb{Z}\}. \tag{4.2}$$

Therefore, a direct relation for each observation window with the objective region, observation configuration and observation chance is established:

$$j \Leftrightarrow r, k, e.$$

The observation windows subset generated by a certain satellite, s, definition will be useful for the resolution:

$$\bigcup_{j=j(s)} j = OW_s$$

Transmission windows set

The transmission windows set, TW, is composed by the D transmission windows, d:

$$\bigcup_{\forall d} d = TW.$$

A certain transmission window is established by the e-th transmission chance between the g ground station and the s satellite. Given the previous entities the start, τ^s_{gse}, and finish, τ^f_{gse}, times are extracted for each transmission window d. Therefore:

$$d = \{[\tau^s_{gse}, \tau^f_{gse}] : g \in GrdSt, s \in ObsSat, e \in \mathbb{Z}\}. \tag{4.3}$$

Similar to the observation windows case, a direct relation for each transmission window with the ground station, observation satellite and transmission chance is established:

$$d \Leftrightarrow g, s, e.$$

Other characteristic transmission windows subsets are defined:

- **Satellite transmission windows**: formed by the transmission windows involving a certain satellite, s:

$$\bigcup_{d=d(s)} d = TW_s.$$

- **Ground station transmission windows**: formed by the transmission windows involving a certain ground station, g:

$$\bigcup_{d=d(g)} d = TW_g.$$

Subregions set

The subregion set, SR, is composed by the I subregions, i, created by the intersection of all the observation window, j, with the objective regions, r:

$$\bigcup_{\forall i} i = SR.$$

It is useful to define additional subregions subsets:

- **Covered subregions:** formed by the subregions observed at an observation window, j:

$$\bigcup_{\forall i \in j} = SR_j.$$

- **Satellite subregions:** formed by the subregions observed by a satellite, s:

$$\bigcup_{\forall i \in OW_s} = SR_s.$$

Acquisitions set

The acquisitions set, Acq, is composed by the scheduled observation windows, $j^\star$:

$$\bigcup_{\forall j=j^\star} j = Acq; \quad j \in OW.$$

Once the problem is finished, the acquisition set represent the solution for the observation scheduling problem.

Downloads set

The downloads set, Dwn, is composed by the scheduled transmission windows, $d^\star$:

$$\bigcup_{\forall d=d^\star} d = Dwn; \quad d \in TW.$$

Once the problem is finished, the downloads set represent the solution for the transmission scheduling problem.

4.1.2 Mathematical relations

Observation windows coverage

The observation windows coverage is modelled by the coverage matrix, Q_{ij}, which states whether the i subregion is covered by the j observation window or not.

$$Q_{ij} = \begin{cases} 1 & \text{if } i \in j \\ 0 & \text{if } i \notin j \end{cases} ; \quad i \in SR,\, j \in OW. \tag{4.4}$$

Windows incompatibility

The time incompatibility between windows is modelled using a series of matrices. These matrices states whether two generic windows are incompatible, i.e. if both windows are allowed to be scheduled together (Sec. 3.4).

- **Observation windows incompatibility ($R^{obs}_{j_1,j_2}$):** establishes whether the observation windows j_1 and j_1 are incompatible or not.

$$R^{obs}_{j_1 j_2} = \begin{cases} 1 & \text{if } j_1,\, j_2 \text{ incompatible} \\ 0 & \text{if } j_1,\, j_2 \text{ compatible} \end{cases} ; \quad j_1,\, j_2 \in OW. \tag{4.5}$$

- **Transmission windows incompatibility($R^{trs}_{d_1,d_2}$):** establishes whether the transmission windows d_1 and d_2 are incompatible or not.

$$R^{trs}_{d_1 d_2} = \begin{cases} 1 & \text{if } d_1,\, d_2 \text{ incompatible} \\ 0 & \text{if } d_1,\, d_2 \text{ compatible} \end{cases} ; \quad d_1,\, d_2 \in TW. \tag{4.6}$$

- **Mixed windows incompatibility($R^{mix}_{j,d}$):** establishes whether the observation window j and the transmission window d are incompatible or not.

$$R^{mix}_{jd} = \begin{cases} 1 & \text{if } j,\, d \text{ incompatible} \\ 0 & \text{if } j,\, d \text{ compatible} \end{cases} ; \quad j \in OW,\, d \in TW. \tag{4.7}$$

4.1.3 Variables

Observation scheduling

The observation scheduling variable, x_j, states whether an observation window j is adopted as an acquisition for the solution or not:

$$x_j = \begin{cases} 1 & \text{if } j \in Acq \\ 0 & \text{if } j \notin Acq \end{cases} ; \quad j \in OW. \tag{4.8}$$

Transmission scheduling

The transmission scheduling variable, y_d, states whether an transmission window d is adopted as a download for the solution or not:

$$y_d = \begin{cases} 1 & \text{if } d \in Dwn \\ 0 & \text{if } d \notin Dwn \end{cases} \quad ; \quad d \in TW. \tag{4.9}$$

Storage

The storage variable, $L_{s\tau}$, describes the storage level of the satellite s at the time τ. The storage is measured by the time of observation still not transmitted gathered in memory, T, at the specific time.

$$L_{s\tau} = T_{s\tau}; \quad s \in ObsSat,\ \tau \in \mathbb{Z},\ 0 \leq \tau \leq N. \tag{4.10}$$

4.1.4 Constraints

Complete coverage

The complete coverage of the objective regions must be fulfilled. To address this the constraint which states that each subregion, i, must be covered at least once by the acquisition set, Acq, is defined:

$$\sum_{\forall j \in OW} Q_{ij} x_j \geq 1; \quad \forall i \in SR. \tag{4.11}$$

This constraint in some cases might be very restrictive, typically on analysis where the time span, t_{span}, is not big enough, the area of observation regions, $Area(\bigcup_{\forall r \in ObsReg} r)$, is too big and/or the observation parameters do not allow to get a feasible solution for this constraint. In these situations and when the resolution procedure allows it, the problem description will hold a relaxation of this constraint in which the coverage of the maximum number of subregions is pursued.

Schedule compatibility

The windows chosen for the schedule solution must not interfere between them, every window incorporated to the solution must be compatible with the other ones. This constraint is defined for each scheduled observation and transmission windows as follows:

- **Acquisitions:** Every scheduled observation, $j^\star$, must not be incompatible with the rest of the scheduled observations and transmissions:

$$\sum_{\forall j \in OW} R^{obs}_{j^\star j} x_j < 1; \quad \forall j^\star \in Acq. \tag{4.12}$$

$$\sum_{\forall d \in TW} R^{mix}_{j^\star d} y_d < 1; \quad \forall j^\star \in Acq. \tag{4.13}$$

- **Downloads:** Every scheduled transmission, $d^\star$, must not be incompatible with the rest of the scheduled transmissions and observations:

$$\sum_{\forall d \in TW} R^{trs}_{d^\star d} y_d < 1; \quad \forall d^\star \in Dwn. \tag{4.14}$$

$$\sum_{\forall j \in OW} R^{mix}_{j d^\star} x_j < 1; \quad \forall d^\star \in Dwn. \tag{4.15}$$

Storage range

The storage of each satellite, s, must remain within the safe range at every instant of time, τ. The safe range is defined by it minimum value, set to zero, and a maximum value, $MaxStg$.

$$0 \leq L_{s\tau} \leq MaxStg; \quad \forall s \in Sat, \forall \tau \in \mathbb{Z},\ 0 \leq \tau \leq N. \tag{4.16}$$

Data acquisition and download

Each observation and transmission operation involves a modification of the storage level of the satellite that mus be reflected in the storage variable, $L_{s\tau}$. Depending on the typology of the acquisition, the constraint will be describe on different ways:

- **Acquisitions:** After an acquisition $j^\star$ involving a satellite $s_{j^\star}$ during an observation window $[\tau^s_{j^\star}, \tau^f_{j^\star}]$, the storage level of the satellite $L_{s_{j^\star}\tau^f_{j^\star}}$ rises the exact amount of the observation time:

$$L_{s_{j^\star}\tau^f_{j^\star}} = L_{s_{j^\star}\tau^s_{j^\star}} + (\tau^f_{j^\star} - \tau^s_{j^\star}); \quad \forall j^\star \in Acq. \tag{4.17}$$

- **Downloads:** After a download $d^\star$ involving a satellite $s_{d^\star}$ during a transmission window $[\tau^s_{d^\star}, \overline{\tau}_{d^\star}]$, the storage level of the satellite $L_{s_{d^\star}\overline{\tau}_{d^\star}}$ decreases the exact amount of the transmission time multiplied by the transmission-observation speed ratio, δ^{trs}:

$$L_{s_{d^\star}\overline{\tau}_{d^\star}} = L_{s_{d^\star}\tau^s_{d^\star}} - \delta^{trs}(\overline{\tau}_{d^\star} - \tau^s_{d^\star}); \quad \tau^s_{d^\star} \leq \overline{\tau}_{d^\star} \leq \tau^f_{d^\star}, \forall d^\star \in Dwn. \tag{4.18}$$

  Note that, in case of the transmission windows, the download might finish before the window closes. This commonly happens when there is no more data left to transmit in the satellite's memory.

4.1.5 Objective function

The objective function is directly related with the purpose of the schedule. Consequently for each different purpose there is a specific objective function. Here below, a few examples are shown:

- **Minimization of number of acquisitions:** In this case the objective function to minimize is equal to the number of observation windows, j, scheduled:

$$f = \sum_{\forall j \in OW} x_j; \tag{4.19}$$

- **Minimization of costs:** For the minimization of costs, the objective function needed to be minimized is the cost, c_j,of every observation included in the solution:

$$f = \sum_{\forall j \in OW} c_j x_j; \tag{4.20}$$

- **Minimization of observations makespan:** The observations makespan refers to the time needed to complete the observations and it is defined by the completion time of the last acquisition. Hence the objective function is equal to the maximum value of the scheduled completion times:

$$f = \max_{\forall j \in OW} \{\tau^f_j x_j\}; \tag{4.21}$$

In this project, the scheduling objective is to cover the objective regions with the less number of acquisitions, consequently, the objective function chosen corresponds to the first one (4.19) of the explained above.

4.2 Mathematical resolution

At this point, the resolution of the scheduling problem can be addressed as an optimization problem, supported by the mathematical approach made. Once an optimization problem is defined by the N-dimensional variable x, the objective function $f(x)$, the m inequality constraints and p equality constraints related to $g_i(x)$ and $h_j(x)$ functions, its general form is defined by:

$$\begin{aligned} \min \quad & f(x) \\ s.t. \quad & g_i(x) \leq 0, \quad i = 1, \dots, m \\ & h_j(x) = 0, \quad j = 1, \dots, n \end{aligned} \tag{4.22}$$

An entire field of study of computational science analyses the methods used to solve the optimization problems, among others. The complexity of these problems frequently jeopardise the computational capabilities

of the employed devices, consequently a plenty of solving methods are designed to solve the optimization problems depending on their nature minimising the computational demands.

Regarding this methods, they are based in algorithms which guarantee an optimal solution (Exact algorithms) or find a feasible solution presumably close to the optimal one. The exact algorithm for specific optimization problems, such as the observation and transmission scheduling one (NP-hard), may not determine the solution within polynomial time, which means their running time is not upper bounded by a polynomial expression in the size of the inputs. This can lead to unfeasible huge computational times which constitutes the reason why simpler non-exact algorithms are preferred in some situations.

Focusing on the specific optimization of this project, the algorithms used are now selected depending on the complexity of the problem. A first approach for the observations sub-problem in which the transmission are no needed is previously solved to make way to the complete observations and transmissions problem consideration. Two alternatives to get the solution for these problems have been considered:

- **Commercial Integer Programming solvers:**

  These are specialised in this kind of optimisation problems and provide directly the solution once the objective function and constraints are properly defined. In general, the user has not the ability to totally customize the algorithms employed by the solver to get the solution. In addition, the requirement to express the objective function and constraints on a certain way might become an inconvenience if their complexity is noticeable.

- **Heuristic algorithms:**

  These are specifically designed for the problem and their performance is easier to be understood. In this algorithms the heuristic decides which of the available observation and transmission windows are adopted as acquisitions and downloads based on heuristic indices which measure the contribution of each one to the problem. This technique does not guarantee the optimal solution but a feasible solution presumably close to the optimal one. The heuristic algorithms usually randomly pick the entity joining the solution from a subset of candidates with the best heuristic indices. Depending on the size of this subset, i.e. its cardinality p, the algorithms can be classified into two groups:

  – ***GREEDY*** **($p = 1$):**

    In this algorithm, always the best candidate is chosen to be become part of the solution. Consequently, the randomisation of the process is lost and the solutions are always the same for a given set of problem instances.

  – ***GRASP*** **($p > 1$):**

    Opposite to the previous ones, this algorithm randomly pick one of the candidates selected. The randomisation increase with the cardinality of the candidates subset and the algorithm is repeated a number of times, N_{sol}, in order to finally adopt the best solution from the generated ones as the final solution. In general the GRASP algorithms, although their computational time is greater, achieve better solutions than the GREEDY ones.

4.2.1 Observations scheduling sub-problem

As a first step, the transmission scheduling are removed from the problem and, with them, the storage range and data acquisition and download constraints.

Thanks to this simplification, the observations scheduling problem became a linear problem which involves the observation scheduling binary variable, x_j:

$$\begin{array}{lll} \min & \sum_{\forall j \in OW} x_j & \\ s.t. & \sum_{\forall j \in OW} Q_{ij} x_j \geq 1, & \forall i \in SR \\ & \sum_{\forall j \in OW} R^{obs}_{j'j} x_j - B(1-x_{j'}) \leq 0, & \forall j' \in OW \end{array} \tag{4.23}$$

establishing B as a large constant which ensures the compatibility constraint only affects the observation windows adopted as acquisitions.

This problem is solved using the Integer Lineal Programming algorithm (ILP) included in the *Optimization Toolbox* from the software *MATLAB*, to be precise, the *intlinprog.m* function is used.

Alongside, an heuristic approach (Algo. 3) is developed in order to be able to upgrade it with transmissions scheduling capabilities for the complete problem. Therefore, the objective of this heuristic algorithm used in the observations sub-problem is to represent a middle step which helps to link both results obtained from the exact resolution of the observation sub-problem and the heuristic resolution of the complete problem.

The algorithm iterates picking acquisitions from the observation windows set until there are no subregion left to be observed or no observation windows left for acquiring the remaining subregions, which would imply the complete coverage constraint (4.11) is not satisfied.

In the algorithm the function $HeuristicIndex$ define an index for each observation window, j, based on the remaining ones and the subregions not yet acquired. This index, h_j models how good the contribution of the observation window presumably is in order to minimize the objective function of the problem. In this index lies the heuristic of the method, being its design a crucial point for the quality of the algorithm. Regarding the minimization of the number of acquisitions, as an example, some possible definitions for the heuristic index, h_j, might consist on the number of unobserved subregions, the unobserved area or the ratio between the unobserved and total areas covered by the observation window. Moreover, the function *RandomPick* randomly choose an observation window, $j^\star$ to be scheduled from the observation nominees subset OW_{nom} of cardinality p.

$Acq \leftarrow \emptyset$;
while $SR \neq \emptyset$ **or** $OW \neq \emptyset$ **do**
  $h_j \leftarrow HeuristicIndex(SR, OW)$;
  $OW_{nom} \leftarrow \bigcup j' \ : \ h_{j'} \geq h_{\forall j \neq j'}, |OW_{nom}| = p$;
  $j^\star \leftarrow RandomPick(OW_{nom})$;
  $OW_{R_{j^\star}} \leftarrow \bigcup j' \ : \ R^{obs}_{j'j^\star} \neq 0$;
  $SR_{j^\star} \leftarrow \bigcup i' \ : \ Q_{i'j^\star} = 1$;
  $Acq \leftarrow Acq \cup j^\star$;
  $OW \leftarrow OW - (OW_{R_{j^\star}} \cup j^\star)$;
  $SR \leftarrow SR - SR_{j^\star}$;
end

Algorithm 3: Heuristic algorithm for observations sub-problem

4.2.2 Observations and transmissions scheduling problem

The incorporation of both observations and transmission features substantially increase the complexity of the problem. In addition, the constrains stated to guarantee the storage safe level and the consequences after a data operation thereof present a non-linear behaviour which complicates the resolution by means of the ILP solver incorporated in *MATLAB* which is used on the observations scheduling sub-problem.

With the objective of facing this problem, the previously developed heuristic algorithm for the resolution of the observations sub-problem is upgraded to include the transmissions and storage considerations (Algo. 4). For the transmission decision, a *foresee-download* policy is adopted. The algorithm chooses an observation candidate as previously designed. However, in this occasion the storage level of the satellite involved, $L_{\bar{s}\tau}$, is checked to remain within the safe range, OK_L, thanks to the function *StorageCheck*. If the storage exceeds the maximum level after including the observation candidate, the function *ScheduleDwn* chooses the less conflictive transmission window which allows the observation candidate to be included as an acquisition. In case there is no available transmission window, the observation is discarded and no observation neither transmission are scheduled.

Once all subregions have been covered or there are no more available observation windows, a final routine solves the decoupled transmissions scheduling problem in order to guarantee the data collected is transmitted to the ground stations as possible. To do so, the algorithm detects the intervals of inactivity of each satellites after the observations and transmissions have been scheduled thanks to the *foresee-download* policy. Given the inactivity intervals whose storage level is not null, the algorithm tries to schedule the less conflictive download for the satellite from the compatible transmission windows set, prioritizing those inactivity intervals whose storage level is greater.

On every iteration the storage level along time, $L_{s\tau}$, is updated by including the data acquisition and download activities scheduled, Eq. (4.17) and (4.18). The function $UpdateSto$ carries out the update redefining the idle times, t^{idle}, for previously scheduled transmission which are no longer completely exploited.

$Acq \leftarrow \emptyset$;
$Dwn \leftarrow \emptyset$;
while $SR \neq \emptyset$ **or** $OW \neq \emptyset$ **do**
  $h_j \leftarrow HeuristicIndex(SR, OW)$;
  $OW_{nom} \leftarrow \bigcup j' \ : \ h_{j'} \geq h_{\forall j \neq j'}, |OW_{nom}| = p$;
  $\overline{j} \leftarrow RandomPick(OW_{nom})$;
  $OK_L \leftarrow StorageCheck(\overline{j}, L_{\overline{s}\tau})$;
  if OK_L **then**
    $j^\star \leftarrow \overline{j}$;
    $d^\star \leftarrow \emptyset$;
  else
    $TW_{R_{\overline{j}}} \leftarrow \bigcup d' \ : \ R^{mix}_{\overline{j}d'} \neq 0$;
    $\overline{d} \leftarrow ScheduleDwn(L_{\overline{s}\tau}, TW_{\overline{s}}, TW_{R_{\overline{j}}})$;
    if $\overline{d} \neq \emptyset$ **then**
      $j^\star \leftarrow \overline{j}$;
      $d^\star \leftarrow \overline{d}$;
    else
      $OW \leftarrow OW - \overline{j}$;
      $j^\star \leftarrow \emptyset$;
      $d^\star \leftarrow \emptyset$;
    end
  end
  $OW_{R_{j^\star d^\star}} \leftarrow \bigcup j' \ : \ R^{obs}_{j'j^\star} + R^{mix}_{j'd^\star} \neq 0$;
  $TW_{R_{j^\star d^\star}} \leftarrow \bigcup d' \ : \ R^{trs}_{d'd^\star} + R^{mix}_{j^\star d'} \neq 0$;
  $SR_{j^\star} \leftarrow \bigcup i' \ : \ Q_{i'j^\star} = 1$;
  $Acq \leftarrow Acq \cup j^\star$;
  $Dwn \leftarrow Dwn \cup d^\star$;
  $L_{\overline{s}\tau} \leftarrow UpdateSto(L_{\overline{s}\tau}, j^\star, d^\star)$;
  $OW \leftarrow OW - (OW_{R_{j^\star d^\star}} \cup j^\star)$;
  $TW \leftarrow TW - (TW_{R_{j^\star d^\star}} \cup d^\star)$;
  $SR \leftarrow SR - SR_{j^\star}$;
end
$Inact \leftarrow InactivityIntervals(Acq, Dwn, L_{s\tau})$;
while $Inact \neq \emptyset$ **do**
  $\overline{l} \leftarrow [\tau^s_l, \tau^f_l] \in Inact \ : \ L_{\overline{s}\tau \in \overline{l}} = \max\{L_{s\tau}\}$;
  $d^\star \leftarrow ScheduleDwn(TW_{\overline{s}}, TW_R, \overline{l}) \ : \ [\tau^s_{d^\star}, \tau^f_{d^\star}] \subseteq \overline{l}$;
  $Dwn \leftarrow Dwn \cup d^\star$;
  $L_{\overline{s}\tau} \leftarrow UpdateSto(L_{\overline{s}\tau}, d^\star)$;
  $Inact \leftarrow Inact - \overline{l}$;
end

Algorithm 4: Heuristic algorithm for observations and transmissions problem

5 Results

On this chapter the results obtained for both observations sub-problem and observations and transmissions problem are exhibited. A certain scenario composed by different resources and regions of interest is defined for each resolution.

5.1 Resources

The company *Planet Labs Inc.* has been contacted and asked about some relevant parameters in order to analyse a real scenario. Hence, as far as possible, the real parameters from the company will be selected.

5.1.1 Satellites

For every considered scenario, the constellations of satellites *FLOCK 2P* and *FLOCK 3P* (Table 2.1) have been used, considering a total number of 100 satellites. The sensors on board these satellites are simply modelled thanks to the following parameters (Sec. 2.4 and Subsec. 2.6.1) provided by *Planet Labs*:

$$\begin{aligned} \Gamma_{max} &= 5^o \\ FOV &= 4^o \\ \Omega_x &= 1\frac{^o}{s} \end{aligned}$$

With respect to the modes of observation which generate the swaths, they consist in 5 different attitude configurations, varying equidistantly their roll angle, while pitch remains null:

$$\begin{aligned} M &= 5 \\ \varphi_m &= \{-5^o, -2.5^o, 0^o, 2.5^o, 5^o\} \\ \chi_m &= 0^o \end{aligned}$$

Concerning the temporal parameters, the objective regions must be covered in the time interval from 23/08/2019 00:00:00, until 24/08/2019 00:00:00. The algorithm uses a time resolution of 1 second, $t_{step} = 1\ s$, hence the number of time instant considered:

$$N = 86401.$$

Once this parameters are set, the computation of the satellite ground-tracks and visibility swaths is carried out. The number of tracks, N_{track}, corresponds to the number of total satellites, while the number of continuous swaths, N_{cont}, takes into account the number of modes, M, for each satellite. Finally each continuous swath is divided into normalised ones which fit into the geographical longitudes interval, generating a total amount of swaths considered, N_{swath}. This process spent a certain amount of computing time, T_{TS}:

$$\begin{aligned} N_{track} &= 100 \\ N_{cont} &= 500 \\ N_{swath} &= 8605 \\ T_{TS} &= 773.254\ s \end{aligned}$$

5.1.2 Ground stations

Regarding the ground stations, the locations shown on Fig. 2.13 and described in Table 2.2 are used, with the exception of no. **6** in Antarctica, which is no longer available. In addition,a total of 4 antennas are located on each site, establishing a total number of 28 antennas considered for every scenario.

Moreover, the parameters involved in the communications with the ground stations are established as well thanks to the indications of *Planet Labs*. The reset time of each antenna, t_{reset} and the satellite's minimum elevation required, γ_{min}, are defined bellow:

$$\begin{aligned} t_{reset} &= 4\ min \\ \gamma_{min} &= 10^{o} \end{aligned}$$

For the transmission-observation speed ratio value, δ^{trs} (2.78), some estimations have been made about the size of the observation area [5] and the downlink speeds [2].

$$\begin{aligned} Observed\ area\ ratio &\simeq 250\,\tfrac{km^2}{s} \\ \tfrac{Data\ size}{Observed\ area} &\simeq 15\,\tfrac{kB}{km^2} \\ \Rightarrow DR_{obs} &\simeq 3750\,\tfrac{kB}{s} \\ DR_{trs} &\simeq 220\,Mbps \\ \Rightarrow \delta^{trs} &\simeq 7.5 \end{aligned}$$

5.2 Scenarios

Several scenarios are considered for the previous resources varying in the objective regions considered. For each of them the computational demands for the instances definition and the final resolution are exhibit.

Instances

The following entities are computed:

- **Observation windows:** After the definition of the swaths and the objective region, a total number of N_{OW} observation windows are computed. From all of them, the only ones occurring at daytime, N_{OW^D}, are selected. The computing time needed for this algorithm is provided, T_{OW}.
- **Subregions:** Next, the objective region is divided into N_{SR} subregions and the coverage matrix is calculated. The computing time needed for this process is provided, T_{SR}.

  The computational costs of this process strongly depends on the morphology of the observation windows considered. The number of subregion increases rapidly when working with observation windows that cross between them, while if they remain parallel less subregions are created and the cost of the computation decrease.

  In the particular case of the sun-synchronous orbits with which the scenarios are solved, the pair of different directions of the observation windows for each satellite belong to the two observation chances during the whole day, of which only one occurs at day time. The constellations selected have parallel directions of their observation for the daytime passes (Fig. 2.12), hence the number of subregions, N_{SR^D}, and the computing time, T_{SR^D} are much lower than the values for the consideration of both passes, $N_{SR^{tot}}$ and $T_{SR^{tot}}$.
- **Transmission windows:** Afterwards, the number of transmission windows between each satellite and each ground station antenna, N_{TW}, is computed. The computing time needed for this process is provided, T_{TW}.
- **Incompatibility matrices:** Finally, an algorithm computes the three incompatibility matrices for each observations and/or transmissions combinations. The computing time needed for this algorithm is provided, T_R.

Resolution

Once the Instances for each scenario are set, the resolutions are carried out for both observations sub-problem and observations and transmissions complete problem. Different methods are employed for the resolution depending on which problem is addressed:

Observations sub-problem

- ***Matlab* ILP solver:** The *intlinprog.m* function of the software an be used thanks to the linearity of this sub-problem. The algorithm first look for the optimal solution of the continuous linear problem (LP) and provides the value of its objective function, $f^{\star}_{LP}$. Afterwards, it applies different kind of cuts in order to obtain a lower bound of the objective function value for the integer linear problem (ILP), f^{lb}. Ultimately, it performs the computation of the optimal solution for the integer linear problem thanks to a *Branch and Bound* method and the optimal objective function value is obtained, $f^{\star}$. The computing time taken for this resolution is given, $T^{\star}$.

- **Observations heuristic algorithm:** The previously mentioned heuristic algorithm (Algo. 3) is used as an intermediate step between the optimal solution of the observations sub-problem and the heuristic one of the complete problem. The algorithm is executed for different sizes for the candidates subset, p, and number of repetitions, N_{sol}, in order to obtain different heuristic solutions, f^{heu}, to compare. As previously mentioned (Subsec. 4.2.1) the Algo. 3 might not fulfill the full-coverage constraint (Eq. (4.11)). The decision made in this project is to accept the results as feasible even though portions of the objective regions is not covered, and to evaluate the size of the area from the objective regions which remains uncovered,

  $$A^{uncov}_{rel} = \frac{Area\ not\ covered}{Area\ of\ objective\ region}.$$

  In case a number of solution is generated, as in GRASP algorithm, the process also provides the best solution which covers the entire regions if it is found. On each case the computing times for the resolutions are evaluated, T^{heu}.

Observations and transmissions sub-problem

- **Observations and transmissions heuristic algorithm:** On the complete problem, the only method used is the observations and transmissions heuristic algorithm designed (Algo. 4). As done for the heuristic resolution of the observations sub-problem, the algorithm is executed for different sizes for the candidates subset, p, and number of repetitions, N_{sol}, in order to obtain different heuristic solutions, f^{heu}, to compare. In addition, index A^{uncov}_{rel} is presented as for the observations sub-problem algorithms. The computing time for each case is evaluated, T^{heu}.

As introduced in Sec. 4.2 and in the previous paragraphs, the way the heuristic algorithms are designed for this project also requires the previous computation of the subregions, N_{SR}, in which the objective regions are divided. This fact substantially increase the overall necessary computing time with respect to other heuristic resolutions which avoid the computation of the mentioned subregions; specially on scenarios where a variety of constellations is used and observation windows which cross between them are generated, rising the number of the created subregions.

Nevertheless, the objective of the designed heuristic algorithms, and in particular the of Algo. 4, is to provide the closest solution to the optimal one for the observations and transmissions scheduling problem, since the exact algorithms are not able to address this complete problem. Therefore, in order to contextualise the results obtained from the heuristic algorithm used for the resolution of the complete problem and link them with the exact resolution of the observations scheduling sub-problem, the results provided by the heuristic algorithm solving the observations sub-problem (Algo. 3) are as well presented, representing a middle step between both main resolutions of sub-problem and complete problem.

5.2.1 SPAIN

In this case, the political territories of Spain are considered as objective regions for the resolution of the scheduling problems.

$$A_{obj} = 5.1602 \times 10^5\ km^2.$$

Figure 5.1 Spanish territories.

Instances

The parameters evaluating the problem instances computation performance for this particular scenario are shown in Table 5.1.

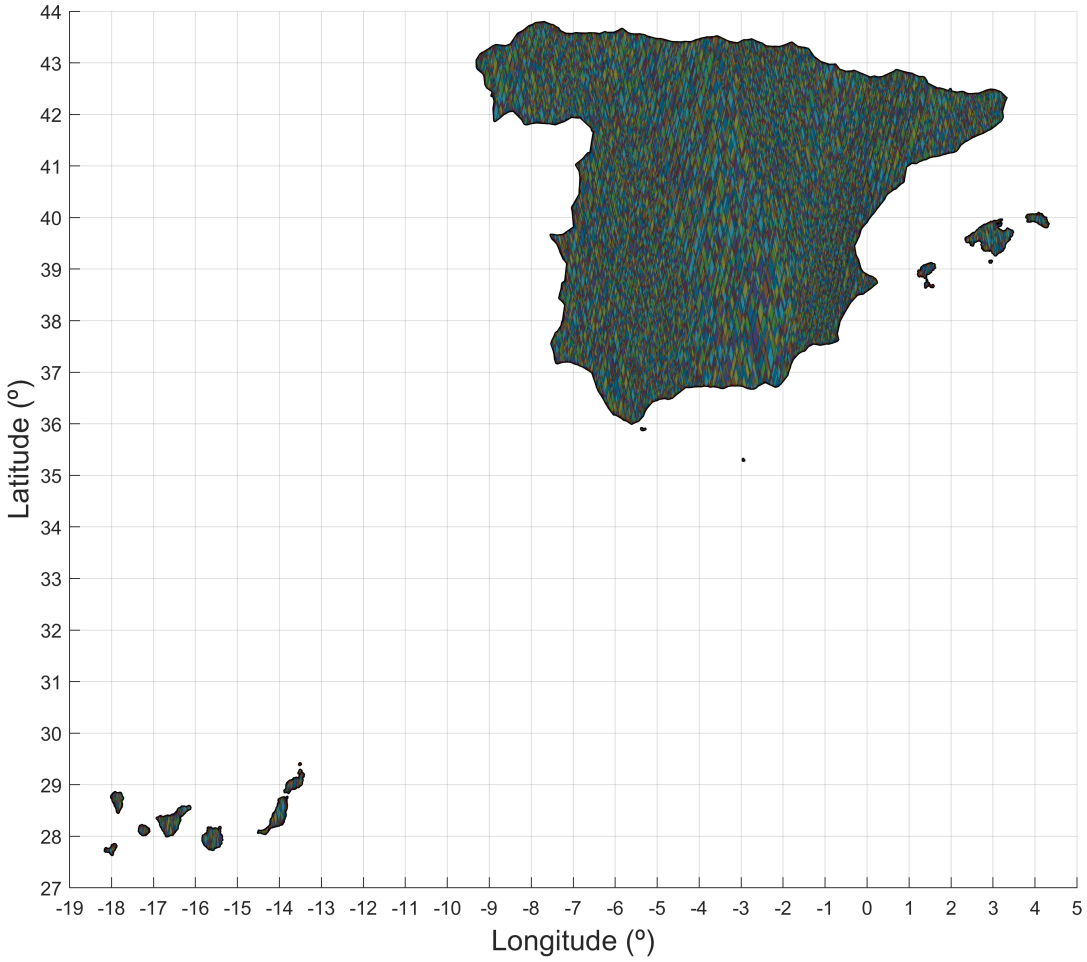

(a) Subregions created by all the observation windows.

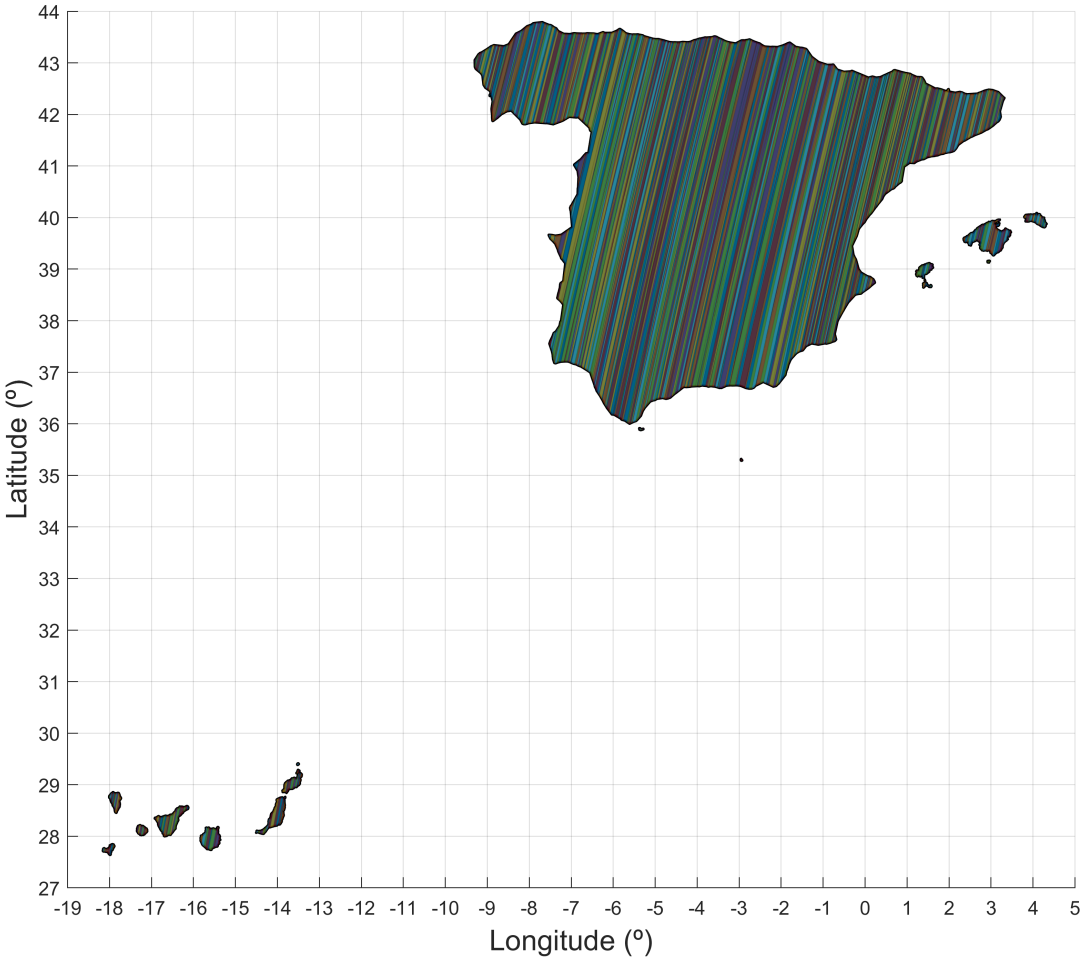

(b) Subregions created by daytime observation windows .

Figure 5.1 Subregions created .

Table 5.1 Instances computation for Spanish territories coverage .

	Observation windows		Subregions		Transmission windows	Incompatibility matrices
Entities	$N_{OW} = 976$	$N_{OW^D} = 488$	$N_{SR^{tot}} = 59611$	$N_{SR^D} = 1359$	$N_{TW} = 12668$	-
Computing time $[s]$	$T_{OW} = 51.246$		$T_{SR^{tot}} = 2165.456$	$T_{SR^D} = 25.412$	$T_{TW} = 67.781$	$T_R = 0.741$

Resolution

The resolutions for both sub-problem and complete problem and the performance of the algorithms used are finally analysed for the scenario with the Spanish territories as objective regions.

- **Observations scheduling sub-problem**

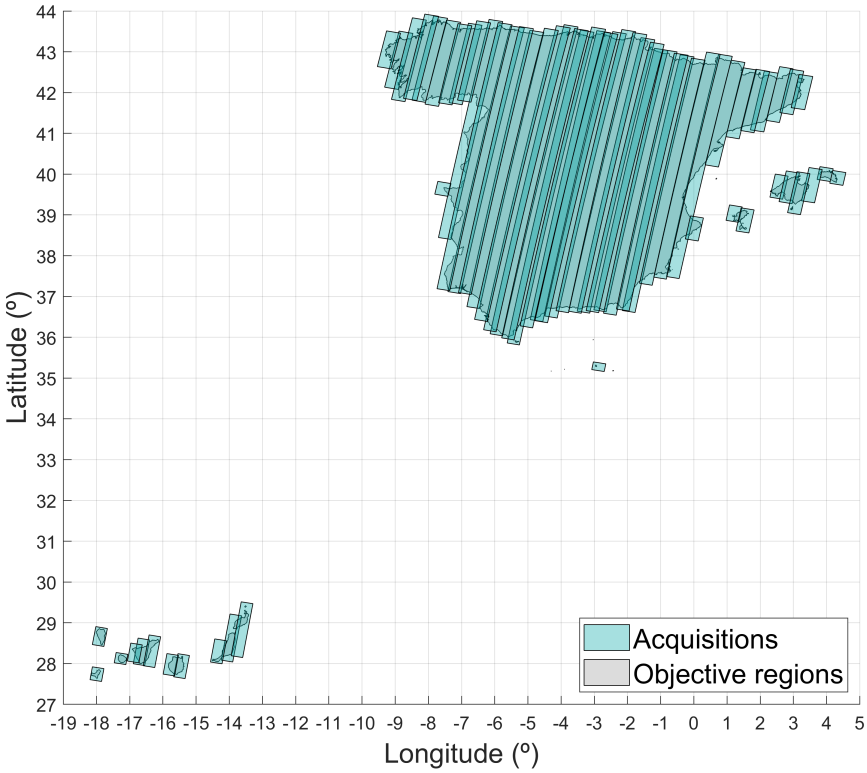

(c) Scheduled observations.

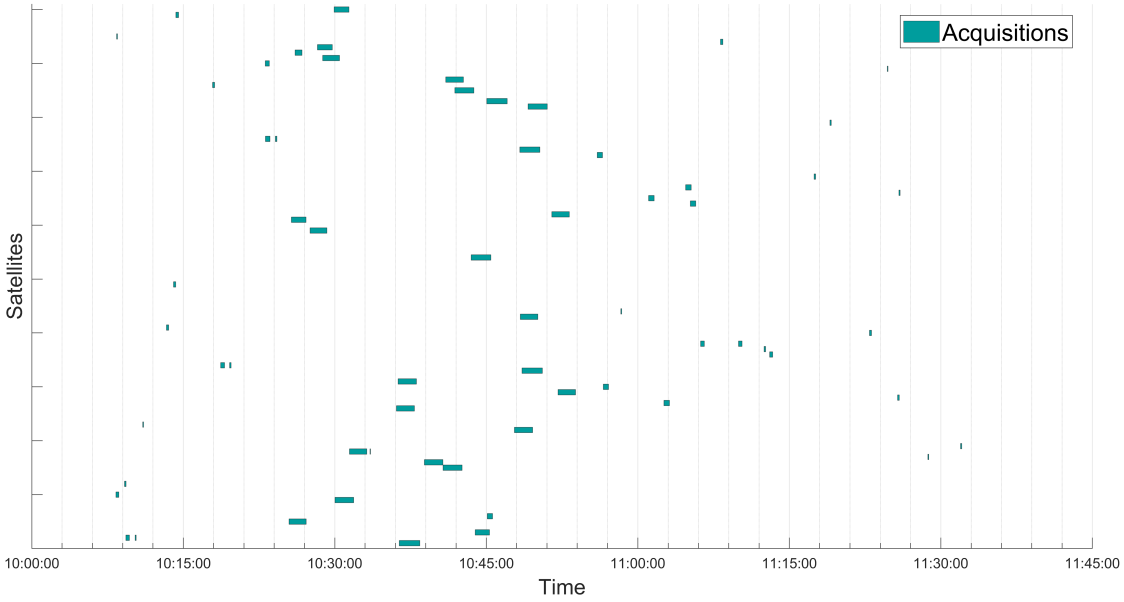

(d) Gantt chart for acquisitions.

Figure 5.2 Optimal solution provided by ***MATLAB*** **ILP solver** for the observations scheduling sub-problem concerning the coverage of the Spanish territories.

Table 5.2 Spain coverage observations sub-problem: Algorithms performances.

***MATLAB* ILP solver**	
$f^{\star}_{LP}$ $[acq.]$	62.000010
f^{lb} $[acq.]$	63
$f^{\star}$ $[acq.]$	63
$T^{\star}$ $[s]$	0.151

GREEDY algo. *Partial coverage allowed*	
f^{heu} $[acq.]$	72
A^{uncov}_{rel} [-]	0
T^{heu} $[s]$	0.377

GRASP algo. *Partial coverage allowed* ($p = 2$)

Solutions obtained	$N_{sol} = 10$		$N_{sol} = 50$		$N_{sol} = 100$		$N_{sol} = 500$	
Full coverage	No	Yes	No	Yes	No	Yes	No	Yes
f^{heu} $[acq.]$	70	-	68	73	66	73	66	71
A^{uncov}_{rel} [-]	0.465%	-	0.491%	0	1.082%	0	3.237%	0
T^{heu} $[s]$	1.904		5.786		11.677		56.922	

GRASP algo. *Partial coverage allowed* ($p = 4$)

Solutions obtained	$N_{sol} = 10$		$N_{sol} = 50$		$N_{sol} = 100$		$N_{sol} = 500$	
Full coverage	No	Yes	No	Yes	No	Yes	No	Yes
f^{heu} $[acq.]$	69	74	67	70	66	70	67	69
A^{uncov}_{rel} [-]	3.910%	0	6.348%	0	6.818%	0	1.084%	0
T^{heu} $[s]$	1.290		6.020		11.561		57.557	

GRASP algo. *Partial coverage allowed* ($p = 6$)

Solutions obtained	$N_{sol} = 10$		$N_{sol} = 50$		$N_{sol} = 100$		$N_{sol} = 500$	
Full coverage	No	Yes	No	Yes	No	Yes	No	Yes
f^{heu} $[acq.]$	68	70	68	72	65	71	65	70
A^{uncov}_{rel} [-]	2.837%	0	0.644%	0	1.698%	0	3.047%	0
T^{heu} $[s]$	1.795		6.023		12.047		57.478	

GRASP algo. *Partial coverage allowed* ($p = 8$)

Solutions obtained	$N_{sol} = 10$		$N_{sol} = 50$		$N_{sol} = 100$		$N_{sol} = 500$	
Full coverage	No	Yes	No	Yes	No	Yes	No	Yes
f^{heu} $[acq.]$	67	-	67	-	67	71	65	70
A^{uncov}_{rel} [-]	1.175%	-	2.625%	-	3.459%	0	4.739%	0
T^{heu} $[s]$	2.502		6.171		11.849		57.952	

GRASP algo. *Partial coverage allowed* ($p = 10$)

Solutions obtained	$N_{sol} = 10$		$N_{sol} = 50$		$N_{sol} = 100$		$N_{sol} = 500$	
Full coverage	No	Yes	No	Yes	No	Yes	No	Yes
f^{heu} $[acq.]$	67	-	67	73	67	70	65	71
A^{uncov}_{rel} [-]	1.606%	-	5.352%	0	3.578%	0	2.605%	0
T^{heu} $[s]$	1.809		6.198		11.856		58.351	

- **Observations and transmissions scheduling problem**

Table 5.3 Spain coverage observations and transmissions problem: Algorithms performances.

GREEDY algo. *Partial coverage allowed*	
f^{heu} $[acq.]$	72
A_{rel}^{uncov} [-]	0
T^{heu} $[s]$	20.753

GRASP algo. *Partial coverage allowed* ($p = 4$)						
Solutions obtained	$N_{sol} = 10$		$N_{sol} = 50$		$N_{sol} = 100$	
Full coverage	No	Yes	No	Yes	No	Yes
f^{heu} $[acq.]$	68	72	67	71	67	71
A_{rel}^{uncov} [-]	1.829%	0	2.740%	0	2.305%	0
T^{heu} $[s]$	108.021		514.922		987.790	

GRASP algo. *Partial coverage allowed* ($p = 6$)						
Solutions obtained	$N_{sol} = 10$		$N_{sol} = 50$		$N_{sol} = 100$	
Full coverage	No	Yes	No	Yes	No	Yes
f^{heu} $[acq.]$	70	-	67	71	68	72
A_{rel}^{uncov} [-]	0.832%	-	4.758%	0	1.019%	0
T^{heu} $[s]$	105.097		510.122		984.468	

GRASP algo. *Partial coverage allowed* ($p = 8$)						
Solutions obtained	$N_{sol} = 10$		$N_{sol} = 50$		$N_{sol} = 100$	
Full coverage	No	Yes	No	Yes	No	Yes
f^{heu} $[acq.]$	67	-	67	72	66	71
A_{rel}^{uncov} [-]	0.791%	-	3.069%	0	2.843%	0
T^{heu} $[s]$	104.390		104.390		986.837	

The solution provided by the **GRASP algo.** which randomly chooses between $p = 8$ candidates and provides $N_{sol} = 10$ has been selected to illustrate the results obtained. In this case, 99.2% of the total area is covered by 67 acquisitions. In this solution, 62 downloads are scheduled to gather the data acquired before the end of the day.

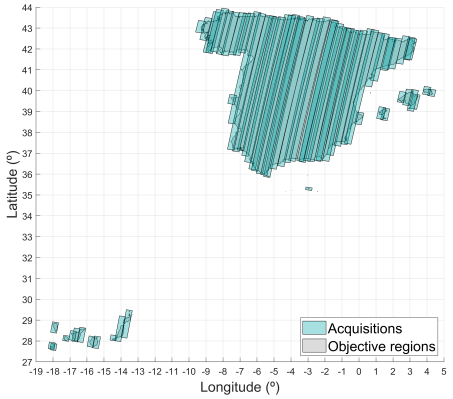

(a) Scheduled observations.

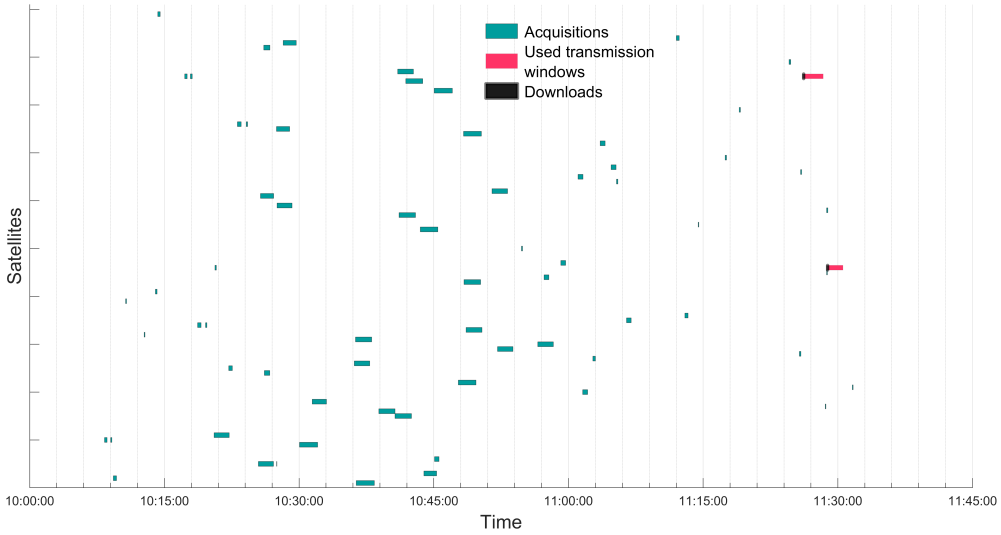

(b) Gantt chart for acquisitions .

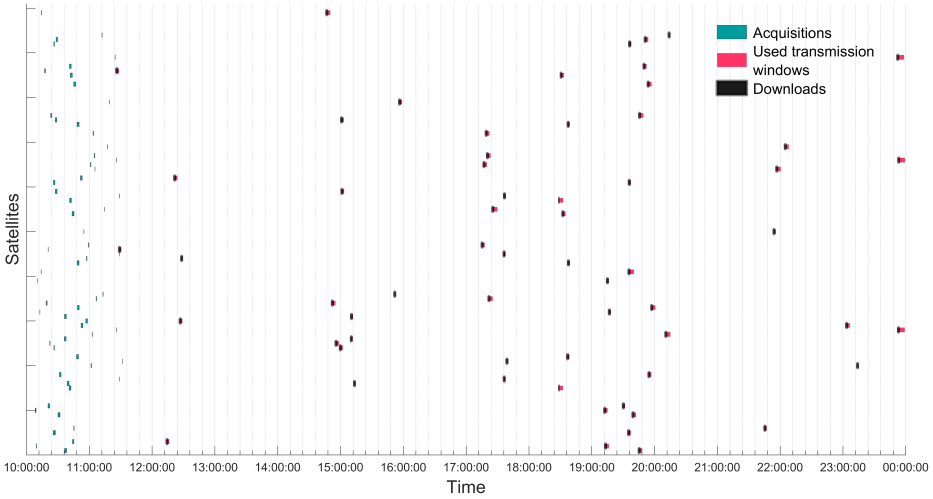

(c) Gantt chart for acquisitions and downloads .

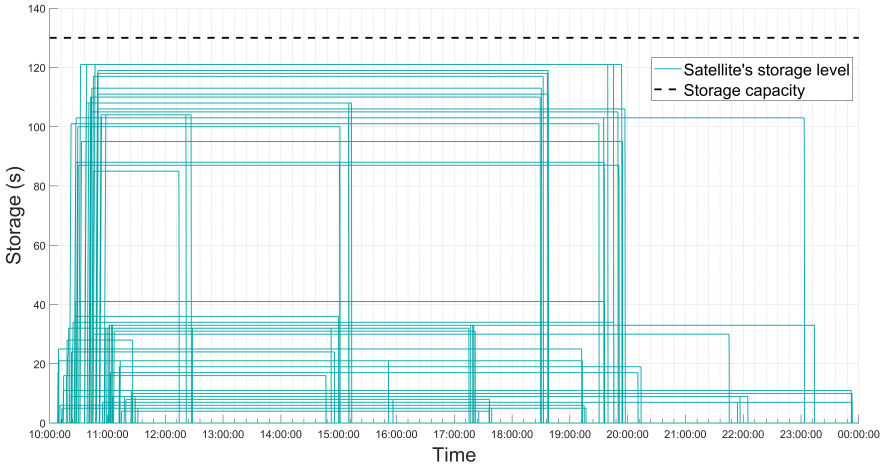

(d) Storage evolution on satellites.

Figure 5.2 Solution provided by **GRASP heuristic algo.** ($p = 8$, $N_{sol} = 10$) for the observations and transmissions scheduling problem concerning the coverage of the Spanish territories.

5.2.2 SPAIN AND ITALY

In the next scenario, the Italian political territories, together with the Spanish ones, are considered in order to increase the size of the problem.

$$A_{obj} = 8.3654 \times 10^5 \ km^2.$$

Figure 5.3 Spanish and Italian territories.

Instances

The parameters evaluating the problem instances computation performance for this particular scenario are shown in Table 5.4.

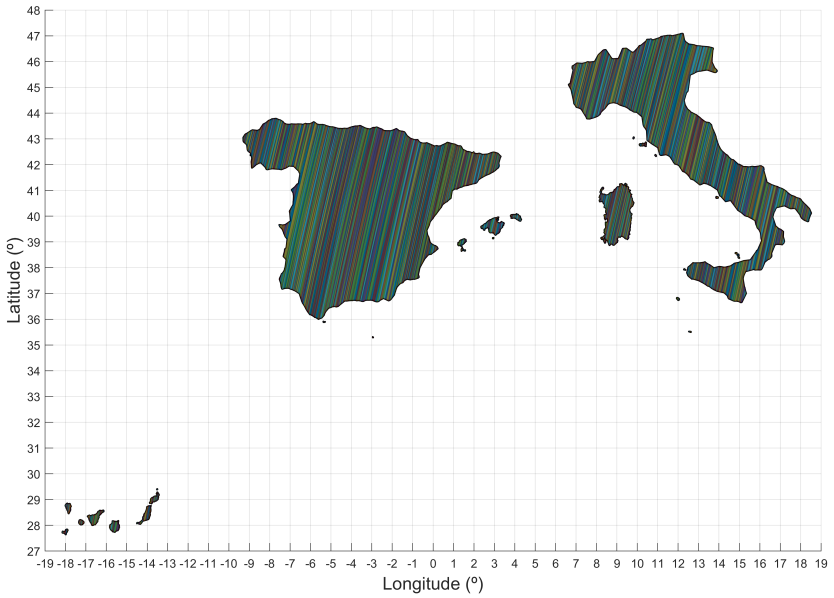

Figure 5.4 Subregions created by daytime observation windows.

Table 5.4 Instances computation for Spanish and Italian territories coverage .

	Observation windows		Subregions	Transmission windows	Incompatibility matrices
Entities	$N_{OW} = 1968$	$N_{OW^D} = 981$	$N_{SR^D} = 2579$	$N_{TW} = 12668$	-
Computing time $[s]$	$T_{OW} = 85.821$		$T_{SR^D} = 53.780$	$T_{TW} = 76.340$	$T_R = 0.826$

Resolution

The resolutions for both sub-problem and complete problem and the performance of the algorithms used are finally analysed for the scenario with the Spanish territories as objective regions.

- **Observations scheduling sub-problem**

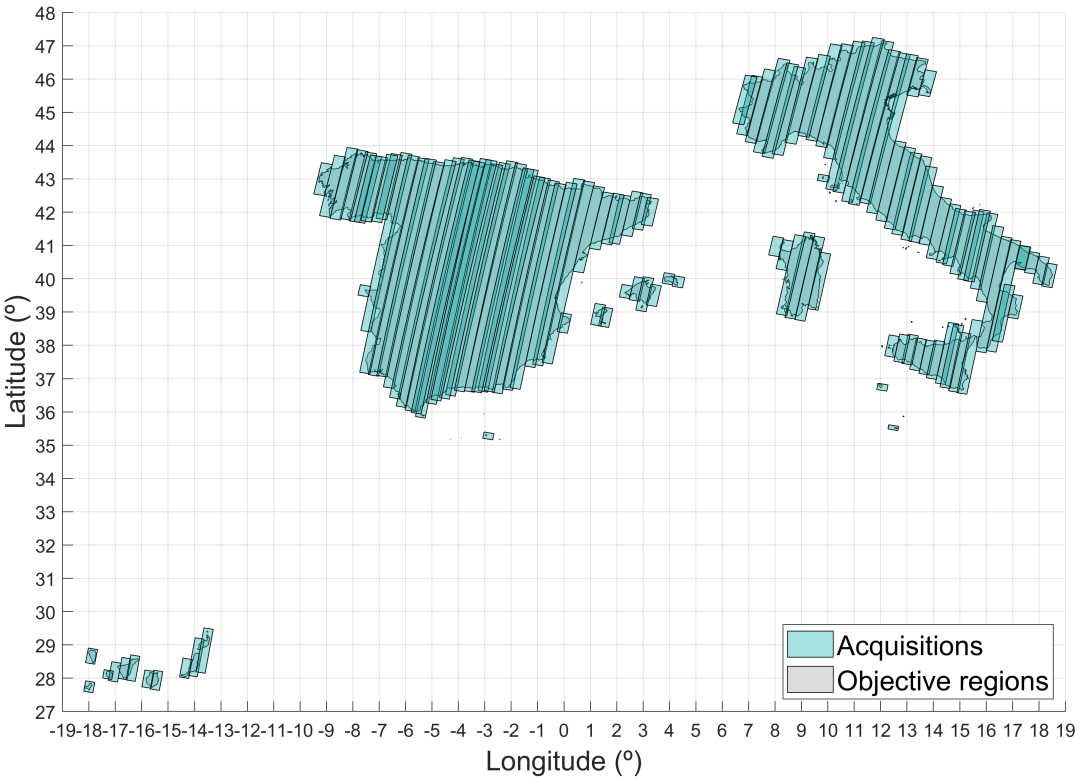

(a) Scheduled observations.

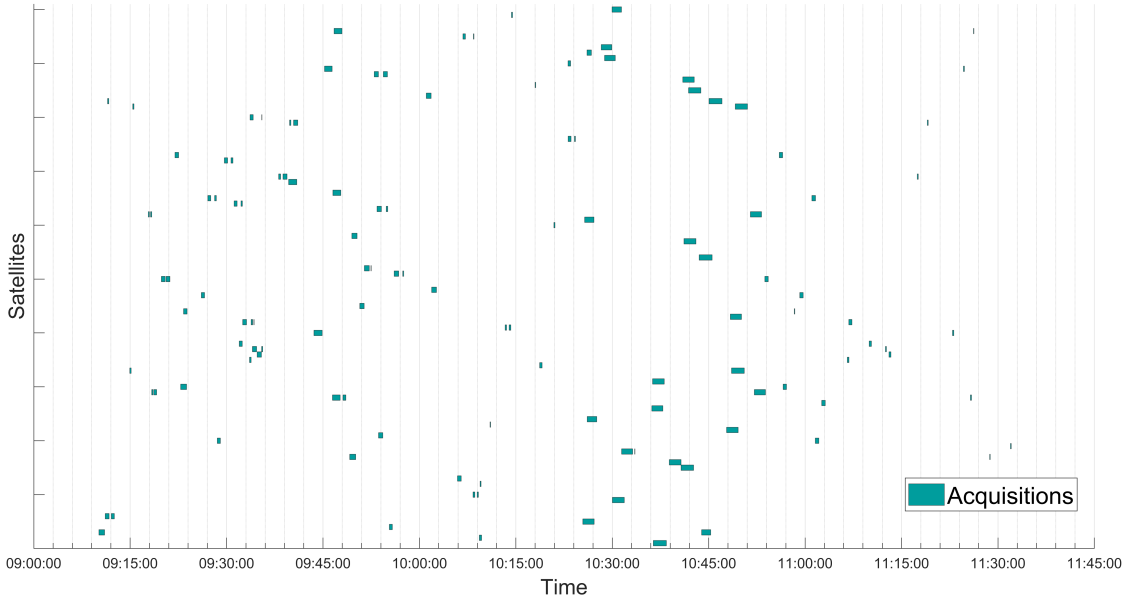

(b) Gantt chart for acquisitions.

Figure 5.5 Optimal solution provided by ***MATLAB* ILP solver** for the observations scheduling sub-problem concerning the coverage of the Spanish and Italian territories.

Table 5.5 Spain and Italy coverage observations sub-problem: Algorithms performances.

***MATLAB* ILP solver**	
$f^{\star}_{LP}$ $[acq.]$	122.500010
f^{lb} $[acq.]$	124
$f^{\star}$ $[acq.]$	124
$T^{\star}$ $[s]$	0.412

GREEDY algo. *Partial coverage allowed*	
f^{heu} $[acq.]$	142
A^{uncov}_{rel} [-]	0.085%
T^{heu} $[s]$	3.869

GRASP algo. *Partial coverage allowed* ($p = 2$)

Solutions obtained	$N_{sol} = 10$		$N_{sol} = 50$		$N_{sol} = 100$		$N_{sol} = 500$	
Full coverage	No	Yes	No	Yes	No	Yes	No	Yes
f^{heu} $[acq.]$	140	-	139	-	138	144	137	142
A^{uncov}_{rel} [-]	1.136%	-	1.245%	-	1.106%	0	1.016%	0
T^{heu} $[s]$	10.321		50.479		96.098		494.721	

GRASP algo. *Partial coverage allowed* ($p = 4$)

Solutions obtained	$N_{sol} = 10$		$N_{sol} = 50$		$N_{sol} = 100$		$N_{sol} = 500$	
Full coverage	No	Yes	No	Yes	No	Yes	No	Yes
f^{heu} $[acq.]$	136	-	137	-	137	146	135	142
A^{uncov}_{rel} [-]	1.426%	-	1.562%	-	1.077%	0	1.123%	0
T^{heu} $[s]$	9.570		48.783		96.420		490.829	

GRASP algo. *Partial coverage allowed* ($p = 6$)

Solutions obtained	$N_{sol} = 10$		$N_{sol} = 50$		$N_{sol} = 100$		$N_{sol} = 500$	
Full coverage	No	Yes	No	Yes	No	Yes	No	Yes
f^{heu} $[acq.]$	138	-	135	-	135	-	135	145
A^{uncov}_{rel} [-]	0.486%	-	1.597%	-	2.420%	-	1.650%	0
T^{heu} $[s]$	10.456		47.506		94.140		475.803	

GRASP algo. *Partial coverage allowed* ($p = 8$)

Solutions obtained	$N_{sol} = 10$		$N_{sol} = 50$		$N_{sol} = 100$		$N_{sol} = 500$	
Full coverage	No	Yes	No	Yes	No	Yes	No	Yes
f^{heu} $[acq.]$	138	-	137	-	137	-	135	143
A^{uncov}_{rel} [-]	1.889%	-	1.537%	-	0.745%	-	1.286%	0
T^{heu} $[s]$	10.527		49.418		99.889		491.895	

GRASP algo. *Partial coverage allowed* ($p = 10$)

Solutions obtained	$N_{sol} = 10$		$N_{sol} = 50$		$N_{sol} = 100$		$N_{sol} = 500$	
Full coverage	No	Yes	No	Yes	No	Yes	No	Yes
f^{heu} $[acq.]$	139	-	137	-	135	-	134	147
A^{uncov}_{rel} [-]	2.130%	-	1.002%	-	1.736%	-	1.669%	0
T^{heu} $[s]$	11.561		51.674		96.310		488.577	

- **Observations and transmissions scheduling problem**

Table 5.6 Spain and Italy coverage observations and transmissions problem: Algorithms performances.

GREEDY algo. *Partial coverage allowed*	
f^{heu} $[acq.]$	142
A_{rel}^{uncov} [-]	0.085
T^{heu} $[s]$	44.554

GRASP algo. *Partial coverage allowed* ($p = 4$)						
Solutions obtained	$N_{sol} = 10$		$N_{sol} = 50$		$N_{sol} = 100$	
Full coverage	No	Yes	No	Yes	No	Yes
f^{heu} $[acq.]$	138	-	137	-	137	-
A_{rel}^{uncov} [-]	0.616%	-	0.749%	-	1.549%	-
T^{heu} $[s]$	205.076		987.603		2035.061	

GRASP algo. *Partial coverage allowed* ($p = 6$)						
Solutions obtained	$N_{sol} = 10$		$N_{sol} = 50$		$N_{sol} = 100$	
Full coverage	No	Yes	No	Yes	No	Yes
f^{heu} $[acq.]$	140	-	137	142	136	144
A_{rel}^{uncov} [-]	1.369%	-	2.532%	0	1.296%	0
T^{heu} $[s]$	209.443		990.156		1930.192	

GRASP algo. *Partial coverage allowed* ($p = 8$)						
Solutions obtained	$N_{sol} = 10$		$N_{sol} = 50$		$N_{sol} = 100$	
Full coverage	No	Yes	No	Yes	No	Yes
f^{heu} $[acq.]$	140	-	137	-	136	142
A_{rel}^{uncov} [-]	2.941%	-	1.122%	-	1.758%	0
T^{heu} $[s]$	204.070		976.691		1970.310	

The solution provided by the **GRASP algo.** which randomly chooses between $p = 4$ candidates and provides $N_{sol} = 10$ has been selected to illustrate the results obtained. In this case, 99.4% of the total area is covered by 138 acquisitions. In this solution, 114 downloads are scheduled to allow the scheduling of other observations and to gather the data acquired before the end of the day.

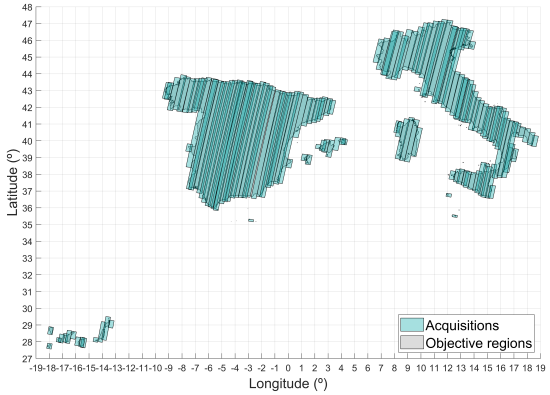

(a) Scheduled observations.

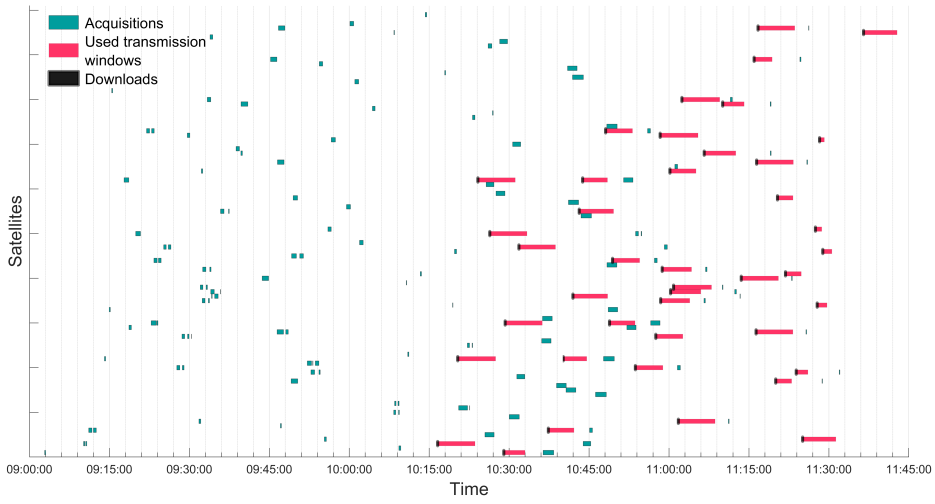

(b) Gantt chart for acquisitions and *foreseen* downloads .

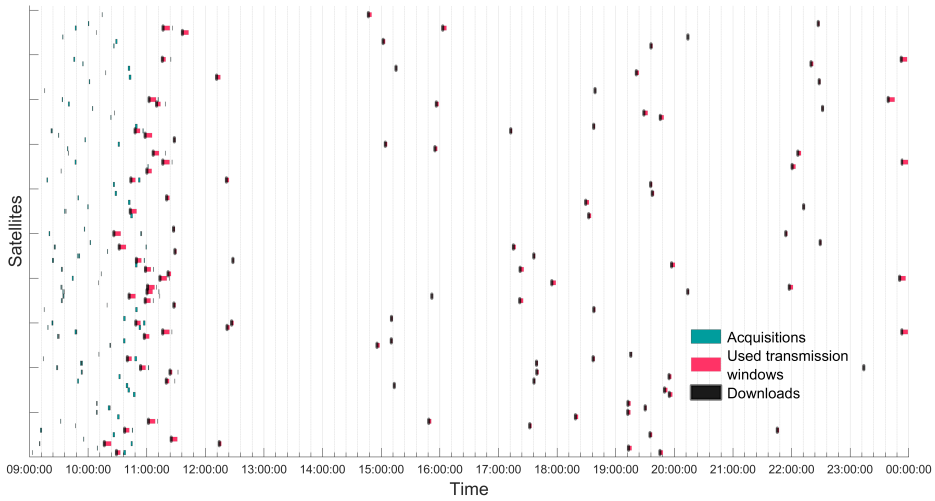

(c) Gantt chart for acquisitions and downloads .

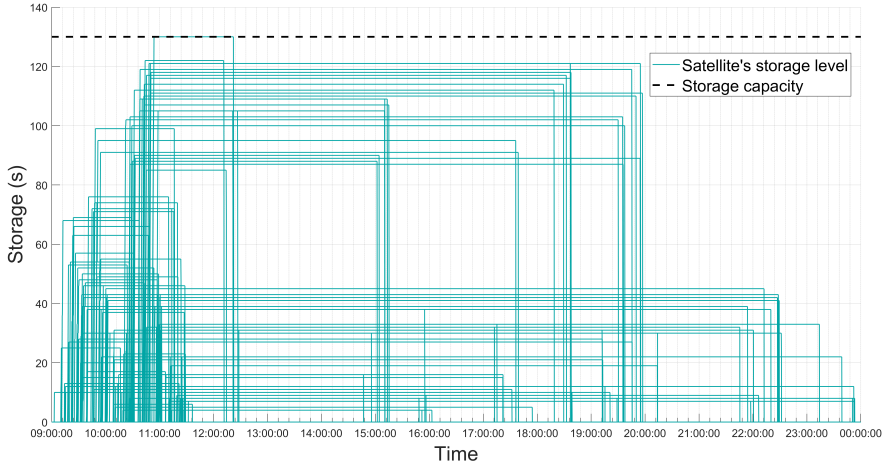

(d) Storage evolution on satellites.

Figure 5.5 Solution provided by **GRASP heuristic algo.** ($p = 4$, $N_{sol} = 10$) for the observations and transmissions scheduling problem concerning the coverage of the Spanish and Italian territories.

5.3 Final analysis

After the computation of the results is made, a final analysis of the overall process is carried out.

- **Instances:** With respect to the problem's instances, their computating demands cannot be neglected. The determination of the satellite's tracks and swaths take a significant amount of time and its behaviour will remain proportional to the number of satellites and modes considered, i.e. the number of swaths generated. The demands of the observation and transmission windows determination are similar and their computing times proportionally depend on the size of the problem. In the other hand, the computation of the subregions not only depends on the number of observation windows but, as previously introduced, depends also on the distribution of these observations and their morphology. As shown in Table 5.1 and Fig. 5.1, the total number of subregions rapidly increase when more intersections are created between the observations, and even more abrupt is the growth for the necessary computing times. To conclude the computation of the instances, the incompatibility matrices are defined without great computing efforts.
- **Resolution:** For the resolution of the relaxed observations problem, *MATLAB* ILP solver is capable to find the full-coverage optimal schedule. In terms of the heuristic algorithm performances for both sub-problem and complete problem, as expected, the optimisation of the solution increase with the number of solutions generated, N_{sol}, especially when increasing the cardinality of the candidates subset, p. However, the increment on the candidates considered, p, not always improves the solution generated. In general, the growth of this cardinality, p, hinders the ability of the algorithms to find full-coverage solution due to the considered heuristic index, the number of subregions added. In terms of computing times, they are proportional to the number of solutions generated and remain unaffected by the number of candidates considered. The size of the problem strongly influences the resolution efforts, since the computing times between the only Spanish regions and Spanish and Italian regions problems, which doubles the number of observation windows and subregions, increase by a factor of around 10.

  Regarding the solutions provided for the complete problems, in the Spanish scenario no download is needed to clear the satellites RAM since their total observing time is low (Fig. 5.2b), hence the transmissions are scheduled only after the observations scheduling is completed (Fig. 5.2c). Contrarily, in the Spanish-Italian scenario, due to the growth of the problem, the satellites observing time increases and the necessary downloads are successfully placed (Fig. 5.5b). Once this is done, the rest of the transmissions are scheduled in order to gather the acquisitions (Fig. 5.5c).

  In terms of overall computing time, as introduced in previous sections, the heuristic algorithms do not improve the necessary time since they also need the computation of the subregions set due to the way they are designed. However, despite the worse performance of the heuristic observations sub-problem resolution (Algo. 3), it helps to calibrate the heuristic resolution of the complete problem (Algo. 4), where no exact resolution is available, with respect to the exact resolution of the observations sub-problem. As a result, the comparison of the three different resolutions provides a better analysis of certain aspects. For example, it helps to realise that the growth in the number of acquisitions needed between the exact resolution in the sub-problem and the heuristic resolution of the complete problem is not caused by the addition of downloading activities, since approximately the same growth manifests itself in the heuristic observations scheduling resolution, but only due to the inherent characteristics of the heuristic approaches, which cannot guarantee the global optimum of the problem.

6 Conclusions and future work

As mentioned in Ch. 1, the interest of this project lies in the growing activities of the small satellites market in the space sector. Due to the technological progress on the miniaturization fields, smaller but numerous devices grouped into constellations which perform a cooperative work are becoming the trend for the future artificial satellites missions. One of the main industries affected by this trend is the Earth observation ones, with companies now being able to perform remote sensing of the Earth with a higher time resolution. Consequently, due to the rise on the amount of the entities needed to be arranged, the development of an automatised and optimal scheduling tool, not only for the observations but also for the transmissions to make accessible the data acquired, becomes essential for these new capabilities.

For the work done in the project, some real parameters have been partially used thanks to the data provided by the company *Planet Labs Inc.*, pioneering this new concept of Earth observation missions. Their satellites from constellations *Flock 2P* and *Flock 3P* have been used as well as other specifications concerning their ground stations and equipped sensors. However, while this company pursues the complete coverage of Earth on each day, a simpler approach has been taken at this project in which specific regions have been considered as the objective regions due to the great computational demands of the full Earth coverage problem. As mentioned in the introduction, the work developed on this project has also been based in other previously done bachelor's thesis ([7] and [6]) and research ([13] and [9]) related with the matter of study.

Firstly, the project has addressed some preliminary matters:

- An exhaustive 3D-model for the determinations of the visible regions and swath for a satellite with certain attitude has been developed. Even though this model consider the Earth as an ideal sphere instead of an ellipsoid, it presents undeniable advantages as its reliability for all possible latitudes and its potential extension for other fields, such as telecommunications.
- The determination of the available transmission windows has been carried out constraining the feasible elevations of the satellites from the involved antenna location. Beyond the scope of the project remains the considerations about failed transmissions and downlink ratio variabilities.
- The *Computational Geometry Toolbox* from *MATLAB* software [4] has been used to describe the geometrical entities for the problem. The swaths created by the satellites are computed and processed in order to fit into the standard geographical longitudes interval. The observations windows are defined from the swaths and objective region overlaps, establishing the starting and finishing times for each one. From each swath different observations can be created, related with different objective regions or a single one whose geometry interrupts the observations. Finally, the subregions are computed using a *divide-compute-assemble* process which performs a separated calculation dividing the big objective regions into smaller ones in order to reduce the computing time.

Afterwards, the mathematical model for the resolution is stated. This model generates an observations scheduling sub-problem which, thanks to the linear character of its constraints and objective function, can be easily solved with any integer linear programming algorithm. The inclusion of the storage constraints for the transmissions scheduling sets the non-linear character of the complete problem and the integer linear programming algorithms are not able to solve it the way it is modelled. Therefore, an heuristic approach has been developed for the resolution. It is important to identify the observations scheduling sub-problem resolution not only as a preliminary step for the complete one, but also as a potential implementation for the

scheduling of constellations with *transmit-while-observe* capabilities or with large storage capacities which relax the downloading demands.

Finally, the resolution of the scheduling problems is carried out using different methodologies. For the observations scheduling sub-problem the performance of the *MATLAB* ILP solver make the designed heuristic algorithm uninteresting, since it is capable to reach the exact solution in less computing time. Regarding the complete problem, the heuristic algorithm designed successfully accomplishes its objective and places the required downloads in order to allow the scheduling of more observations when the storage capacity constraint block them. In addition, although the algorithm occasionally is not able to find solutions which full-cover the objective regions, the areas remaining uncovered are small in comparison with the total area of the objective. An analysis for the different combinations of the number of candidates, p, to join the solution on each iteration of the algorithm, and the number of solutions generated, N_{sol}, has been established for each scenario. This analysis shows that when more candidates are considered, more number of solutions must be generated to get better solutions, substantially increasing the computing time of the resolution. Furthermore, the rise of the parameter p complicates the detection of full-coverage solutions. Therefore, small number of candidates, p, are preferred to decrease the time needed to obtain a proper schedule.

Improvements and future work

Here are now presented a series of considerations which have not been addressed in this project but might be interesting for future studies:

- As mentioned, in this project, the Earth's surface is modelled as a perfect sphere in order to determine the swaths of the satellites. This fact might produce inaccurate coordinates for the limits of the visibility region. Hence, a better modelling of the Earth is proposed using an ellipsoid in stead of a sphere, e.g. the *WGS-84* standard ellipsoid.
- In the approach taken in this document, the available attitudes take discrete values and the slew operations of the satellites are only allowed while they are not observing. The consideration of continuous values of attitude and their capability to slew and observe simultaneously might be interesting for full-coverage better solutions.
- As previously introduced, the resolution carried out address the problem concerning specific regions to be covered. A bigger scale analysis might be performed for the scheduling pursuing the complete coverage of the Earth land mass.
- For future projects, other considerations constraining the scheduling problem could be analysed. Some of them might include the *duty cycle* constraints for satellites and ground stations or possible failed observations and transmissions due to meteorological or misalignment uncertainties.
- The procedure taken on the project detects the transmission windows and their incompatibility between the rest of the operation windows. Then, once one transmission is scheduled in the resolution, all their incompatible windows are discarded even though only a brief downloading lapse is used from the entire transmission window. A more optimised solution might be achieved considering this fact and positioning the download interval at the best moment within the transmission window.
- In stead of analysing a *transmit-or-observe* policy in which no simultaneous observations and transmissions are allowed, future projects can address problems concerning *transmit-while-observe* constellations, removing the observation-transmission incompatibility constraint.
- Due to the growth in the amount of satellites in LEO orbit, space agencies are developing constellations of satellites whose task is to relay the information and data between the entities involved, such as the *European Data Relay System* (*EDRS*). For future concerns, this constellations might substitute the ground stations for better transmission availabilities.
- In terms of the algorithms employed for the resolution, more efficient heuristic algorithms, which do not need the computation of elements needed for the exact resolution, could be used in order to improve their time performances. In addition, commercial integer programming solvers (Gurobi, SCIP, ...) might be also used to solve the coupled observations and transmissions scheduling problem.

List of Figures

List of Tables

Bibliography

[1] Howard D. Curtis, *Orbital mechanics for engineering students*, Butterworth-Heinemann, 2013.

[2] Kiruthika Devaraj, Ryan Kingsbury, Matt Ligon, Joseph Breu, Vivek Vittaldev, Bryan Klofas, Patrick Yeon, and Kyle Colton, *Dove high speed downlink system*, (2017).

[3] Felix R Hoots and Ronald L Roehrich, *Models for propagation of norad element sets*, Tech. report, Aerospace Defense Command, Peterson AFB (CO): Office of Astrodynamics, 1980.

[4] The MathWorks Inc., *Computational geometry: Elementary polygons*.

[5] Bryan Klofas, *Planet labs ground station network*, Tech. report, 13th Annual CubeSat Developers Workshop, Cal Poly SLO, 2016, 13th Annual CubeSat Developers Workshop, Cal Poly SLO.

[6] Ana Laura Zabala López, *Análisis y desarrollo de algoritmos para la planificación optimizada de adquisición de imágenes terrestres*, Master's thesis, Escuela Técnica Superior de Ingeniería (Universidad de Sevilla), 2013.

[7] Sergio Rubio Madroñal, *Análisis y desarrollo de algoritmos para la planificación optimizada de misiones espaciales de observacion de la tierra*, Master's thesis, Escuela Técnica Superior de Ingeniería (Universidad de Sevilla), -.

[8] NASA, *Remote sensors | earthdata*, Aug 2019.

[9] Federico Perea, Rafael Vazquez, and Jorge Galan-Viogue, *Swath-acquisition planning in multiple-satellite missions: an exact and heuristic approach*, IEEE Transactions on Aerospace and Electronic Systems **51** (2015), no. 3, 1717–1725.

[10] Planet Labs, *Planet labs specifications: spacecraft operations and ground systems*, 1.0 ed., 2015.

[11] Jérôme Théau, *Temporal resolution*, pp. 1150–1151, Springer US, Boston, MA, 2008.

[12] David Vallado, Paul Crawford, Ricahrd Hujsak, and TS Kelso, *Revisiting spacetrack report# 3*, AIAA/AAS Astrodynamics Specialist Conference and Exhibit, 2006, p. 6753.

[13] Rafael Vazquez, Federico Perea, and Jorge Galán Vioque, *Resolution of an antenna–satellite assignment problem by means of integer linear programming*, Aerospace Science and Technology **39** (2014), 567–574.

[14] Pei Wang, Gerhard Reinelt, Peng Gao, and Yuejin Tan, *A model, a heuristic and a decision support system to solve the scheduling problem of an earth observing satellite constellation*, Computers & Industrial Engineering **61** (2011), no. 2, 322–335.